UNIVERSIDADE ESTADUAL DE CAMPINAS

INSTITUTO DE BIOLOGIA

TATYANA ALMEIDA TAVELLA

Antiplasmodial activity and mode of action of violacein in *Plasmodium falciparum*

Atividade antiplasmodial e mecanismo de ação da violaceína em *Plasmodium falciparum*

CAMPINAS

2019

TATYANA ALMEIDA TAVELLA

Antiplasmodial activity and mode of action of violacein in *Plasmodium falciparum*

Atividade antiplasmodial e mecanismo de ação da violaceína em *Plasmodium falciparum*

Thesis presented to the Institute of Biology of the University of Campinas in partial fulfillment of the requirements for the degree of Doctor of Philosophy in the field of Genetics and Molecular Biology in Immunology field.

Tese apresentada ao Instituto de Biologia da Universidade Estadual de Campinas como parte dos requisitos exigidos para a obtenção do Título de Doutora em Genética e Biologia Molecular na área de Imunologia

ESTE ARQUIVO DIGITAL CORRESPONDE À VERSÃO FINAL DA TESE DEFENDIDA PELA ALUNA TATYANA ALMEIDA TAVELLA E ORIENTADA PELO PROF. DR. FABIO TRINDADE MARANHÃO COSTA.

Orientador: Fabio Trindade Maranhão Costa

Co-orientadora: Elizabeth Bilsland

CAMPINAS

2019

Ficha catalográfica
Universidade Estadual de Campinas
Biblioteca do Instituto de Biologia
Mara Janaina de Oliveira - CRB 8/6972

T198a

Tavella, Tatyana Almeida, 1990-
Antiplasmodial activity and mode of action of violacein in *Plasmodium falciparum* / Tatyana Almeida Tavella. – Campinas, SP : [s.n.], 2019.

Orientador: Fabio Trindade Maranhão Costa.
Coorientador: Elizabeth Bilsland.
Tese (doutorado) – Universidade Estadual de Campinas, Instituto de Biologia.

1. Violaceína. 2. Mecanismo de ação (Bioquímica). 3. Malária. 4. Chaperonas moleculares. 5. Proteínas de choque térmico HSP70. I. Costa, Fabio Trindade Maranhão, 1972-. II. Bilsland, Elizabeth, 1973-. III. Universidade Estadual de Campinas. Instituto de Biologia. IV. Título.

Informações para Biblioteca Digital

Título em outro idioma: Atividade antiplasmodial e mecanismo de ação da violaceína em *Plasmodium falciparum*
Palavras-chave em inglês:
Violacein
Mechanism of action (Biochemistry)
Malaria
Molecular chaperones
HSP70 heat-shock proteins
Área de concentração: Imunologia
Titulação: Doutora em Genética e Biologia Molecular
Banca examinadora:
Fabio Trindade Maranhão Costa [Orientador]
Marcelo Brocchi
Anna Caroline Campos Aguiar
Célia Regina da Silva Garcia
Carsten Wrenger
Data de defesa: 06-08-2019
Programa de Pós-Graduação: Genética e Biologia Molecular

Identificação e informações acadêmicas do(a) aluno(a)
- ORCID do autor: https://orcid.org/0000-0001-7440-7143
- Currículo Lattes do autor: http://lattes.cnpq.br/4783818797134341

Campinas, 06 de agosto de 2019.

COMISSÃO EXAMINADORA

Prof. Dr. Fabio Trindade Maranhão Costa (orientador)

Prof. Dr. Marcelo Brocchi

Dra. Anna Caroline Campos Aguiar

Dra. Célia Regina da Silva Garcia

Dr. Carsten Wrenger

Os membros da Comissão Examinadora acima assinaram a Ata de Defesa, que se encontra no processo de vida acadêmica do aluno.

Dedico essa tese aos meus pais, sem os quais não estaria onde estou. Obrigada por todo esforço para que eu me tornasse tudo que sempre quis ser, pelos kits de ciência no natal, pelos tubos de ensaio, pelas vidrarias, obrigada por sempre priorizarem a minha educação. Obrigada pelo apoio, pelas madrugadas e fins de semana no laboratório, por minimizarem meus medos, minhas frustrações, por aliviarem meu estresse, obrigada pelas incontáveis orações que sei que fizeram para que eu superasse todos os meus problemas. Aos meus irmãos Alex e Yuri, agradeço pela paciência, pelo amor e pelo exemplo, vocês são as pessoas que mais admiro nesse mundo.

Não existem palavras para descrever quão importante vocês foram/ são nessa fase da minha vida.

Estamos juntos 

AGRADECIMENTOS

Ao professor Fabio Trindade Maranhão Costa, por abrir as portas de seu laboratório para me receber como sua aluna de doutorado direto. Obrigada por estimular minha independência científica e por ter colocado ao meu dispor todas as ferramentas necessárias para que eu desempenhasse meu trabalho.

À Bessie por ter sido minha co-orientadora e por me proporcionar a chance de aprender diferentes técnicas e amadurecer cientificamente em solos nórdicos.

À Drª.Leann Tilley, minha orientadora no exterior, que provavelmente nunca saberá quão importante foi para minha formação científica o nosso encontro, nossas reuniões, discussões e jantares. Obrigada por me aceitar e por confiar em mim.

À Drª.Natalie Spillman e ao Dr. Mattew Dixon, vocês também nunca saberão o quanto aprendi profissionalmente com vocês, e nunca saberão que se tornaram a referência de um autêntico cientista para mim, não apenas pelo vasto (vaaaasto) conhecimento sobre malária, mas também pela dedicação e respeito com o trabalho, pela ética, pela didática, pela paciência para o ensino.

Agradeço aos meus colaboradores, que tornaram esse projeto possível: Elizabeth Bilsland, Per Sunnerhagen, Carolina Horta Andrade, Bruno Neves, Daniel Youssef Bargieri, Juliana Calit, Pedro Cravo, Júlio Cesar Borges e Noeli Silva. Destaco a importância da participação da aluna de doutorado Noeli Silva, com quem trabalhei intensamente durante um curto intervalo de tempo para a obtenção dos dados mais importantes desse trabalho!

Agradeço a Carla por me ajudar nos experimentos de real time, pelas conversas.

À Carol, que além de ser a minha personal figure stylish, me ajudou tanto experimentalmente quanto psicologicamente nesse projeto, com uma participação essencial nos meus primeiros ensaios de drogas *in vitro*, *in vivo* e também nos experimentos super-mega-hiper desafiadores (que nunca funcionaram).

Aos colegas de LIPEX, Najara, João Conrado, João Luiz, Catarina, Juliana e Letícia por tornarem as tardes de trabalho mais leves e as noites de partidas de Catan mais divertidas.

Aos colegas de cultura de células, Gustavo, Letícia, Kaira e Luis, por compartilharem deste trabalho que insiste em ser fora de hora, por cobrirem meus fins de semana de fuga e pelo trabalho sincronizado que faz de nós uma equipe.

Agradeço ainda especialmente ao Gustavo pelas inúmeras vezes que me tirou dúvidas, corrigiu e ensinou – seu companheirismo e boa vontade me ajudaram muito a encarar qualquer problema de maneira mais fácil. Obrigada também, você e Najara, pelas noites de filosofia de buteco.

Um agradecimento aos meus amigos mais próximos, mais distantes, amigos de infância, amigos de República Doriana, amigos de República Tosca, Tospa, Toscamp, com um agradecimento especial à futura doutora Camila Ferezin, popularmente conhecida como Peitinho, que sempre me ajudou a segurar essa barra que é gostar de você (pós-graduação Brasil).

Gostaria de agradecer ao financiamento da agência de fomento FAPESP, dado através da verba do Projeto Temático de n° 2012/165254-2 e 2017/18611-7.

O presente trabalho foi realizado com apoio da Coordenação de Aperfeiçoamento de Pessoal de Nível Superior – Brasil (CAPES) – Código de Financiamento 001.

Agradeço também ao Instituto de Biologia e à UNICAMP pela infraestrutura que possibilitou o desenvolvimento deste projeto de pesquisa, e a todos aqueles que direta ou indiretamente contribuíram para a concretização deste trabalho, a minha eterna gratidão.

SARAPALHA

Guimarães Rosa

Tapera de arraial. Ali, na beira do rio Pará, deixaram largado um povoado inteiro: ... E o lugar já esteve nos mapas, muito antes da malária chegar.

Ela veio de longe, do São Francisco. Um dia, tomou caminho, entrou na boca aberta do Pará, e pegou a subir. Cada ano avançava um punhado de léguas, mais perto, mais perto, pertinho, fazendo medo no povo, porque era sezão da brava - da 'tremedeira que não desamontava' - matando muita gente.

- Talvez que até aqui ela não chegue... Deus há-de...

Mas chegou; nem dilatou para vir. E foi um ano de tristezas. Então, houve gente tremendo, com os primeiros acessos da sezão.

- Talvez que para o ano ela não volte, vá s'embora...

Ficou. Quem foi s'embora foram os moradores: os primeiros para o cemitério, os outros por aí a fora, por este mundo de Deus.

RESUMO

Na malária, parasitas do gênero *Plasmodium* precisam lidar com diferentes tipos de estresse para estabelecer infecções bem sucedidas. As espécies tóxicas reativas de oxigênio e o heme livre (ferro / ferrroprotoporfirina IX) gerados como resultado da degradação da hemoglobina representam uma ameaça à sobrevivência do parasita. Além disso, o protozoário enfrenta um choque térmico de aproximadamente 10°C durante a transmissão do mosquito anofelino para o hospedeiro humano, enfrentando variações constantes de temperatura decorrentes de episódios de febre do hospedeiro infectado. Assim, é compreensível que genes do sistema chaperônico componham cerca de 2% do seu genoma. Moléculas orgânicas derivadas do metabolismo secundário de microorganismos são fontes preciosas de "*probes*", ou sondas naturais que nos permitem entender a função de proteínas específicas e vias importantes dentro de um contexto biológico. Nos últimos 200 anos, os produtos naturais ocuparam um lugar de destaque no tratamento e controle da malária, com os principais antimaláricos da história sendo direta ou indiretamente derivados de produtos naturais. A violaceína é um composto natural de coloração púrpura, produzido pelo metabolismo secundário de bactérias gram-negativas (e.g. *Chromobacterium violaceum*). Apesar de centenas de estudos publicados na literatura reportando sua atividade biológica *in vitro e in vivo* contra células cancerosas e diferentes patógenos como vírus, bactérias, fungos e protozoários, incluindo a capacidade de controlar a malária em camundongos, um mecanismo de ação que explique a toxicidade da violaceína em uma gama de organismos distintos permanece desconhecido. No presente trabalho utilizamos o *Chemical Genomic Profiling,* ou HIP (*Happloinsufficiency proffiling*) em modelo de levedura para elucidar o mecanismo de ação da violaceína. A estratégia abordada nos forneceu uma lista com 6 potenciais hits para o composto, sendo 2 deles cochaperonas da HSP90. Quando observamos o crescimento de todas as leveduras heterozigotas para genes componentes do sistema chaperônico, nota-se uma suceptibilidade comum ao tratamento com o composto, sugerindo que a violaceína possa afetar a via das chaperonas de maneira geral. Nós investigamos a capacidade da violaceína de interagir com 3 chaperonas principais em *Plasmodium*: PfHsp90,

TriC e PfHsp70. Consistente com os dados encontrados, o composto mostrou-se capaz de se ligar e termoestabilizar o domínio N-terminal da PfHSP90 e inibir completamente a atividade ATPásica da PfHSP70 em doses baixas, comprometendo sua capacidade de prevenir a formação de agregados proteicos em aproximadamente 70% em doses equimolares de proteína e composto (Hsp70: violaceina), além de induzir a aceleração da agregação de um modo independente de chaperonas. Outras características típicas de inibidores de chaperonas também foram observadas em parasitos tratados com violaceína, como o *unfolding* de proteínas e intensa degradação proteica via proteasoma. Apesar da intensa proteólise em parasitos tratados com violaceína, a síntese protéica não foi inibida, possivelmente na tentativa de compensar a perda de proteínas essenciais pelo proteasoma. No entanto, o processo de síntese proteica é altamente dependente de chaperonas para que seja bem sucedido, reforçando o colapso da proteostase induzido pela violaceína. Curiosamente, gametócitos *falciparum* maduros (Estágio V), os responsáveis pela transmissão da doença, são mais suceptíveis a ação da violaceína do que estágios assexuados. Esse dado reforça que estratégias que afetam o turnover de proteínas parecem ser importantes para o bloqueio da transmissão da malária.

ABSTRACT

Parasites of *Plasmodium* genus must deal with different types of stress to establish the malarial infection. The toxic reactive species of oxygen and free heme (iron / ferriprotoporphyrin IX) generated as a result of haemoglobin degradation represent a threat to parasite survival. In addition, the protozoa faces a heat shock of approximately 10°C during the transmission from the anopheline mosquito to human host, experiencing constant temperature variations due to patients' episodes of fever. Thus, it is understandable that chaperone system genes make up about 2% of parasite genome. Organic molecules derived from the secondary metabolism of microorganisms are precious sources of natural probes that allow us to understand function of specific proteins and important pathways within a biological context. In the last 200 years, natural products have been prominent in malaria chemotherapy and control, with the major antimalarials in history being directly or indirectly derived from natural products. Violacein is a naturally occurring purple-colored compound produced by the secondary metabolism of gram-negative bacteria (e.g. *Chromobacterium violaceum*). Although hundreds of studies published in the literature report its biological activity *in vitro* and *in vivo* against cancer cells and different pathogens such as viruses, bacteria, fungi and protozoa, including the ability to control malaria in mice; a mechanism of action that fulfills violacein general toxicity against a wide variety of organisms remains unknown. In the present work, we used the Chemical Genomic Profiling (CGP), or HIP approach using yeast model to elucidate the mechanism of action of violacein. Interestingly, the strategy provided us a list of 6 possible hits, 2 of which are cochaperones of Hsp90. When we analyze fitness defect scores for all yeast strains carrying heterozygous genes for components of the chaperone system (178 genes out of ~6000), we can observe a common susceptibility to the compound, providing a strong indication that violacein might be affecting the chaperone system as a whole. We have investigated violacein interaction with three major components of chaperone system: PfHsp90, PfTRiC and PfHsp70. In agreement with our CGP data, the compound was able to bind to PfHSP90 and completely inhibit PfHSP70 activity at low doses, in a way to compromise, in about 70%, its ability to prevent protein aggregates at equimolar doses of protein and

compound. Violacein was also shown to induce acceleration of aggregation in a chaperone independent manner. In addition, other typical characteristics of chaperone inhibitors have been observed in parasites treated with violacein, such as protein unfolding and intense proteasome degradation. Curiously, we were unable to detect activation of the Unfolded Protein Response, as eIf2-α remained unphosphorylated. Regardless of intense proteolysis, protein synthesis was not inhibited, possibly in an attempt to compensate for the loss of essential proteins by the proteasome. However, the protein synthesis itself is a process highly dependent on chaperones to succeed, reinforcing parasite proteostasis collapse induced by violacein. Interestingly, mature *falciparum* gametocytes (Stage V), those responsible for transmitting the disease, are more susceptible to violacein than asexual stages. This data reinforces that strategies targeting protein turnover seem to be important for blocking malaria transmission.

FIGURE LIST

Figure 1- Malaria Cycle…….....……....23

Figure 2- Malaria Incidence and Death rates from the period 2000 to 2015 …....24

Figure 3- Percentage in malaria incidence from the period 2010 to 2016 ….....25

Figure 4- ER stress response across different eukaryotes…….....29

Figure 5- Scheme of Ubiquitin Proteasome System (UPS) and Unfolded Protein Response (UPR) in cellular stress……..……..……30

Figure 6- The ubiquitination cascade.....32

Figure 7- Composition of the 26S proteasome……..…….....34

Figure 8- Artemisinin proposed mode of action……..……....37

Figure 9- Gin tonic old recipe……..……...…….....38

Figure 10- Chemical Structure of Violacein……..…….....39

Figure 11- Schematic representation of *in vitro* violacein EC50 Speed assay….46

Figure 12- Schematic design of generation of Yeast Heterozygous Library through chromosomal Integration by homologous recombination……..……...49

Figure 13- Schematic representation of Chemical Genomic Profiling in yeast model……..50

Figure 14- *P. falciparum in vitro* growth curves upon violacein treatment …….....59

Figure 15- Violacein stage specificity within asexual parasites…..……..……..61

Figure 16- Violacein speed of action……..…..…….……62

Figure 17- *P. berghei* liver stages infection rates upon violacein treatment ……..64

Figure 18- Violacein activity against early stage gametocytes…..……65

Figure 19- Violacein activity against stage V gametocytes……..…….66

Figure 20- Gametocyte ookinete conversion upon violacein treatment..……67

Figure 21- Hypothetical scheme showing Chemical Genomic Profiling assay ……..……..……..…....68

Figure 22- BY4743 wild-type yeast growth curve upon violacein treatment…….…….……....69

Figure 23- Haploinsufficiency profile of heterozygous yeast strains treated with violacein compared to the untreated control……..……..70

Figure 24- Predicted intermolecular interactions of violacein with ATP binding sites of *P. falciparum* and human HSP90……..……..…….....74

Figure 25- Unfolded protein response in *P. falciparum* upon violacein treatment. ……...…….....77

Figure 26- *P. falciparum* UPS response upon violacein treatment…….……80

Figure 27- PfHSP90 CD far-UV spectra in the presence or absence of violacein…….…….82

Figure 28- DSC data for full length PfHSP90 incubated with ADP, violacein or both……..……84

Figure 29- PfHSP90 ATPase activity following violacein treatment……..…87

Figure 30- PfHSP90 ATPase folding cycle……..……..88

Figure 31- PfHSP90 capability to prevent MDH aggregation upon violacein treatment…….89

Figure 32- Chemical genomic profiling data from all yeast strains carring heterozygous mutant for proteins involved in the chaperone system…….91

Figure 33- Schematic outlining the strategy used to design PfΘTRiC conditional knockdown……..94

Figure 34- PfΘTRiC conditional knockdown parasites……..…….…….95

Figure 35- PfTRiC knockdown EC50 shift upon violacein treatment……..…..95

Figure 36- PfHSP70 ATPase activity following violacein treatment…..……..…..97

Figure 37- PfHSP70 capability to prevent MDH aggregation upon violacein pre-treatment…….……99

Figure 38- Proposed violacein mechanism of action in *Plasmodium*……..103

TABLE LIST

Table 1. Antiplasmodial activity of violacein……..……..……..……60

Table 2. Liver stage activity of violacein……..……..…63

Table 3. Ookinete conversion under violacein treatment……67

Table 4. Top Hits Fitness defect. Hits for CGP, violacein 10G…….……..……...71

Table 5. Details of grids used in molecular docking studies and corresponding Chemgauss4 scores for violacein……..……..……75

Table 6. Differential Scanning Calorimetry analysis……....84

ABBREVIATIONS

WHO- World Health Organization

ITNs- Insecticide treated nets

ACTs- Artemisinin combined therapies

ART- Artemisinin

PV- Parasitophorous vacuole

RBCs- Red blood cells

HSP90- Heat shock protein 90

HSP70- Heat shock protein 70

TRiC/CCT- Chaperonin containing TCP-1 ring

HSP60- Heat shock protein 60

PfEMP1- Plasmodium falciparum Exported membrane protein -1

XBP1- X-box binding protein 1

CREBH- Cyclic adenosine monophosphate (cAMP) responsive element binding protein H

HSP40- Heat shock protein 40

mRNA- Messenger RNA

PROSC- Proline synthetase co-transcribed [bacterial homolog]

UPS- Unfolded protein response

ER- Endoplasmatic reticulum

ATF6- Activating transcription factor 6

PERK- Protein kinase RNA-like endoplasmic reticulum kinase

IRE1- Inositol-requiring enzyme 1

BiP- Binding immunoglobulin protein

PK4- *Plasmodium* eIF2 kinase

UPR- Unfolded protein response

eIf2-α- Eukaryotic Initiation Factor 2 alpha

E1- Ubiquitin-activating enzyme

E2- Ubiquitin-conjugating enzyme

E3- Ubiquitin protein ligase

AAA type ATPase- ATPases Associated with diverse cellular Activities

Rpt- Regulatory particle of triple-ATPase

Rpn- Regulatory particle of non-ATPase

DUBs- Deubiquitinating enzymes

FDA- Food and Drug Administration

MPl-1- Myeloproliferative leukemia vírus-1

DHA- Dihydroartemisinin

K13- Kelch 13

DDT- Diclorodifeniltricloroetane

HL60- Acute promyelocytic leukemia cell line

TNF receptor-1- Tumor necrosis factor receptor 1

TF1 - Human growth factor-dependent cell line

MDM2- Mouse double minute 2 homolog

EDTA- Ethylenediamine tetraacetic acid

GFP- Green fluorescent protein

CQ- Chloroquine

DV- Digestive vacuole

EC50- Concentration of a drug that gives half-maximal response

Huh7- Hepatocarcinoma cell line

CGP- Chemical genomic profiling

DMSO- Dimethyl sulfoxide

TPR- Tetratricopeptide repeat

PK4- *Plasmodium* eIF2α Kinase

CD- Circular Dichroism

DSC- Differential scanning calorimetry

ADP- Adenosine diphosphate

Tm- Melting temperature

∆**H-** Enthalpy variation

ATP- Adenosine triphosphate

Pi- Inorganic phosphate

GA- Geldanamycin

Tau- Microtubule-associated protein

MDH- Malate Dehydrogenase

TeTR- Tetracycline repressor-

DOZI- Development of zygote inhibited

NBD- Nucleotide binding domain

PBD- Peptide binding domain

pH- Potential of Hydrogen

HSP104- Heat shock protein 104

ClpB- Caseinolytic peptidase B protein homolog

Hip- Haploinsufficiency profile

ERAD- Endoplasmic reticulum-associated protein quality control and degradation

SUMMARY

INTRODUCTION……..…….....21

The Disease…….....21

The Human Host……...…..26

Unfolding Malaria…….…….....27

Unfolding Protein Response…….28

The Ubiquitin Proteasome System……..……....31

Artemisinin: The resistant……..……35

Malaria and natural products: more than just gin and tonic….....37

Violacein…….....39

RATIONAL……..…….....42

OBJECTIVES……...43

MATHERIALS AND METHODS…….....44

RESULTS AND DISCUSSION…….....58

FINAL REMARKS…….……..…….....100

CONCLUSIONS…….....104

REFERENCES…….....105

SUPPLEMENTARY MATERIAL…...……127

Annex I: Scientific publications……..……127

Annex II: Financial support.....128

Annex III: Authors declaration.....129

Annex IV: Bioethics declaration……...130

1. INTRODUCTION

1.1. The disease

Although unprecedented constant improvement in shrinking malaria map have put several endemic countries in elimination and control phase of the disease, nearly half of the world's population is still at risk of contracting malaria [1]. According with the latest world malaria report, in 2017 there were more than 200 million cases of malaria, with an estimative of 435.000 related deaths worldwide [2]. Despite the wide distribution along the tropical zone of the globe, Sub-Saharan Africa still carries the highest percentage of malaria burden, comprising in 2015, 90% of total cases and deaths.

In 2016, US $2.7 billion was invested in measurements to defeat the disease. What looks like a reasonable investment is actually well below the US $6.5 billion annual investment projected by WHO to meet the 2030 targets of malaria eradication strategy [1]. We can understand the socio-economic impact that malaria has on the tropical world, especially in low-income countries, but what causes malaria and what are the challenges to eradicate it?

Despite first beliefs that this ancient disease was caused by bacteria [3] and transmitted by the air (mal'aria; "bad air", from medieval Italian), thanks to Alphonse Laveran (Nobel prize, 1907) Malaria was discovered to be caused by the infection of protozoans from genus *Plasmodium*. There are hundreds of different *Plasmodium* species but only five of them are well known to cause malaria in humans: *P. falciparum, P. vivax, P. malarie, P. ovale and P. knowlesi.* Out of these five species, two of them are responsible for the main burden of the disease: *P. vivax*, the most widespread specie, and *P. falciparum*, the most virulent one, responsible for nearly half million deaths/ year in the past couple of years [1], [4], [5].

After Laveran, several scientists around the world put puzzle pieces together to solve the malaria causative agent life cycle [3], [6]. The infection in humans starts with the intradermal inoculation of sporozoites through the female anopheline mosquito blood meal. The sporozoites are transported to the liver through the vasculature, where they infect hepatocytes and undergo schizogony, originating thousands of merozoites released in packs of merossomes into the blood stream. This

part of the cycle precedes the erythrocytic phase of the disease, and is known as hepatic phase or malaria pre-erythrocytic phase. On the vasculature, merozoites infect red blood cells, remodeling host cells until parasite maturation that ranges from early stages (rings) to mature stages (trophozoites and schizonts). Schizonts represents the highest stage of maturation, which goes through several rounds of replication (schizogony) originating dozens of daughters merozoites that burst the erythrocyte releasing themselves into the blood stream where they will invade new red blood cells, establishing a chronic cycle of asexual replication [7], [8] (Figure 1). A small percentage of the asexual parasites differentiate into sexual gametocytes, which are taken by the mosquito during blood meal giving continuity to the parasite cycle in the anopheline. This phase is known as the erythrocytic phase or symptomatic phase, and is responsible for the common symptoms of the disease like high fever, chills, headache, weakness, myalgia and vomit in non-complicated malaria, being also responsible for harsh symptoms in the severe manifestation of the disease promoting severe anemia, splenomegaly, renal failure, spontaneous bleeding, convulsions and coma.

Pregnant women are 3 times more likely to develop severe malaria compared with their non-pregnant counterparts, with mortality rates approaching 50%. It is hypothesized that this risk factor results mainly from placental sequestration of infected erythrocytes combined with immunocompromisation due to pregnancy [9]. Patients HIV/AIDS positive, Infants and children under five also comprise high-risk group, mostly because the immune system is deteriorated or not fully develop to combat the disease on its severe form [1], [4], [5].

Beside the high-risk patients, it is interesting to call attention to another edge of people affected by malaria, the asymptomatics. Even though these present no symptoms and have no death risk, the asymptomatic carriers represent a treat to eradication polices. Like silent reservoirs, they do not seek medical care as they are unaware of infection, continuing to spread the disease. Asymptomatic malaria is a chronic and debilitating infection that needs to be treated [10], [11], but it is just the tip of the iceberg when we talk about challenges in eradication.

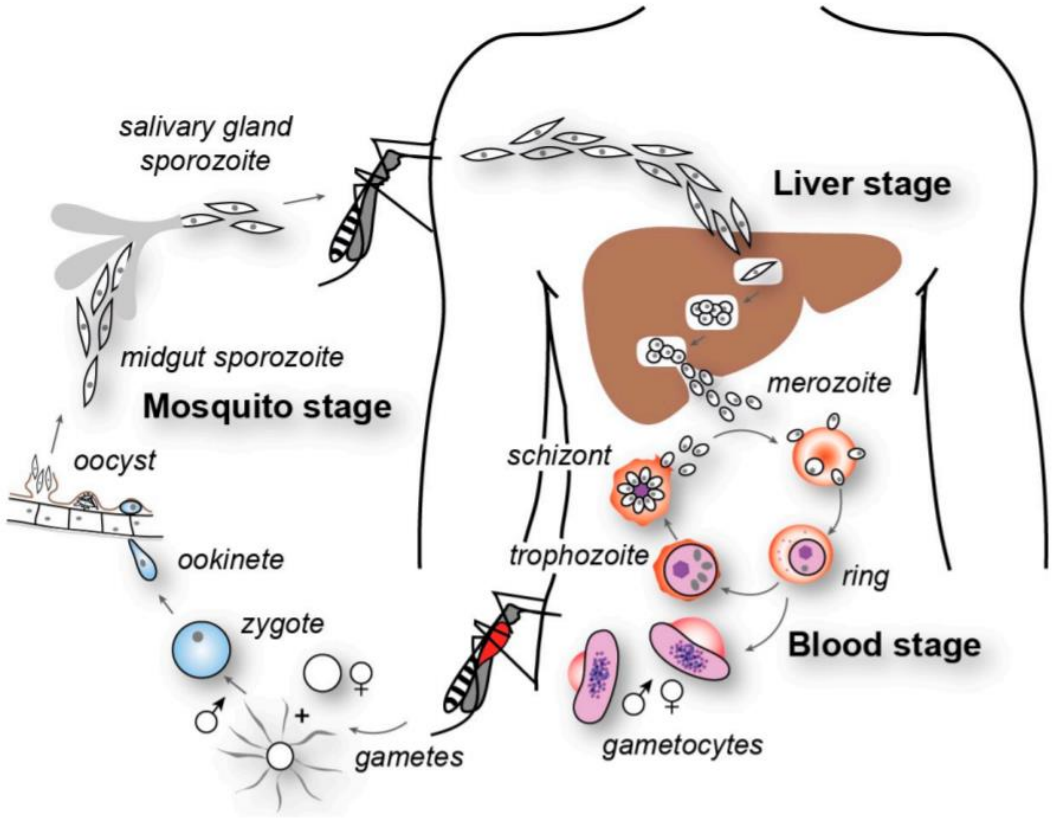

Figure 1: Plasmodium life cycle (adapted from Cowman and colleagues, 2012). Sporozoites are inoculated into the vasculature during the mosquito blood meal and travel to the liver parenchyma, infecting hepatocytes inside. There, they differentiate into thousands of daughter merozoites. Merozoites leave hepatocytes in packs of merossomes and reach the blood stream, where they infect red blood cells, starting the symptomatic phase of malaria. Inside red blood cells the parasites develop from ring to trophozoites and after successive rounds of schizogony, at schizonts stage they will burst the erythrocyte releasing dozens of merozoites that will reinvade new red blood cells. A small fraction of the asexual parasites differentiates into sexual gametocytes, which will be taken by the mosquito during blood meal to give continuity to the parasite cycle in the mosquito. When male and female gametocytes reach the mosquito gut, they go through gametogenesis, differentiating themselves into micro and macrogametes respectively. Fusion of male and female gametes originates the zygotes, that develop into motile ookinete, which migrate to the midgut epithelium differentiating themselves into oocysts. Growth and development of oocysts results into generation of thousands of sporozoites that will further infect humans giving continuity to *Plasmodium* life cycle.

According to WHO, vector control strategies such as the wide distribution of insecticide treated mosquito nets (ITNs), as well as the use of Artemisinin Combined Therapy (ACTs) as first-and-second-line of treatment for uncomplicated *falciparum* malaria and chloroquine-resistant *vivax* malaria, were the main responsible for malaria massive drop in both incidence (37%) and mortality (60%) from 2010 to 2015 [4] (Figure 2). The latest World Malaria Report showed resistance evidence of vectors to the four classes of insecticide mainly used in ITNs. Out of the 76 countries surveyed between 2010-2016, 61 reported vector resistance to at least one insecticide used [1].

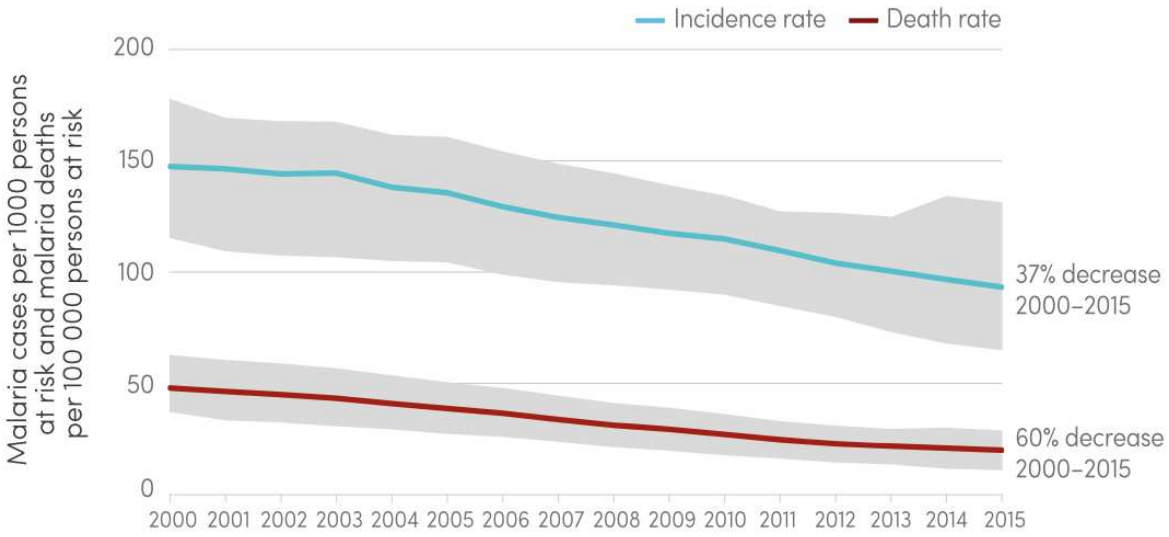

Figure 2: Malaria Incidence and Death rates from the period 2000 to 2015 (Adapted from WHO, World Malaria Report, 2015)

Problems with resistance are not restricted to vectors. In the early 2000s, several groups reported delay in the clearance of *P. falciparum* infections upon artemisinin (ART) treatment in the Great Mekong Region [1], [12]–[14]. After the emergence of chloroquine resistance in the 80'ths, artemisinin was the only drug capable of killing multidrug-resistant parasites, earning the Chinese researcher Youyou Too, the Nobel Prize in Medicine for its characterization and contribution to malaria control [15][16]. Worryingly, recent studies have demonstrated that partial artemisinin resistance has emerged independently in different regions of the Great Mekong as well as in Guyana, South America [17].

Despite a significant decrease in malaria cases all over the world from 2010-2015, when we consider data from the past couple of years (2014-2016), the incidence of the disease increased in all continents with exception of Europe [1] (Figure 3). It worth notice that according with the latest World Malaria Report, there was no relevant progress in reducing malaria cases during the period 2015-2017 [2].

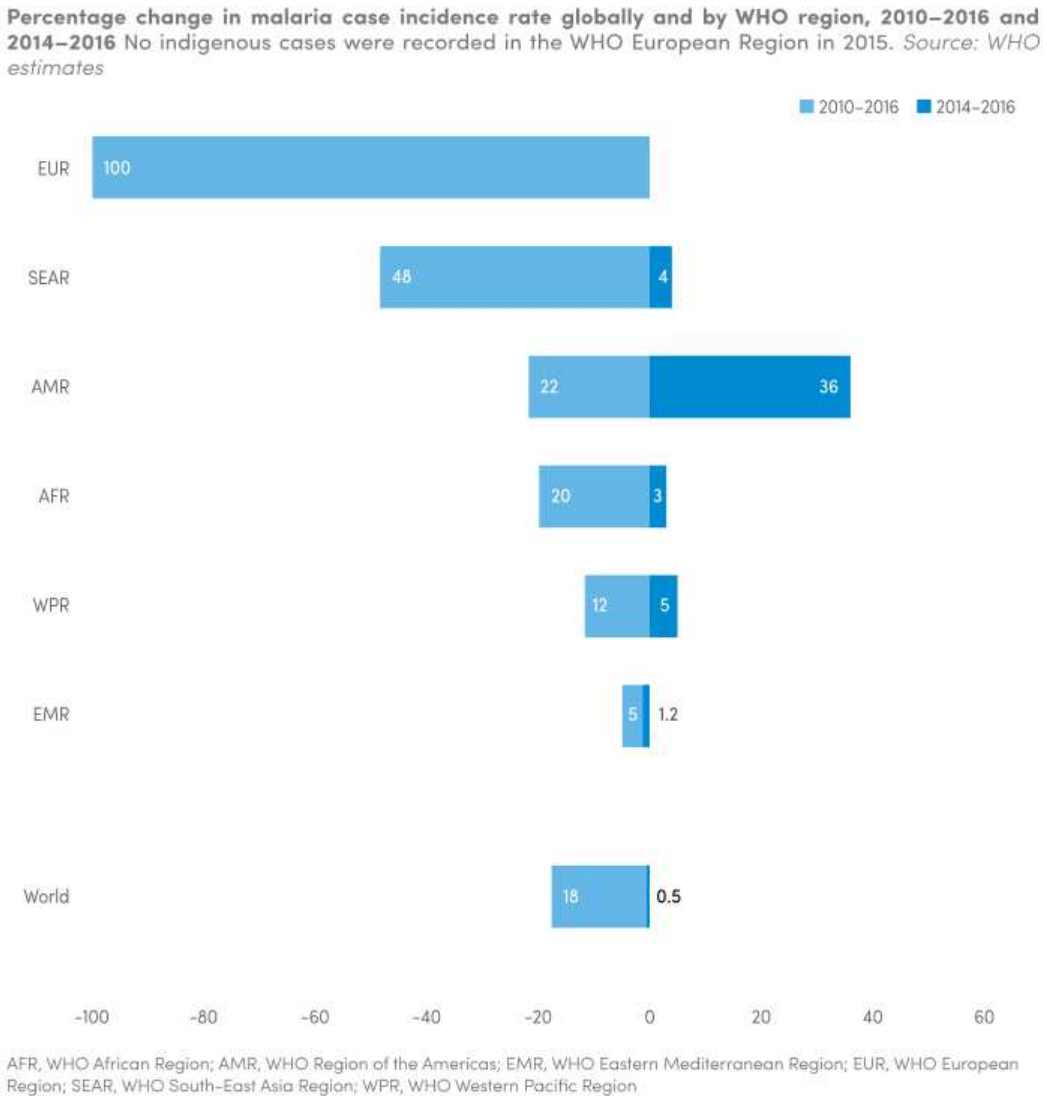

Figure 3: Percentage in malaria incidence from the period 2010 to 2016 (Adapted from WHO, World Malaria Report 2017)

Many factors could have contributed to the recent rise of malaria incidence, such as the emergency of resistance among parasites and vectors against commonly

used drugs and insecticides, combined with political instabilities in countries like Venezuela, South Sudan, Bangladesh, and Yemen; as malaria control demands commitment to public health policies, investment and infrastructure [18].

1.2. The Human Host

Plasmodium parasites depend on mammalian cells for intracellular development and replication. The first obligatory site of infection within the human host takes place in the liver, where infection occurs after sporozoites release into bloodstream through the bite of infected female *Anopheles* mosquito. Once sporozoites enter in the liver parenchyma, they invade hepatocytes sheltering themselves inside a protective parasitophorous vacuole (PV), where they create a replication-competent niche [19], [20]. Although with an active metabolism, *Plasmodium* parasites are highly dependent on host cells for nutrient acquisition, waste removal, protein traffic, turnover and several processes that require secretory pathways from the host [21].

The following site of infection within humans happens on red blood cells (RBCs). Unlike hepatocytes, here, the *falciparum* parasite has adapted itself to invade an “empty” cell, devoid of nuclei, mitochondria, endoplasmatic reticulum, besides numerous cellular receptors that were expelled or degraded during red blood cell maturation [22], [23]. The lack of default organelles is accompanied by metabolic restrictions in several processes, which obligates the parasite to develop mechanisms to overcome host limitations by creating nets of tubular-like membranes connecting parasite and host cytoplasm with the extracellular environment [21]. Even though RBCs shed almost the totality of their content giving place to haemoglobin, some proteins as chaperones persist in the erythrocyte cytosol [24]. The importance of chaperones for erythropoiesis and RBC maintenance is suggested by the accumulation of HSP70 within erythroid precursors [25], requirement of HSP90 for haemoglobin maturation [26] and TRiC translocation from cytosol to a membrane-bound state under high physiologically relevant temperatures, implying a role on cytoskeleton stabilization over thermal stress [27].

Despite intrinsic value in maintenance of cellular stability, this essential class of folding machines is an important part of the unfolding protein response (UPR) and

can work as an Achilles heel, exploited by many pathogens to successfully establish infections. In malaria for instance, human chaperonin containing TCP-1 complex, a Hsp60 chaperone, also known as CCT complex or TRiC, from the red blood cell, appears to be recruited by the parasite for the traffic of PfEMP1, a cytoadhesion protein that correlates with high virulence in severe malaria [28].

Curiously, apparently *P. berghei* infections on hepatocytes are benefited by host's unfolded protein response activation. In liver, the different UPR signaling cascades, XBP1 and CREBH, are known to regulate lipid and iron homeostasis respectively; ∆xbp1 and ∆crebh mice showed reduced parasite burden in hepatocytes, suggesting that host UPR activation might provide important sources of fatty acids and iron required for parasite development during this phase of infection [29].

1.3. Unfolding malaria

Beside innumerous error-prone processes by which cells are normally subjected to, such as transcription and protein translation, *Plasmodium* parasites are exposed to a wide range of temperature shocks, with temperatures variations reaching up to 10°C during the transition from mosquito vector to human. During malaria symptomatic phase, parasites are exposed to successively episodes of fever suffered by the host, haem detoxification [30] and host immune response [31]; making it understandable that genes encoding chaperones represent around 2% of total genome in *Plasmodium* [32]. Not surprisingly, several intracellular pathogens utilize not only endogenous chaperones but also host chaperone systems to overcome adverse conditions and effectively establish infections [24], [33]–[36].

Chaperones and chaperonins are highly conserved protein folding machineries that can bind and dissociate from macromolecules through non-covalent bonds in order to ensure proteins are kept under native conformation, guaranteeing its function within the cell. Misfolded intermediates and unassembled polypeptides generally expose their hydrophobic sites prone to aggregation, a common feature in many pathologic disorders. Proteins that aggregate or that cannot be correctly folded by these machineries are usually degraded by the proteasome pathway, allowing vital equilibrium between protein synthesis and proteolysis, a process called proteostasis

[37]. Thus, keeping an army of chaperones together with an efficient proteolytic system, is crucial for cell survival, once protein concentrations can reach over 300mg/ml, a favorable environment for unwanted interactions as protein aggregation, insolubility and denaturation [38].

In addition to folding properties, chaperones are known to regulate several essential processes in which different families, highly conserved across species, are involved in chromatin remodeling, signal transduction and protein traffic [34], [39], [40]. The major heat shock families in *Plasmodium* are: Hsp40, Hsp60, Hsp70 and Hsp90 [40].

In 2011, a group of scientists shed light on possible mechanisms by which *Plasmodium* acquires resistance to artemisinin. Transcriptomic analysis of 1043 *P. falciparum* isolates from patients from Southeast Asia with malaria, correlated the increased levels of mRNAs for the chaperone systems PROSC and TRiC, with parasite drug resistance [41], [42].

Protein ubiquitination also seems to be involved in *Plasmodium* resistance to artemisinin, as resistant parasites show reduced protein poly-ubiquitination after drug treatment when compared to their sensitive counterparts [43]. Yet, ubiquitination is a key component of the ubiquitin proteasome system (UPS), a crucial proteolytic network for parasite progression through its life cycle, being an essential post-translational modulator of several biochemical processes in *Plasmodium* [44]. Thus, understanding perturbations of the unfolded protein response and ubiquitin proteasome system in malaria is fundamental, not only to unravel the mechanisms used by the parasite to overcome artemisinin's activity, but also to highlight important pathways passive of being targeted for drug discovery and drug development strategies.

1.3.1. Unfolding Protein Response

The Ubiquitin Proteasome System (UPS) and Unfolded Protein Response (UPR) form two major regulatory branches of cell stress signaling. In the UPS pathway, proteins damaged by cellular stress are mainly refolded by chaperones, or ubiquitin tagged for degradation by the proteasome. In UPR, biochemical pathways that lead to increased transcription of chaperones, cytokines and proteins involved in proteolytic systems are activated while translation of other proteins is shut down [36].

Whilst in mammalian systems, UPR is composed by three majoritarian arms represented by ER resident membrane proteins: IRE-1, PERK and ATF6, in *Plasmodium* this response is simplified, being restricted to a modified PERK pathway that lacks transcriptional regulatory response [36], [45], [46]. Interestingly, although the absence of canonical UPR transcriptional pathways (Figure 4), some studies propose that up-regulation of genes from proteins involved at ERAD response can be achieved with chemical treatment in *Plasmodium* [47]–[49]. These studies suggest the existence of folding stress transducers, different from the ones found for higher eukaryotes. Curiously, this was previously considerate to happen in *Giardia lamblia*, a protozoan that also lacks the Unfolded Protein Response adaptative wing [50]. However, a different study couldn't observe alterations on *Plasmodium* UPS transcription pattern upon DTT treatment, a compound known to activate the UPR, reinforcing the lack of transcriptional regulation at Plasmodium ER stress response [45].

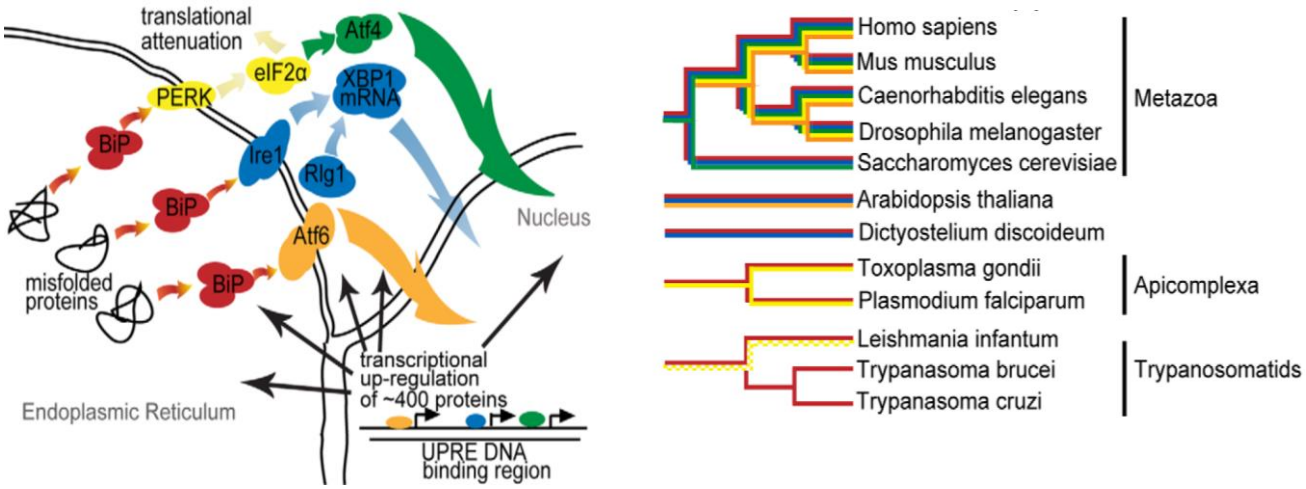

Figure 4. **ER stress response across different eukaryotes** (Adapted from Gosline, 2011). The colors of the branches indicates that the proteins represented with the same colors are present at the organism.

During ER stress response, the accumulation of misfolded proteins leads to the dissociation of BiP from PK4, a transmembrane kinase that undergoes autophosphorylation prior to phosphorylating eIF2α, resulting downregulation of protein translation (Figure 5). Decrease in protein synthesis avoids chaperone

overload, since protein biogenesis is an error-prone process highly dependent on chaperone machineries to succeed. Thus, stress response in *Plasmodium* is controlled by decrease of protein synthesis (UPR branch) and refolding/degradation of misfolded proteins (UPS branch) [36], [37], [46].

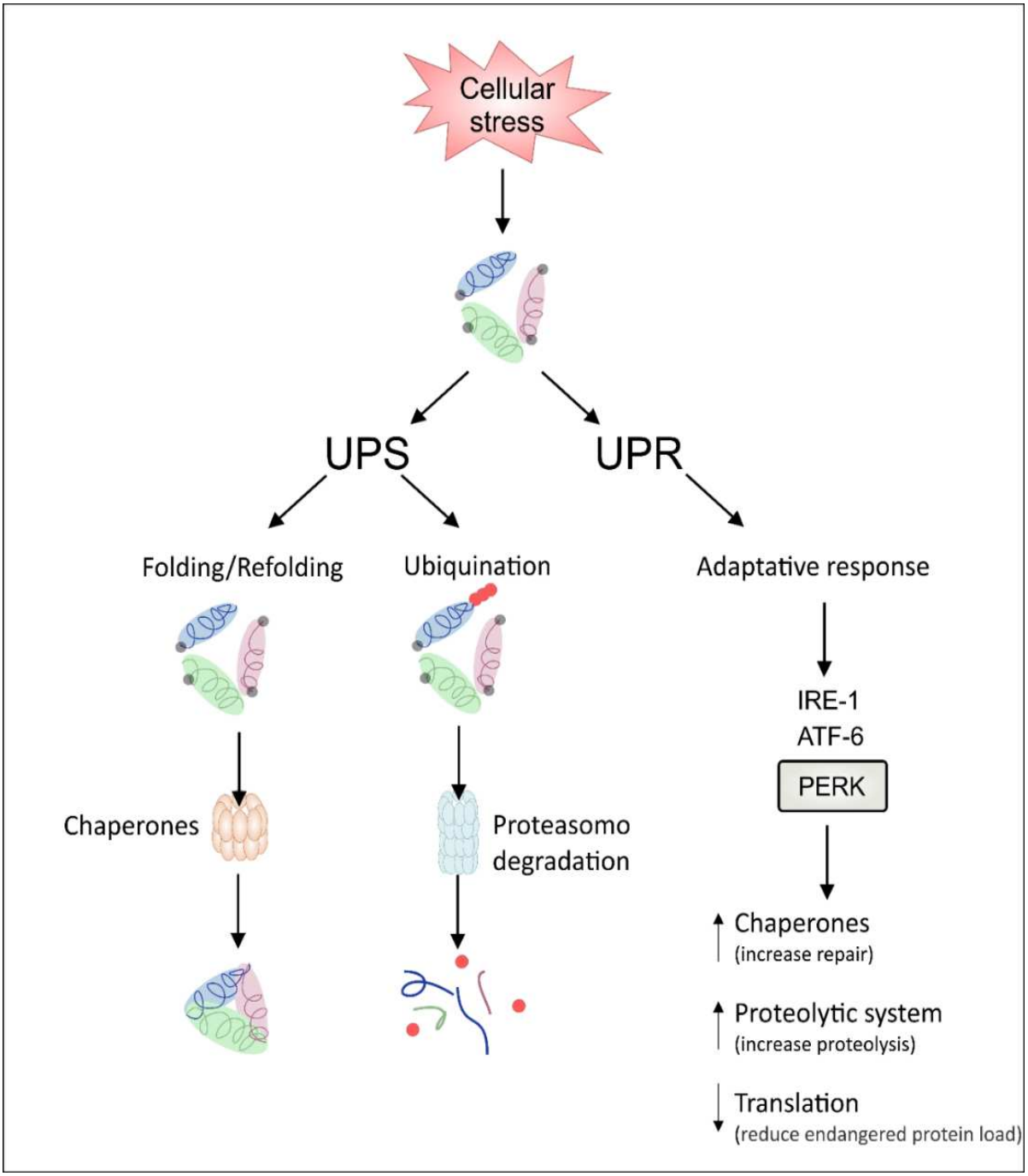

Figure 5. **Scheme of Ubiquitin Proteasome System (UPS) and Unfolded Protein Response (UPR) in cellular stress.** In UPS, proteins damaged by cellular stress are preferentially refolded by chaperones. When proper folding cannot be achieved, misfolded intermediates are ubiquitinated and sent to the proteasome for degradation. Mammalian cells produce a robust UPR, with three major branches: IRE-1, ATF6 and PERK, each one leading to reinforcement of quality control network through transcriptional regulation and downregulation of translation. In *Plasmodium,* UPR is reduced to a modified PERK pathway that results in downregulation of protein translation to decrease chaperone overload.

1.3.2. Ubiquitin Proteasome System

Plasmodium is highly dependent on proteolytic systems to survive, relying on three distinct protease complexes: ClpQ, ClpP and 26S proteasome. ClpQ and ClpP have prokaryotic origin residing on parasite mitochondria and apicoplast respectively [51]–[53]. The typical eukaryote 26S proteasome is a multisubunit enzyme complex, core of the ubiquitin proteasome system (UPS), which controls innumerous functions within the cell through life-span regulation of short living and damaged proteins, labeled with ubiquitin signals for degradation.

Computational analysis suggested that nearly 80% of parasite proteins are putative targets for ubiquitination, post-translational modification present along all stages of parasite life cycle. This data is reinforced by the high frequency of lysine rich sequences present on its proteome [44]. Lysine, the second most abundant amino acid in *Plasmodium*, works as an anchor for poly-ubiquitination, in which ubiquitin is attached to the protein through a bond between ubiquitin's C-terminal-end and lysine from the substrate. Each ubiquitin possess seven lysine residues, providing innumerous possibilities of linkage chains with distinct spatial conformations that can be attached to substrate [54]. Client ubiquitination requires at least three groups of enzymes: E3, an ubiquitin ligase, E2, an ubiquitin conjugating enzyme and E1, an ubiquitin-activating enzyme. The ubiquitination cascade starts with the formation of E1-ubiquitin complex that acts like a donor of ubiquitin to E2. Substrate selection and ubiquitination depend on an orchestrated interaction between E3 ligase and E2 enzyme, in which E3 binds to the substrate and recruits E2 charged with ubiquitin molecules that will be further transferred to the target protein (Figure 6) [54], [55].

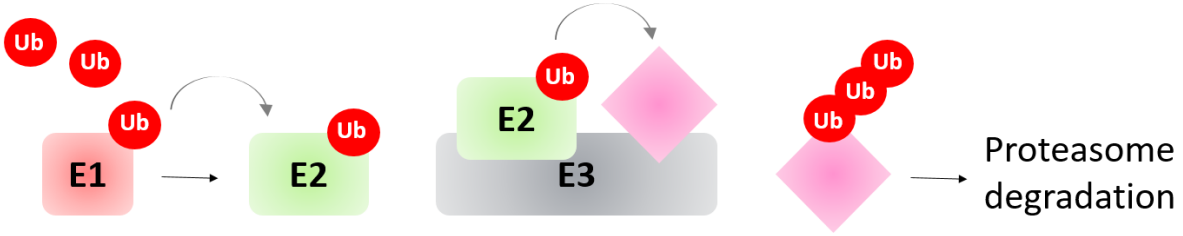

Figure 6. The ubiquitination cascade. The ubiquitin-activating enzyme (E1) charges itself with ubiquitin molecule that will be further donated to an ubiquitin-conjugating enzyme (E2). Substrate ubiquitination relies on ubiquitin ligase enzyme (E3) simultaneous binding to both, client protein and E2 enzyme, allowing enough proximity for ubiquitin transferring from E2 to the target substrate. Proteins can undergo several rounds of ubiquitination and depending on the type of polyubiquitin chain it will be guided for proteasome degradation.

In *P. falciparum genome*, all the components of the ubiquitination cascade were identified, including four genes for ubiquitin, along with more than 50 E3 ubiquitin ligases, 14 E2 enzymes and 8 E1 ubiquitin-activating proteins [44].

Not all ubiquitinated proteins are shuttled for degradation, as the length and linkage type of ubiquitin chain determines the fate of each protein. Substrates that are ubiquitinated at a single or at multiple sites where previously shown to play regulatory roles in the cell performing functions like DNA repair and vesicle traffic [56], [57]. Studies suggested that degradation signal requires a chain with at least four associated ubiquitin molecules for proteolysis targeting[54]. However, the mechanisms implied in substrate selection for degradation are not fully understood and possibly involve specific ubiquitin receptors associated with different kinds of degradation/biochemical pathways [54].

The proteasome is composed by nearly 30 subunits disposed in a barrel shape forming the proteolytic 20S core, capped by two 19S regulatory regions. Proteins tagged with poly-ubiquitin chains are recognized and unfolded by the 19S regulatory region that is divided into two sub-complexes, the base and the lid. The base is structured by six AAA-type ATPases, responsible for substrate recognition, unfolding and α-ring gate opening (Rpt 1-6), together with four non-ATPase subunits: Rpn1, Rpn2, Rpn10 and Rpn13. Rpn1 and Rpn2 work as scaffolds, and Rpn10 and Rpn13 are integral ubiquitin receptors. The lid is built by nine Rpn subunits: Rpn3, Rpn5-9,

Rpn11-12 and Rpn15, whose primary function is to recycle ubiquitin through deubiquitination process. Four heptameric rings compose the 20S core. The outer rings are structured by α-subunits, while the inner rings are formed by seven β-subunits each, being three of them well studied proteolytic proteins: β1 with caspase activity (cleaves acid residues), β2 with trypsin activity (cleaves basic residues) and β5 with chymotrypsin-like activity (cleaves non-polar residues) [58]. In addition, the proteasome rely on accessory proteins that aid in deubiquitination (DUBs), and activators that ensure unfolded proteins are correctly translocated to the 20S core for degradation (proteasome activators) [55].

In *P. falciparum*, most of the components of the proteasome were identified ad characterized [59], [60]. The proteasome has intrinsic role in *Plasmodium* viability, as parasites need to rapidly adapt to different hosts while going through several morphologic changes during its life cycle. Aminake et al, reported the expression of proteasome α and β subunits in all blood stages of the parasite, with continuously expression during sexual differentiation into gametocytes [61]. During the past twenty years, different groups around the world emphasized proteasome inhibitors as potent antimalarial agents, as these compounds showed the ability to kill *Plasmodium* at nearly picomolar doses [51], [62]–[66]. Not even Stage V gametocytes, known to be resistant to all antimalarial approved drugs but 8-aminochinolones, could escape the nanomolar effects of epoxomicin, proteasome inhibitor that was modified to become the FDA approved cancer drug, carfilzomib [51], [67]. Interestingly, proteasome inhibitors show potent synergistic activity when administrated with artemisinin and derivatives [68], calling even more attention to the potential of these compounds for development into new antimalarial drugs as they are also efficient killers of artemisinin resistant parasites [69]. The bottleneck of proteasome inhibitors for treating malaria is their poor selectivity for the parasite machinery over the human proteasome, leading to unwanted collateral effects and high toxicity. The search for selective parasite proteasome inhibitors has already begun and involves both public and private initiatives. Recent studies from Melbourne University together with Takeda pharmaceuticals identified MPI-1 as a compound with good selectivity towards *Plasmodium* β5 proteasome subunit. The same study also highlighted important amino acids that can improve selectivity against the parasite target [66], paving a way

for new strategies in designing *Plasmodium* specific proteasome inhibitors to be used in synergy with artemisinin, tackling resistance.

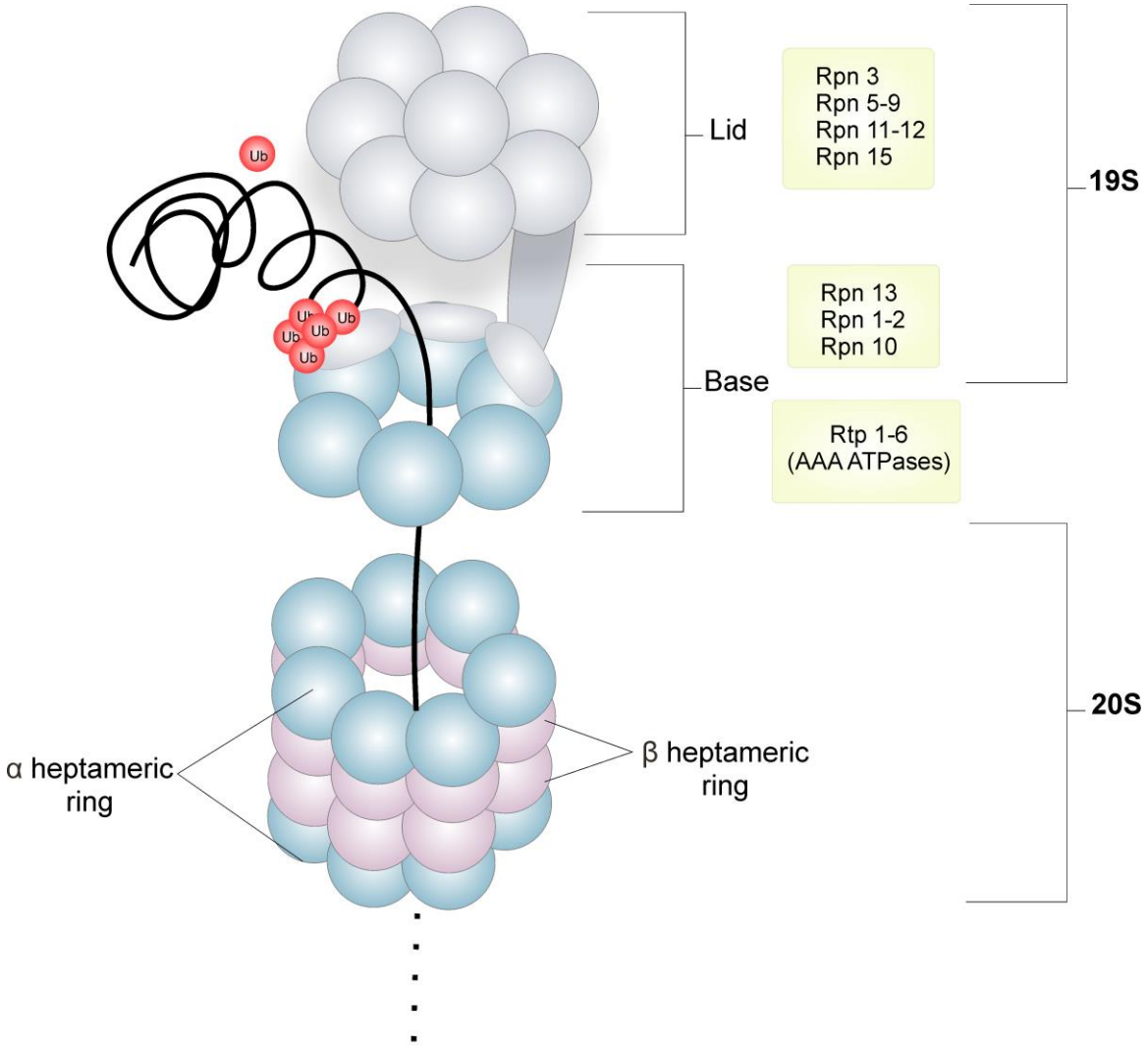

Figure 7. Composition of the 26S proteasome. The proteasome 26S possess three major compartments: one 20S proteolytic core composed by four heptameric rings (two α-rings and two β-rings) and two regulatory regions 19S (shown only one). The 19S conglomerate is subdivided into two sub complexes, the base that is composed by one ring containing six AAA-type ATPases and four non-ATPase subunits (Rpn1, Rpn2, Rpn10 and Rpn13), and the lid, which is composed by nine non-ATPase subunits: Rpn3, Rpn5-9, Rpn11-12 and Rpn15. The 20S core has proteolytic activity while the 19S complex is responsible for substrate recognition, deubiquitination, unfolding and α-ring gate opening.

1.4. Artemisinin: The resistant

"A handful of qinghao immersed in 2 liters of water, wring out the juice and drink it all". This sentence was written more than 1500 years ago in a Chinese medicinal handbook, A Handbook of Prescriptions for Emergencies, by Ge Hong, consisting in the only reference to the use of qinghao (Chinese name of *Artemisia annua L.)* to mitigate malaria symptoms [70]. What Ge Hong could not imagine is that more than a thousand years later, his ancient compilations would influence malaria treatment in a global scale.

After the rise of chloroquine resistance in the 80ths, attempts to eradicate malaria were unsuccessful [71]–[73]. The urgency to find new drugs to treat the disease led to the creation of a Chinese national project whose major goal was to find and isolate potential antimalarial compounds from Chinese traditional herbs. More than 2000 herbal preparations were tested for antimalarial activity without success until finally testing extracts from *Artemisia annua L.*, whose findings drove the isolation of the most important antimalarial drug from XXI century, artemisinin [70]. The characterization of artemisinin as an antimalarial rendered the researcher Youyou Tu the Nobel prize of Medicine in 2015 for its contribution to malaria control [15].

Unfortunately, a couple of decades later several groups reported delay in the clearance of *Plasmodium* infections upon artemisinin treatment in the Great Mekong Region [1], [12]–[14]. Drug cocktails composed by artemisinin and partner drugs are the main line of treatment to tackle *falciparum* malaria as a strategy to avoid resistance [1], [4], [5]; however, it has been reported failure of up to 50% in treatments based on combined therapies (ACT) in Southeast Asia [74]. Now, scientists around the world are trying to understand the biochemical pathways used by the parasite to block artemisinin's activity, together with the mode of action of artemisinin in a view to beat resistance.

Despite low nanomolar activity, artemisinin kills *Plasmodium* in a promiscuous fashion, being able to alkylate hundreds of different parasite proteins [75], [76]. As a pro-drug, ART is administered in an inactive state and is activated by the cleavage of its endoperoxide ring in a heam-dependent way [77]–[79]. Since young ring stage parasites do not digest haemoglobin (main haem source), drug activation on these stages is restricted to parasite haem biosynthesis [76].

The bioactive form of artemisinin, also called dihydroartemisinin (DHA), was shown to cause widespread damage in parasites resulting in accumulation of polyubiquitinated proteins and compromised protein synthesis. Proteostatic stress induced by DHA triggers *Plasmodium* unfolded protein response through activation of a modified mammalian-like PERK pathway, in which PK4 phosphorylates eIf2-α leading to shut down in protein translation [43].

Beside multiple protein damage, dihydroartemisinin functions as a partial proteasome inhibitor. Decreased proteasome activity explains accumulation of polyubiquitinated proteins and reinforces UPR activation by preventing removal of damaged proteins causing proteostasis collapse [43]. Yet, proteasome inhibitors show synergistic activity when administrated with artemisinin, being pointed as promising artemisinin partner drugs [66], [68]. Nevertheless, compounds that inhibit protein polyubiquitination strongly antagonize DHA activity despite proteasome inhibition, suggesting that ubiquitin shortage may play a role in artemisinin mode of action. In a similar way, Nedd8 inhibitor also antagonizes DHA activity, implying that cullin-3 might have important role in ubiquitinating substrates damaged by the drug activity [43]. Interestingly, ART resistant parasites show fewer polyubiquitinated proteins in relation to sensitive parasites. This data is complemented by higher levels of transcripts for chaperone systems found in resistant parasites collected from patients in Southeast Asia, highlights that improved unfolded stress response is intrinsic for resistance [42], [68].

Once resistance is reported, finding molecular markers on parasite's genome is important to track resistant spread. Few years ago, a group of scientists used whole genome sequencing approaches on artemisinin-resistant parasites from Africa and Cambodia and successfully found that mutations in Kelch propeller domain (K13) were associated with resistance [80]. The data was confirmed by many subsequent studies showing that PfKelch-13 mutant parasites had enhanced stress response when compared with their wildtype counterparts [81], [82], [68]. Interestingly, artemisinin resistance appears to be restricted to young ring stage parasites (0-3h post invasion). This can be explained by the fact that ART is not fully activated at this point, selecting parasites that are able to effectively respond to protein damage, which is less likely to

happen at later stages due to high amounts of free haem released from haemoglobin digestion resulting in complete drug activation.

In summary, both, ubiquitin proteasome system and unfolded protein response represent important parasite points of vulnerability, providing insights on new strategies for choosing artemisinin partner drugs for resistance surpass and highlight new pathways to be considerate for antimalarial drug design.

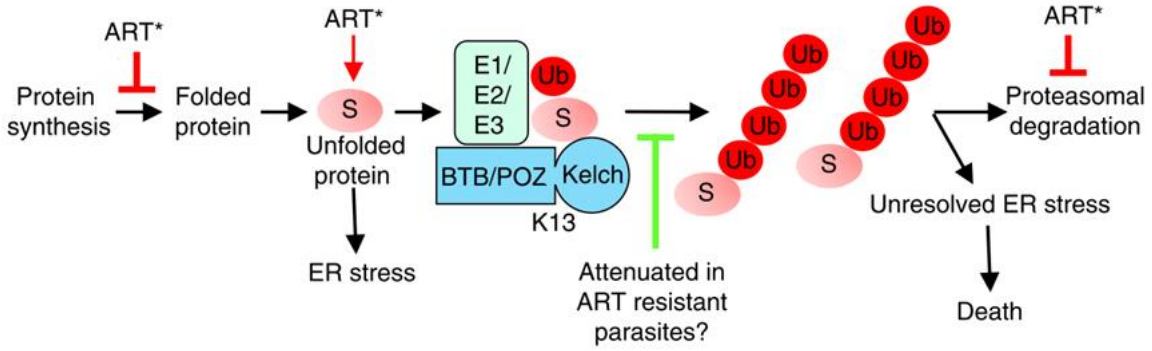

Figure 8. Artemisinin proposed mode of action (Adapted from Bridgford et al, 2018). Activated artemisinin (ART*) causes multi-target protein damage, including in proteasome, preventing unfolded/damaged proteins to be removed. Proteasome partial inhibition results in accumulation of polyubiquitinated proteins that unleashes the unfolded protein response culminating in proteostasis collapse.

1.5. Malaria and natural products: more than tea and tonic

In the last decades, the advance of synthetic chemistry made it possible to construct large libraries of synthetic compounds [83], marking a period in which natural products have been left aside due to difficult extraction and large-scale production. However, approximately one-third of the compounds approved by the FDA in the past thirty years (1981-2010) are of natural origin or are compounds derived from natural sources [84]; a relevant number when taking into account the size of natural libraries when compared to synthetic ones. As an example, until 2015 there were more than 22 million commercially available compounds in the ZINC database, in comparison with 160.000 natural compounds that could be found in the Dictionary of Natural Products [84]–[86]. Small organic molecules provide a great source of natural probes,

allowing us to unravel specific protein function, or important cellular pathways passive of being targeted for drug development.

Natural products hold a special place in history of antimalarial therapy. The use of the “sacred bark”, later known as quinine, molecule extracted from *Cinchona* bark tree, for antimalarial purposes happened almost 400 years ago, being documented by Jesuit missionaries in South America [87]. After its isolation by Pierre Joseph Pelletier and Joseph Caventou in 1820, quinine quickly became the most important antimalarial drug of 19th century (Figure 9) [88].

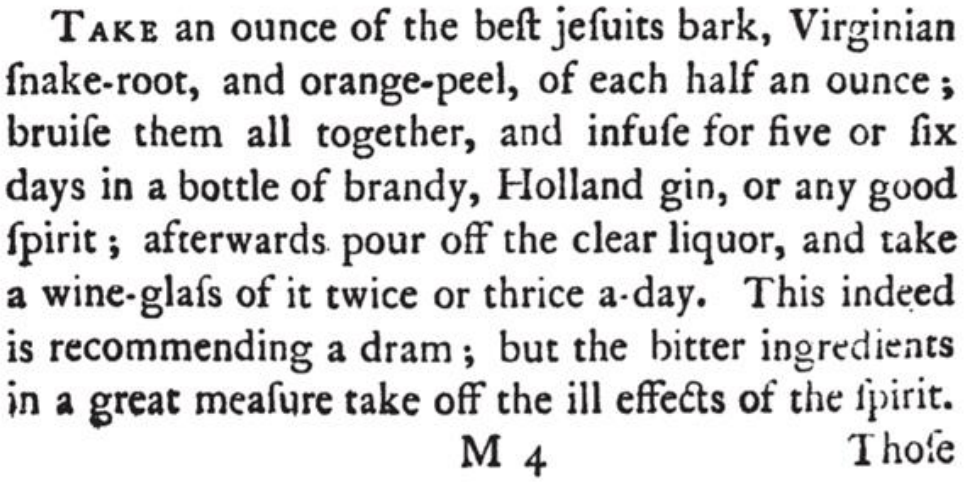
TAKE an ounce of the beſt jeſuits bark, Virginian ſnake-root, and orange-peel, of each half an ounce; bruiſe them all together, and infuſe for five or ſix days in a bottle of brandy, Holland gin, or any good ſpirit; afterwards pour off the clear liquor, and take a wine-glaſs of it twice or thrice a-day. This indeed is recommending a dram; but the bitter ingredients in a great meaſure take off the ill effects of the ſpirit.

M 4 Thoſe

Figure 9. Gin tonic old recipe (Adapted from Meshnick and Dobson, “The history of Antimalarial Drugs”, 2001). Text was reproduced with the permission of The Wellcome Institute Library, London, UK. Extracted from Buchan W. - Domestic Medicine: or, a Treatise on the Prevention and Cure of Diseases by Regimen and Simple Medicines. London: W. Strachan & T. Cadell, 1781.

Efforts to synthesize quinine failed, but led to the creation of “mauve”, the first synthetic textile dye. Importantly, mauve, also known as Methylene blue, was later used by Paul Ehrlich to treat malaria, making Bayern (so far a German dye company) one of the biggest pharmaceutical industries in the world [88]. In 1925, scientists from the big German pharma developed plasmoquine, the first compound capable of killing hypnozoits, avoiding *P. vivax* relapse. Plasmoquine, an 8-aminoquinolone, was created using methylene blue as a prototype and paved the way for the development of primaquine, the only drug used to treat vivax relapses nowadays [89].

During the Second World War, the Japanese cut off quinine's supply when they took control of Java Island, forcing the allies to raise efforts developing new antimalarial drugs. Inspired by the synthetic 8-aminoquinolones, scientists further developed 4-aminoquinolones and amino-alcohols, reaching the creation of the most important antimalarial ever, chloroquine [88], [90].

At late 40s, expressive results in malaria remission were achieved due to the concomitant use of DDT insecticide, for mosquito control, with chloroquine administration in patients carrying the disease [91]. With the rise of mosquito resistance against DDT, malaria control became a world top of concern [92]. Surprisingly, in the 50s, a malariologist from Brazil, Mario Pinotti, introduced the use of chloroquine in the common kitchen salt as a public health measurement to contain malaria resurgence. His method was worldwide known as "Pinotti's method", and quickly spread through endemic areas of the world [88], [93]. Unfortunately, with the emergency of chloroquine resistance in the 80s, scientists were once again pushed to come up with new antimalarial drugs, and once again, they found the "answer" in nature, with the discovery of artemisinin [70], [72].

Now, with the advance of artemisinin resistance, we are another time putting efforts to find and develop new antimalarials agents, vaccines and chemicals that may help us to discover a way to understand and overcome parasite's resistance, contributing towards malaria global elimination.

1.6. Violacein

In the past, the biological role of secondary metabolites was controversial. While some groups believed they were uncharacterized molecules that in a future time might present some functionality, others categorized them as cellular waste or detoxification products [94]. Today it is consensual that the secondary metabolism of microorganisms and plants are precious sources of new bioactive molecules [84]–[86], [90], [95].

Violacein is a natural purple hue compound produced by the secondary metabolism of gram-negative bacteria found in different parts of the world, ranging from glaciers to tropical waters and lands [96]. This bisindole molecule has its

biosynthesis extensively studied, and requires the condensation of two molecules of tryptophan with the help of five bacterial enzymes (VioABCDE) [97], [98].

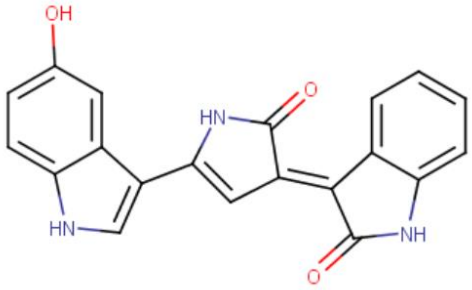

Figure 10. Chemical Structure of Violacein

Its characteristic color increased industry interest over violacein potential use as a dyeing agent. The bright purple hue has attracted attention of food and textile industries, due to consumers' preference for natural food colorants. Its stable pigmentation together with antimicrobial properties opened the possibility for the creation of naturally dyed fabrics without the use of organic solvents [97], [99]. Another function attributed to its color is the use of violacein-producing strains for the exploration of violacein production as a defense mechanism in the presence of bioactive compounds, termed as *quorum sensing* (visible chemical stress response) [100]. However, Violacein's function goes far beyond its attractive color, being widely known for its activity *in vitro* and *in vivo* against cancer cells [101]–[108] and pathogens such as viruses[109], bacteria [110], [111], fungus [112] and protozoans [98], [113]. So far, several groups published possible mechanisms by which violacein kills cancer cells [102], [104], [105], [107], [114]. In summary, violacein was reported to act differently according with the cellular type. HL60 (acute promyelocytic leukemia cell line) was shown to be highly sensitive to violacein treatment, exhibiting clear signs of apoptosis (chromatin condensation, nuclear fragmentation, apoptotic bodies) with increased caspase activities, possible triggering apoptotic events [105]. Another study went deeper on the mode of action of violacein on the same type of cell, proposing that violacein kills HL60 through the activation of TNF receptor-1, resulting in p38MAPK and caspase-8 activation together with upregulation of proinflammatory cytokines [114]. Interestingly, violacein caused decrease in total proteins and

decreased phosphatase activity in lymphocytes [104] and was proposed to kill chemoresistant TF1 leukemia progenitor cells through activation of endoplasmatic reticulum stress response [107]. Yet, another report showed that violacein induced apoptosis in breast cancer cells through down regulation of an E3 ubiquitin ligase MDM2, resulting in upregulation of p53 [115]. Interestingly, a recent study gave us important insights on violacein mode of action against gram-positive bacteria. According with Cauz and colleagues, violacein antibacterial properties are due to interactions with the different types of lipids from the cytoplasmic membrane, causing its disruption followed by cellular permeabilization [116]. However, violacein is able to kill plasmodium parasites at concentrations much lower than the ones required to induce haemolysis [113], which doesn't mean that the compound isn't interacting with lipids from RBC membrane but suggests that cellular permeabilization is not the cause of parasite death.

Regardless of great activity against several pathogens, one must always suspect that, especially when it comes to drug discovery and development, there is no such thing as a bonus without onus. Indeed, the line between violacein treatment and toxicity is blurred, as the compound presents narrow therapeutic window with a selectivity index of nearly 2 and 5 folds when we compare EC_{50} values from human hepatome cells and *P. falciparum* in relation with EC_{50} found for non-tumoral cells, respectively [98]. The poor selectivity of the compound for *Plasmodium* parasites also reflects *in vivo.* Violacein is shown to control malaria in mouse in a dose of 5mg/Kg/ day without compromise any visible changes in appetite or motor function of treated mice when compared with non-treated control groups (data not shown); yet, greatly impairment on both conditions were observed in mice treated with doses higher than that.

Despite clarifying contributions from several works to understand violacein mode of action, the activity against a different range of organisms provides a hint on impairment of a shared cellular mechanism between the distinct phylums affected. With the present work we intent to elucidate the mechanisms of action of violacein in *Plasmodium* and possibly link it with results found in literature for a better understanding on how this compound behaves to promote killing in different organisms.

2. Rational

Small organic molecules provide precious source of natural probes allowing us to unravel specific protein function and important cellular pathways passive of being targeted for drug development. Since the past 200 years, natural products hold a special place regarding malaria chemotherapy and control, with most relevant antimalarials being directly or indirectly derived from natural products.

Violacein is a natural purple hue produced by the secondary metabolism of gram-negative bacteria (e.g. *Chromobacterium violaceum*) found in different landscapes around the globe. Despite previous studies showing that violacein is able to kill blood stage *Plasmodium in vitro* and control malaria in mice, we decided to evaluate chemo-preventive and transmission blocking properties of the compound, testing it against other forms of the parasite cycle. Even though hundreds of studies reporting violacein activity *in vitro* and *in vivo* against cancer cells and distinct pathogens as viruses, bacteria, fungus and protozoans, a mechanism of action that fulfills violacein general toxicity against a wide variety of organisms remains unknown. With the rise of parasite resistance to all currently used antimalarial drugs, understanding the mechanism of action of compounds with antimalarial properties becomes a must in the actual scenario, in which the demand for new bioactive compounds are required to tackle malaria resistant parasites.

With the present work we intent to elucidate the mechanism of action of violacein in *Plasmodium,* paving a way for potential molecule development into a specific probe or future therapeutic compound.

3. Objectives

3.1. General Aim

3.1.1. To characterize violacein activity against different Plasmodium stages

3.1.2. Find essential pathways affected by violacein treatment in *Plasmodium.*

3.2. Specific Aims

3.2.1. Determine *P. falciparum* activity against sensitive Pf3D7 and chemoresistant *P. falciparum* strains, PfDd2 and PfW2;

3.2.2. Verify *P. falciparum* activity against specific asexual stages;

3.2.3. Evaluate violacein speed of action in *P. falciparum* strains *in vitro*;

3.2.4. Access violacein activity against *P. berghei* sporozoite infection in hepatocytes

3.2.5. Determine antimalarial activity of violacein against malaria sexual stages using *P. falciparum* NF54 gametocyte producing cell line and *P. berghei* Ookluc mutant parasites;

3.2.6. Use Chemical Genetic Profiling Technique in yeast as a starting point to track biochemical pathways affected by violacein treatment;

3.2.7. Design and perform biochemical assays to validate affected pathway.

4. Materials and Methods

4.1. Obtention of violacein

Violacein was purchased from Sigma-Aldrich (Janthinobacterium lividum V9389) or produced in an *E. coli* heterologous system [98]. Both sources possess minimum purity of 85% violacein.

4.2. *Plasmodium* spp. culture

P. falciparum sensitive strains (3D7) and multi-drug resistant strains (W2 and Dd2) were used in this study and cultivated at 37 °C in 1 % O_2, 5 % CO_2 and 94 % N_2 [117], [118]. Briefly, erythrocytes infected with *P. falciparum* were cultured in fresh human A+ erythrocytes (UNICAMP, Hemocentro, Brazil) and resuspended at final hematocrit of 5 % in parasite media (RPMI-Sigma-1640 complemented with 2g D-glucose [Lafan], 2 g sodium bicarbonate [Sigma, S5761], 50mg hypoxanthine [Sigma, H9636] and 40mg gentamicin [Schering-Plow] in 1 L milli-Q water) supplemented with 10 % human plasma homologue at pH 7.4. Parasitemia was monitored daily by thin blood smears stained with Giemsa (R66 solution Gurr #VWRC350864X) and slides visualized under an optical microscope [119]. Synchronized cultures were obtained by two consecutive treatments with 5 % solution of D-sorbitol (MP Biomedicals, 194742) at 48 h intervals, as described by Lambros and Vanderberg [120].

4.3. *In vitro* general susceptibility tests of *P. falciparum* asexual strains to violacein

Violacein susceptibility assays in *P. falciparum* were performed in 96-well plates with total volume of 200 µL/well, in which 50 µL composed different concentrations of compound of interest (plus non treated control) in complete parasite medium, and 150µL consisted on *P. falciparum* infected erythrocytes with 0.5% parasitemia at ring stage and 2% hematocrit in complete parasite medium. Chloroquine was used in parallel as standard for assay validation. Drug plates were incubated at 37 °C in 1 % O_2, 5 % CO_2 and 94 % N_2 atmosphere for 72 hours following the candle jar method previously described by W Trager, 1976 [121]. At the end of the incubation phase, plates were frozen at -20 °C for 24 h and subsequently defrosted

for SYBR green staining (1 hour with light protection) prior to plate readings at 483-530 nnm [122]. The Inhibition rate of the compound was determined comparing the concentration required to reach 50 % inhibition of parasite development (EC_{50}), relative to the control. The EC_{50} value was calculated by plotting a non-linear graph of logarithmic values of drug concentration versus inhibition (expressed as a percentage of the control).

SYBR green staining solution: 2.42 g Tris base (Sigma, 10708976001), 1.46 g EDTA (Sigma, E6758), 0.08 g saponin (Sigma, 47036), 0.8 ml Triton X-100 (Sigma, X100) complete solution with milli-Q water up to 1 L, add 0.4 µL SYBR Green 10.000x (Sigma, S9430) per mL solution.

4.4. Violacein Stage specific susceptibility tests of *P. falciparum* asexual strains

Asexual stage specific drug assays and morphology assays require highly synchronized parasites for unbiased experimental approach. Thus, parasites were cultured at standard conditions and hyper-synchronized with two rounds of 5 % sorbitol followed by 65 % percoll (Sigma, P1644) purification for schizonts enrichment. Schizonts were collected and re-incubated for 3 h to allow infected erythrocyte burst and merozoite invasion. After incubation period, parasite culture was sorbitol synchronized again for early-ring stage purification (0-3 h post-invasion). Once highly synchronized ring stage parasites were obtained, they were plated in a 96-well plate following same adjustments and treatments as described in 4.3, with exception that for ring stage susceptibility parasites 0-3 h post-invasion were incubated with drugs for 20 h and washed three times with parasite media prior to re-incubation for 48 h in complete parasite media (parasite media supplemented with 10% human A+ plasma). For trophozoite stage susceptibility assays, parasites 0-3 h post-invasion were incubated in the absence of drugs for 24 h until trophozoite maturation, and further treated with compounds of interest and controls for 20h. After treatment, drug was washed out after three subsequent washes prior to re-incubation for 24 h in complete parasite media. Drug plates were then frozen at -20°C for 24 h, and parasitemia was acquired as described in 4.3.

4.5. Violacein Speed of action

The speed of action of violacein was evaluated according to the protocol described by Le Manach and colleagues [123]. Briefly, we evaluated parasite growth departing from an asynchronous culture in the presence of violacein and control antimalarial compounds: artesunate (quick action) and pyrimethamine (slow action) [123]. *P. falciparum* 3D7 parasites were incubated in the same conditions described in 4.3, with the exception that 96 well plates were treated for 24, 48 and 72 hours (standard time for assay) with compounds of interest and subsequently frozen for 24 h at -20°C. Data was acquired according to the SybrGreen protocol previously described in this work.

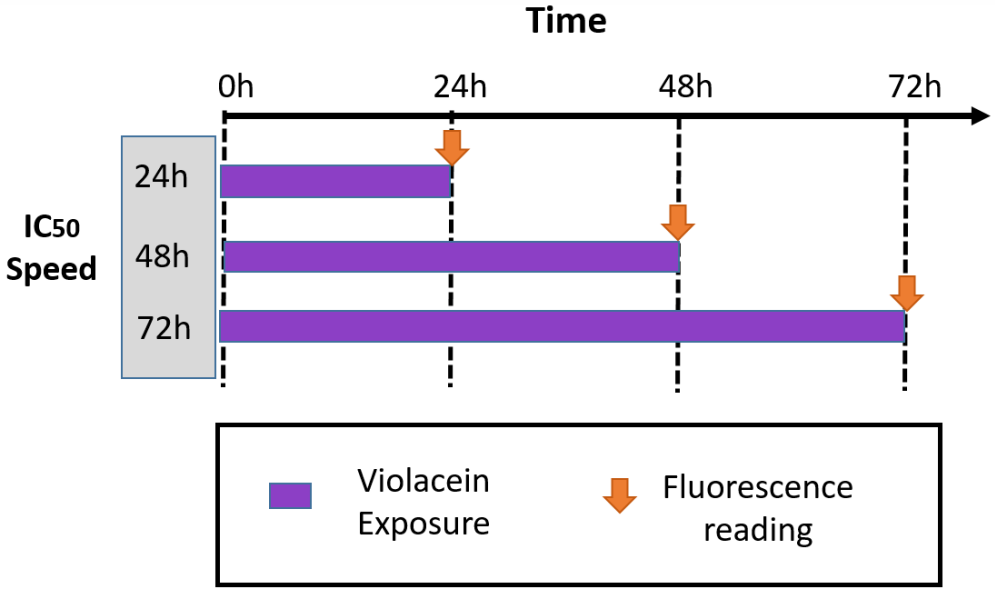

Figure 11. Schematic representation of *in vitro* violacein EC_{50} Speed assay (Adapted from Le Manach, 2013)

4.6. Violacein activity against liver stage parasites

For sporozoite susceptibility assays, Huh7 cells were seeded at $1x10^4$ cells/well of a 96-well plate in 100µL of RPMI medium supplemented with 10% bovine fetal serum at 37ºC, 5% CO_2 overnight. Cells were then incubated with vehicle drug control or different concentrations of violacein in triplicates. Dissected *Pb-Luci* sporozoites from the salivary glands of infected female *Anopheles stephensi* mosquitoes were added to drug treated cellular wells at a proportion of 1:1 ($1x10^4$ sporozoites/well), and centrifuged for 5 min at 1800xg, at room temperature prior incubation for 46 h at 37ºC,

5% CO_2. Compound cytotoxicity was assayed by measuring cell-confluency. For that, drug medium was removed from plate and 80 µL of a solution 1:20 AlamarBlue® (AlamarBlue®, Bio-Rad) prepared in complete RPMI cell medium was added to each well for 1 h 30 min at 37 ºC, 5% CO_2. Fluorescence was read in a plate reader at 530 nm excitation/ 590 nm emission. Infection rates and liver stage drug activity were measured by luminescence. Plate containing AlamarBlue® staining solution was washed and PBS 1x (washing solution) was quickly removed for subsequent addition and incubation of cell lysis buffer (70 µL/ well) for 15 min at room temperature in a 600 rpm shaker. Plate was centrifuged for 5 min at 1800xg to allow all the cell debris/membranes to deposit, and 30 µL of the lysed supernatant was transferred to a 96 nucleon flat white plate followed by subsequent addition of 50 µL/well luciferin solution. Luminescence measurements were read at three subsequent times and data was analyzed using GraphPad prism.

4.7. *In vitro* susceptibility test of *P. falciparum* gametocytes to violacein

High producing gametocyte PfNF54 strain was cultured following standard culture procedures previously described. Gametocytes were produced as showed by Dearnlay [124]. Briefly, culture containing mainly ring stage parasites (6-8 %) was 5 % sorbitol treated twice in intervals of 48 h for synchronization and enrichment of ring stages. Parasites were cultured until they reached ~10 % trophozoite stage and were further subdivided in four flasks containing parasite trophozoites with spent media supplemented with ¾ of fresh complete parasite media and enough non-infected RBCs for 5 % hematocrit adjustment. After this point, no RBCs were added and media was daily changed with pre-warmed complete parasite media solution supplied with 62.5 mM of N-acetyl D-glucosamine (Sigma, A8625) to inhibit merozoite invasion and asexual replication. Gametocyte development was visualized each second day through Giemsa smears and culture was purified through 65 % percoll gradient [125] when parasites reached Stage V maturation. At stage V, parasite culture was centrifuged at 800x g for 5 minutes, media was discharged and hematocrit was adjusted to 20 % with the addition of pre-warmed RPMI media without plasma. 2.5 mL of culture was carefully deposited into 9 mL of 65 % percoll solution, centrifuged at 1870x g for 10 minutes with no break and the gametocyte layer was collected, washed

twice in pre-warmed RPMI media and cultivated in complete parasite media overnight. On the next day media was changed, gametocytemia was assayed by Giemsa smears and a 10% gametocytemia solution in complete parasite media was plated in a 96-well plate at different drug concentrations with a final volume of 100 µL following candle jar incubation for 72 h. After drug treatments, 10 µL of AlamarBlue® (AlamarBlue®, Bio-Rad) staining solution was added to each well and plate was re-incubated for 24 h. After re-incubation time, plate was centrifuged at 1870x g for 5 minutes and 80 µL of supernatant was collected in a new 96-well plate prior to reading at 590/35 nm following excitation at 530/25 nm as described in [125]. The Inhibition rate of the compound was determined by comparing the concentration required to reach 50 % inhibition of parasite development (EC_{50}), relative to the control. The EC_{50} value was calculated by plotting a non-linear graph of logarithmic values of drug concentration versus inhibition (expressed as a percentage of the control).

4.8. *In vitro P. berghei* ookinete conversion inhibition assay

A modified *P. berghei* strain called Ookluc developed by Prof. Dr. Daniel Bargieri from University of São Paulo (USP) was used for violacein ookinete conversion inhibition assay. Ookluc is a mutant *P. berghei* that expresses a Nano-luciferase reporter gene (nLuc) under control of an ookinete specific promoter; thus, luciferase is only expressed in zygote stage reaching its highest light pic at ookinete stage. This experiment can be performed *in vitro* as gametocytes were previously shown to develop into ookinetes in the presence of ookinete medium in conversion assays [126]. Briefly, Balb/c mice were infected with *P. berghei* Ookluc mutant parasites and after four days, parasites were observed through blood smears for circulating gametocytes. The assay was performed in a 96-well plate containing 80 µL of ookinete medium (RPMI 1640, 25 mM HEPES, 50 mg/L of hypoxanthine and 1% of PSN – penicillin/ streptomycin/ neomycin, pH 8.3) supplemented with different concentrations of violacein and 4 µL of mice infected blood per well. After 24 h incubation at 21 °C, 64 µL of the supernatant is collected into another plate with the addition of 20 µL of nLuc substrate (*Nano-Glo® Luciferase Assay System - PROMEGA*) following manufacturer's instructions. After 5 minutes at 37 °C, plates were read in a luminometer, in which the increase of light corresponds to production

of nLuc and luciferase activity due to *in vitro* fertilization and gamete formation. The inhibitory effect of violacein in converting gametocytes to ookinetes was calculated as the percentage of luciferase activity reported on drug treated wells in relation to activity reported in controls [127].

4.9. Haploinsufficiency Chemical Genomic Profiling in Yeast

Haploinsufficiency Chemical Genomic Profiling (HIP) approach is based on the premise that yeast containing a gene expressed in heterozygosis will become hypersensitive to an inhibitor targeting the product of this gene. For this experiment, a collection of ~6000 yeast strains had one copy of each of the predicted *S. cerevisiae* open reading frames (ORF) replaced by an antibiotic resistance marker. Each cassette was flanked by 20-bp DNA barcode sequences, an "uptag" and a "downtag" unique to each of the deleted ORFs [128], [129]. These barcodes were themselves flanked by common known oligonucleotides allowing amplification of all "uptags" and "downtags" by the same primers (Figure 12).

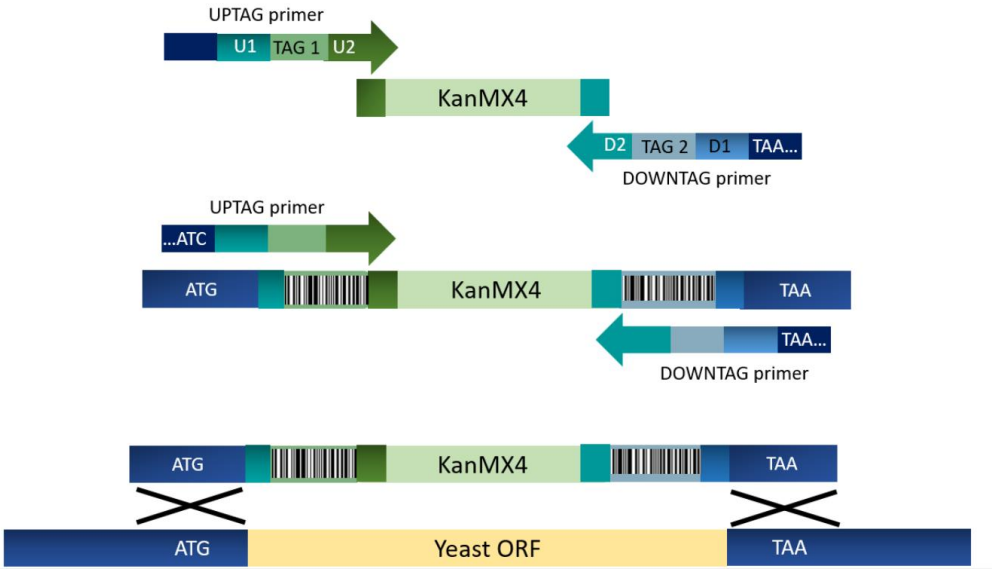

Figure 12. Schematic design of generation of Yeast Heterozygous Library through chromosomal Integration by homologous recombination

To determine which drug concentration to use in the chemo genetic screen, we performed a drug assay in wild-type BY4743 strain for 25 h starting with an OD_{595} of

0.1 and selected the concentration able to inhibit 20 % of growth of a wild type strain relative to control (EC_{20}) [130] . EC_{20} concentration was chosen due to its ability to affect yeast deletion strains measurably without unspecific toxic effects that occurs at higher concentrations (Pierce and colleagues, 2007). After determination of ideal concentration, pools of the 6000 barcoded heterozygous yeast strains were cultured in the presence of violacein or DMSO for 5, 10, 15 and 20 generations prior to genomic analysis. We selected triplicates of mutant pools grown under drug pressure or DMSO for 5 and 10 generations for genomic DNA extraction (Wizard® Genomic DNA Purification Kit, Promega). The selected material was sent to a genomic sequencing center, Centro de Sequenciamento Genômico da Universidade de São Paulo/ ESALQ, for barcode sequencing (Figure 13).

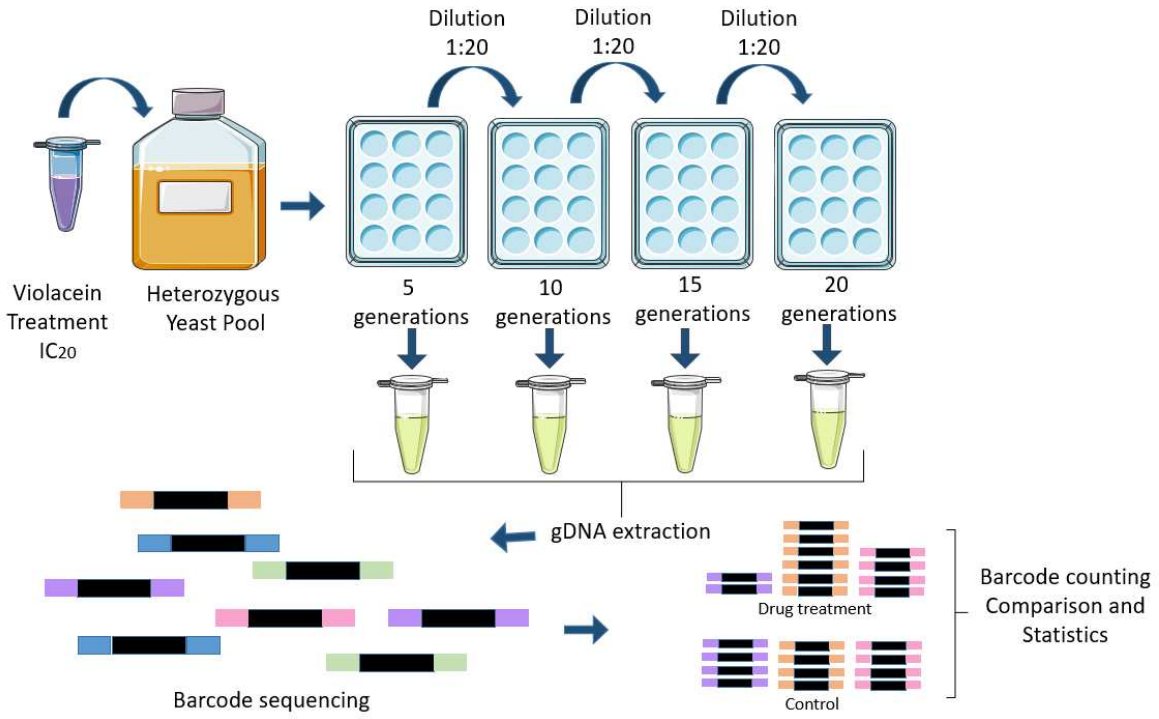

Figure 13. Schematic representation of Haploinsufficiency Chemical Genomic Profiling in yeast model.

Data obtained from Illumina sequencing were subsequently sent for analysis and processing for barcode quantification at LGE, Laboratório de Genômica e Expressão/ UNICAMP. The barcode sequencing (barcode-seq) pre-processing

started with evaluation of the quality of reads generated through the tools FastQC (version 1.6), written by Simon Andrews at the Babraham Institute (for more information see www.bioinformatics.babraham.ac.uk/projects/fastqc) and MultiQC (version 1.6) [131]. Then, adaptors from the primers sequences were removed using Cutadapt (version 1.16) [132]. At this step, primer sequences with insertions and deletions were not allowed and pairs of unprocessed reads were discarded (options –no—indels, --dischard-untrimmed). The resulting sequences were again analyzed with FastQC and MultiQC in order to evaluate the removal efficiency of the primers and adapters. No sample had post-removal adapter contents, and most reads had a 20-basepair size (bp), which is the expected size of the barcode sequence. Single read clustering was done from the identification of amplicon sequence variants (ASV) with the DADA2 denoising algorithm (version 1.9.1) to discard those with more than one expected error (maxEE = 1), quality score less than 2 (minQ = 2) and size smaller than 16 bp or greater than 21 bp (minLen = 16, maxLen = 21). Next, the parameters of the error models were obtained by alternating the sample interference with the parameter estimation until convergence was reached [133]. After base pair denoising, clustered dereplicated reads and error models from all samples were used as input data for the function DADA (options OMEGA_A = 1e-40, BAND_SIZE = 10, USE_KMERS = TRUE, VECTORIZED_ALIGNMENT = TRUE, GREEDY = FALSE, GAPLESS = FALSE). The pairs of reads with a minimum overlap of 10 bp and no mismatch were then fused to obtain the ASVs. In total, DADA2 identified 8395 ASVs, of which 4112 corresponded perfectly to any of the 6337 known barcodes sequences. It was allowed that ASVs with Levenshtein distance of up to 2 were assigned as barcodes with greater similarity. Thus, 5447 ASVs, corresponding to 5405 barcodes, were taken for subsequent analyzes. Finally, the array containing the number of reads per barcode has been updated to replace each barcode sequence by its corresponding mutated ORF code that it represents. Finally, DESeq2 package (version 1.20.0) was used to normalize the barcodes counts and to estimate the differential abundance between treated samples and their respective controls [134]. A filter was further established to remove the barcodes with low count along the samples (less than 10 observations in triplicate). Differentially depleted barcodes were identified using a maximum likelihood ratio test ("LRT"), which consists of a

generalized linear model in which the number of observations of a given barcode is described by a negative binomial distribution whose average is given by the treatment. The normalization between samples was done by the library size factor method, using only ASVs with number of observations greater than zero. Barcodes differentially expressed in the comparisons between treatment and control were considered significant (hits) for p-value <0.001 and log2 fold change <0 [135], [136].

4.10. Cell lysate analysis by Western Blotting

Western blotting lysates were prepared from a culture of 5 % trophozoite at 5 % hematocrit treated with different concentrations of compounds for three hours at 37 °C, as described in the figure legends. For anti-ubiquitin assays, cell pellets were washed twice with cold PBS 1x supplemented with EDTA-free protease inhibitor cocktail (Roche) and 20 mM N-ethylmaleimide (Sigma). In sequence, pellet was incubated with 0.15 % (w/v) saponin in cold PBS for 10 minutes on ice, allowing release of erythrocyte cytoplasmic content, and subsequently washed with PBS twice to remove saponin. For experiments using GFP-DD mutant parasites, 5 % trophozoite culture at 5 % hematocrit as subjected to different drug treatments for three hours. Parasites were then isolated with 0.05 % (w/v) saponin and pellet was washed three times with PBS supplemented with EDTA-free protease inhibitor cocktail (Roche). Parasite pellets were next solubilized in SDS-PAGE on a 4-12 % Bis-Tris acrylamide gel (Life-Technologies) using MES or MOPS running buffer and transferred to nitrocellulose membrane (iBlot; Life Technologies). For ubiquitin western blotting, membranes were boiled in mille-Q water for 10 minutes prior to one hour blocking in 3.5 % skim milk, to improve poly-ubiquitin detection. After blockage, membranes were probed with primary antibodies of interest: mouse anti-GFP (Roche; 1:1000), mouse anti-Pf-BiP (1:1000), rabbit anti- ubiquitin (Dako-Z0458; 1:1000); rabbit anti-phospho-eIf2-α (Cell signaling Technology- 119A11; 1:1000); mouse anti-eIf2-α (Cell signaling Technology- L57A5; 1:1000), rabbit anti- GAPDH (1:1000) and secondary antibodies: goat anti-rabbit IgG-peroxidase (Sigma-Aldrich-A0545; 1:20.000) and goat anti-mouse IgG-peroxidase (Chemicon-AP127P; 1:20.000). Bio-Rad ChemiDocTM MP imaging system was used for detection of chemiluminescence.

4.11. GFP fluorescence measurement using flow cytometry

GFP-DD mutant parasites, 5 % trophozoite cultures at 5 % hematocrit was subjected to different drug treatments for three hours as indicated in figure legend. Parasite samples were stained with 2µM SYTO-61 for 20 minutes and adjusted to 0.1 % hematocrit in PBS for plate reading using FACSCantoTM II cytometer (Becton Dickinson). Fluorescence signals were analyzed in FlowJo (version 10), in which parasites were gated based on SYTO-61 signal and parasite GFP fluorescence was reported as mean fluorescence values. Data were fit by non-linear regression and plotted by GraphPad Prism Software (version 5).

4.12. HSP90 homology modeling and molecular docking

The 3D structure of heat shock protein 90 of *P. falciparum* (*Pf*HSP90, ID: 3K60), as well as human HSP90 (hHSP90, ID: 4YKQ) and PP5 (hPP5, ID: 4ZVZ) were extracted from Protein Data Bank (PDB) [137], [138]. Considering the absence of 3D structures for serine/threonine protein phosphatase of *Plasmodium falciparum* (*Pf*PP5) in PDB, its amino acid sequence (ID: Q962N7) of was retrieved from the UniProt database and used as target for homology modelling in the SWISS-MODEL server [139], [140]. Then, the loop or terminus regions of homology model were refined using GalaxyWEB server .[141] Lastly, the structure reliability of the refined model was evaluated by using MolProbity server [142], [143]. The 3D structure of violacein was drawn in MarvinSketch v.6.3.1 (ChemAxon, Budapest, Hungary, http://www.chemaxon.com) and their protonation and tautomeric states were predicted at pH 7.0 ± 1.0. Subsequently, up to 100 conformers were generated using OMEGA v.3.0.0.1 [144], and the AM1-BCC charges[145] were added using QUACPAC v. 1.7.0.2 (QUACPAC 1.7.0.2: OpenEye Scientific Software, Santa Fe, NM. http://www.eyesopen.com.). In parallel, protonation states of amino acid residues of investigated proteins were predicted using H++ server at neutral pH (7.0 ± 1.0) [146]. The prepared proteins were next submitted to the grid-generation protocol using two strategies for binding pocket detection. In the first strategy, grids were generated using a molecular probe available on OEDocking suite v.3.2.0.2 for detection of binding pockets around the protein. In the second strategy, co-crystallized ligands were considered geometric centers of the grids (Grid details are available in Table 4).

Finally, molecular docking calculations were performed using the high-resolution protocol of FRED program, available on OEDocking suite. [147], [148].

4.13. Recombinant protein expression and purification

Recombinant PfHSP90 protein (XP_001348998.1) and PfHSP70-1 protein were expressed by the synthetic expression vector pET28a::PfHSP90 and pET28a::PfHSP70-1 respectively, commercially obtained from Epoch Life Science Inc. (Missouri City, Texas, USA). Both recombinant proteins, PfHSP90 and PfHSP70-1 were expressed in *E. coli* BL21(DE3) pRARE, grown in LB medium containing 35 µg/mL kanamycin until OD_{600} nm ≈ 0.6-0.8, where 0.4 mM IPTG was added and the temperature set to 20 °C. After 18 h, cells were pelleted by centrifugation and lysed as described for the recombinant Pfp23 proteins. Recombinant proteins were purified using Ni2+ -affinity chromatography, followed by preparative size exclusion chromatography using a Superdex 200 26/60 column in 40 mM HEPES (pH 7.5) buffer containing 100 mM KCl. The purity of all steps was assessed using 10 % SDS-PAGE, and the His-tag on the recombinant proteins were kept. The protein concentration was determined through spectrophotometry using the calculated molar extinction coefficient (ε) for denatured proteins estimated using SEDNTERP software (http: //www.jphilo.mailway.com/download.htm).

4.14. Circular Dichroism for HSP90-violacein interactions

The Circular Dichroism (CD) Spectropolarimetry experiments were performed using a Jasco J-815 spectro-polarimeter (Jasco, Inc). The distant CD was done using a buffer of 12.5 mM Tris-HCl (pH 7.4), 50 mM NaCl, 1 mM EDTA and 0.5 mM β-mercaptoethanol, in a 0.2 mm cuvette optical path and a PfHSP90 concentration of 2.5 µM with or without 30 minutes pre-incubation of equimolar concentrations of violacein. All spectra were collected in a Jasco J-815 spectro-polarimeter (Jasco, Inc), under temperature control by a peltier system and the wavelength ranges of collection for CD in far UV were 260 to 190, respectively. The values generated by the CD curves were converted to ellipticity molar ratio ([θ]). The equation is given below:

$$[\theta] = \frac{\boldsymbol{\theta x 100 x MM}}{\boldsymbol{C x l x n}}$$

Where [θ] is the mean residual molar ellipticity (in degrees cm 2. dmol-1), MM is the molecular weight of the protein in kDa, C is the protein concentration (mg / mL), l is the optical path in cm and n is the number of amino acid residues of the protein. Dichroweb Software (available at: http://dichroweb.cryst.bbk.ac.uk/) was used for spectra deconvolution.

4.15. Differential Scanning Calorimetry for HSP90-violacein interactions

Differential Scanning Calorimetry (Differential Scanning Calorimetry (DSC) is a technique used to measure the thermal properties of materials establishing a link between the specific physical properties of molecules and the temperature. In general, the DSC measures the thermal capacity (Cp) that is released or absorbed by the sample on the basis of a temperature variation. This technique makes it possible to estimate conformational transitions in macromolecules as well as comparing different thermal stabilities [149]. A parameter easily estimated by the DSC is the Tm of a protein, i.e., the average temperature at which half of the protein molecules are coiled and half unraveled. The value of Tm indicates the thermal stability of the macromolecule, that is, the greater the value less susceptible to thermal uncoiling the biomolecule is. The technique was performed on the Nano DSC (TA Instruments), the buffer 25 mM Tris-HCl (pH 7.4), 100 mM NaCl and 2mM EDTA. PfHSP90 proteins were exhaustively dialyzed, and the concentration used for PfHSP90 was 1.0 to 1.4 mg /mL. The thermal range was 20-90 °C, the temperature being elevated in rate of 1 °C / min. The thermograms of protein pre-incubated or not with a concentration 5 times higher of violacein were collected in the DSC-Run software (TA instruments) and data processing was performed in Launch NanoAnalyze software.

4.16. ATPase activity Assays

The inhibition test of both, PfHSP90 and PfHSP70-1, ATP hydrolysis activity was verified under different concentrations of violacein. The entire test was performed on a 96-well microplate and samples were prepared in 40 mM HEPES buffer (pH 7.5) supplemented with 100 mM KCl. The concentration of PfHSP90 and PfHSP70 used was 2μM, which was incubated for 30 minutes in the refrigerator in the presence of 2mM $MgCl_2$ under different concentrations of violacein (proportions protein-violacein are described on figures 28 and 34). To this solution, 1 mM of ATP was added, and

this was again incubated in water bath for 30 minutes at 37 °C. It is important to say that for this test there was no His-tag cleavage for neither PfHSP90 or PfHSP70-1 proteins. After the reaction, the solution was incubated with the PiColorLock ™ Gold kit Phosphate Detection System (Innova Biosciences) for 30 minutes. This kit is based on in a colorimetric reaction, which changes color in the presence of Pi (free inorganic phosphate) due to alterations in absorbance of malachite green dye, induced by the formation of phosphomolybdate complexes. In this way, this reaction allows measurements of Pi released, which will be proportional to the hydrolysis rate of ATP. A standard curve with increasing known values of free phosphate provides an indirect data that correlates color and Pi concentration. After incubation, experiment readings were done in Varioskan TM LUX multimode microplate reader (Thermo Fisher Scientific), with absorbance measurements performed in a range of 590 to 650 nm.

4.17. Aggregation prevention Assays

The molecular chaperone activity of PfHSP90 and PfHSP70 was tested as described by Seraphim and colleagues [150] for their ability to prevent thermal stress aggregation of the client protein model Malate dehydrogenase (MDH), from pork heart (Porcine heart SIGMA M2634). The two chaperones had their ability to avoid protein aggregation assessed in the presence or absence of violacein. In this test, 1 µM of the client protein was subjected to a thermal stress of 42 °C for 3 hours, in the absence or presence of PfHSP90 or PfHSP70 chaperones pretreated or not with equimolar dose of violacein for 30 minutes. The experimental procedure was performed in a 96-well plate and protein aggregation was measured by the readings of light scattering signal at 320 nm in the Varioskan TM LUX multimode microplate reader (Thermo Fisher Scientific). All experiments were performed in the Chromatography buffer of Molecular Exclusion. As control we performed experiments containing only the model client protein, to verify the rate of aggregation of this protein in the absence of chaperones. The effect of violacein on the model protein was also evaluated under thermal stress.

4.18. *Plasmodium* TRiC-ϴ knockdown Assays

Chemical-regulatable TRiC-ϴ knockdown parasites were kindly donated by Natalie Spillman, from Melbourne University, for this work. Parasite culture was performed as described by Spillman and colleagues [151]. Briefly, mutant parasites were cultured at same conditions as described on item 4.2, in complete parasite media supplemented with 0.5 µM anhydrous tetracycline (aTc), for parasite growth expressing wild type ratios of TRiC chaperonin complex. To examine if PfϴTRiC knockdown strains were more sensitive to violacein than parasites with normal expression of PfϴTRiC, we performed a violacein dose-response curve in both parasite culture to see if we could find any shift in EC_{50} concentration. Because of impairment on invasion and ϴTRiC knockdown parasite inability to develop into next cycle, we opted to perform drug assays within the same cycle. Thus, highly synchronized ring stage parasites cultured in complete parasite media supplemented with 0.5 µM aTc (~8 h post invasion) were submitted to 3 rounds of incomplete parasite media washes with intervals of 10 minutes each wash, to allow aTc culture removal. Culture was then split and re-cultured for 20 h until in two different flasks, one containing 0.5 µM aTc and the other without aTc, allowing PfCCT-ϴ mRNA degradation and parasite chemical induced TRiC-ϴ knockdown phenotype. Once parasites reached desired trophozoite maturation, each parasite culture was plated in a 96-well plate under different concentrations of violacein for 3 h preserving previous aTc culture conditions (same variables described on item 4.2). After drug incubation, plates were next washed 3 times in incomplete parasite media, and parasite pellets were resuspended in 180 µL of warm 1x PBS. Trophozoites were subsequently incubated for 10 minutes with the fluorescent dying agent, Rhodamine 123 (Sigma), in a final concentration of 1 µg/mL, for mitochondrial staining as described by Pratt Riccio and colleagues [152]. After mitochondrial staining, plates were washed 3 times in warm 1x PBS prior to flow cytometry plate readings. To quantify whether removal of aTc resulted in PfTRiC-ϴ knockdown, clones B8 and A3 were tightly synchronized, young rings (~ < 8 h post invasion) were washed (3 x 5 min washes in media without aTc). Cultures were then plated with or without 0.5 µM aTc and grown for 20-24 h. Lysates of the total soluble fraction were processed for WB, as described before on item 4.10.

5. Results and discussion

5.1. Violacein sensitive and chemoresistant parasites *in vitro* activity

Violacein was previously shown by our group to have activity against sensitive and chloroquine resistant strains, as well as to control malaria *in vivo* [113]. However, to validate the quality of violacein obtained by our *E. coli* heterologous system [98], we re-tested its activity against *P. falciparum* sensitive strain (Pf3D7) and two chloroquine resistant parasites: PfDd2 and PfW2. Nearly 15 years ago, scientists discovered that mutations on parasite gene *Pfcrt* was related with chloroquine resistance through genomic comparisons between a chloroquine resistant clone PfDd2, from Indochina, and a sensitive strain H3B, from Honduras [153]. Both parasites, multi-drug resistant cell lines, W2 and Dd2 were originated from III/CDC field isolate parasite from Indochina, which contain point mutations in *Pfcrt* and *Pfmdr1*, genes encoding two digestive vacuole membrane transporters [154]. While PfCrt plays a role on drug efflux, PfMdr1 seems to be important for compound import to digestive vacuole [155]. Chloroquine is known to bind ferroprotoporphyrin IX, impairing its conversion to non-toxic β-hematin, poisoning parasite with its own toxic waste derived from haemoglobin degradation. Importantly, as a weak base, CQ is able to freely cross membranes on its neutral form, accumulating at high concentrations inside parasite's acidic digestive vacuole (DV) following Henderson-Hasselbach chemical equilibrium. Parasites carrying mutations on *Pfcrt* membrane transporter gene has significant less amount of drug inside DV, due to its ability to transport protonated CQ upon losing positively charged lysine on its helical structure [156]. Several antimalarial drugs have similar mode of action as chloroquine, thus, mutations on these genes easily confer resistance to other drugs known to accumulate in DV impairing haem conversion to haemozoin, as lumefantrine, quinine, amodiaquine, mefloquine and halofantrine [216]. Importantly, violacein showed EC_{50} values that match literature, confirming that the quality of our compound was at the same range as the one found for commercial violacein (>85% purity) [98], [113]. Similar activity was reported against the three strains tested (Table 1). This data reinforces that this compound is toxic to the parasite through a mechanism that does not involve digestive vacuole membrane transporters (Figure 14).

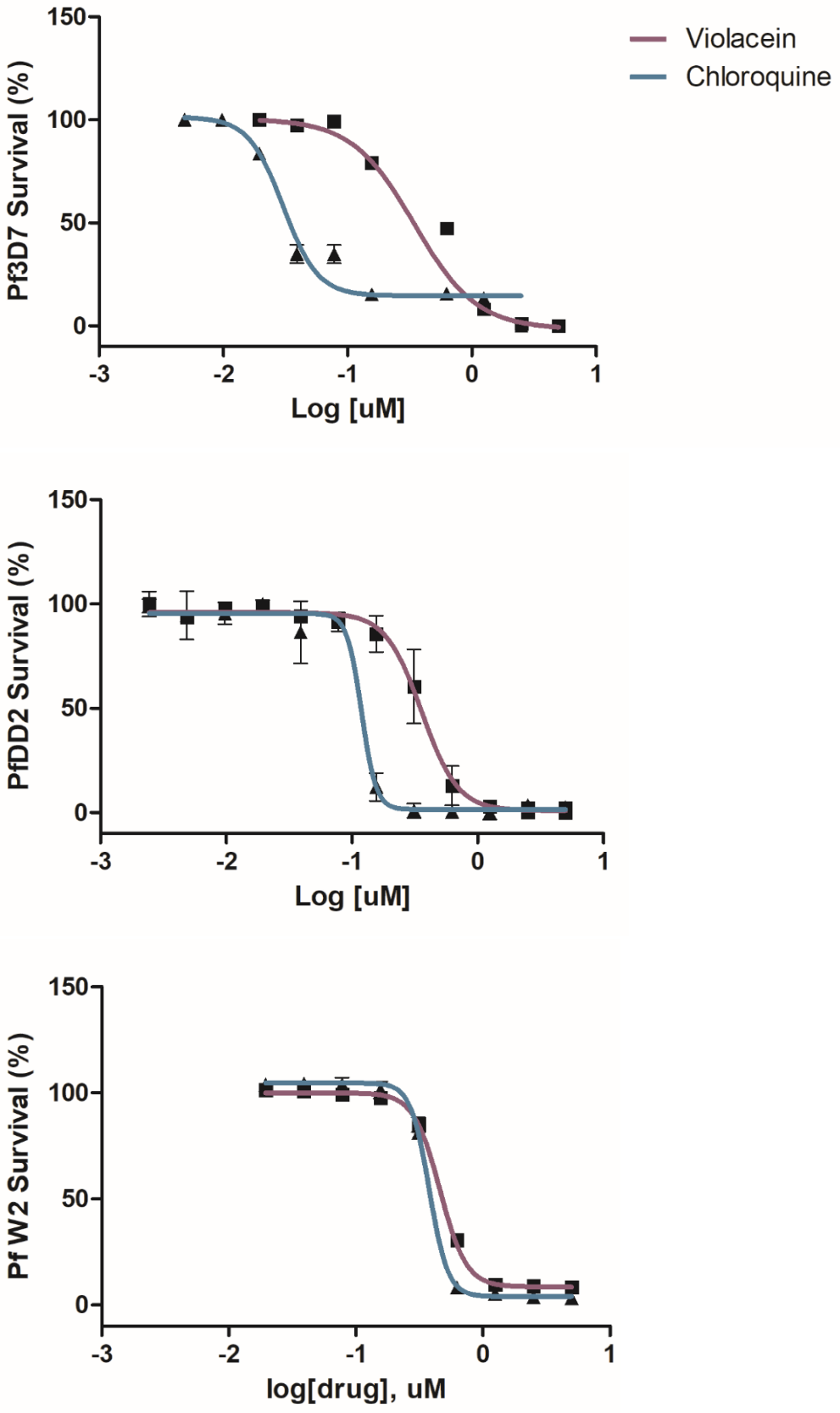
Violacein
Chloroquine
Pf3D7 Survival (%)
150
100
50
0
-3
-2
-1
0
1
Log [uM]
PfDD2 Survival (%)
150
100
50
0
-3
-2
-1
0
1
Log [uM]
Pf W2 Survival (%)
150
100
50
0
-3
-2
-1
0
1
log[drug], uM

Figure 14. ***P. falciparum in vitro*** **growth curves upon violacein treatment**. *In vitro* growth curves of *P. falciparum* sensitive strains (3D7) and resistant (Dd2 and W2) to chloroquine (A, B and C, respectively). 3D7- violacein EC_{50}: 0.5434 µM ± 0.03466, Chloroquine EC_{50}: 0.02410 µM ± 0.001661; Dd2- violacein EC_{50}: 0.43 µM ± 0.1, Chloroquine EC_{50}: 0.12 µM ± 0.005; W2- violacein EC_{50}: 0.42 µM ± 0.01, Chloroquine EC_{50}: 0.54 µM ± 0.04.

Table 1. Antiplasmodial activity of violacein

	Antiplasmodial activity µM (EC_{50}± SE)		
Compound	Pf3D7	PfDd2	PfW2
Violacein	0.5434 ± 0.03466	0.4321 ± 0.1236	0.4287 ± 0.01415
Chloroquine	0.02410 ± 0.001661	0.1211 ± 0.005150	0.5468 ± 0.03928

5.2. Violacein stage specific activity

All commercially available antimalarial drugs have more activity against trophozoite stages rather than rings during the erythrocytic cycle of the disease. That can be explained by their similar mode of action dependent upon haem degradation for drug activation (artemisinin and derivatives) or upon inhibition of haem conversion into inert crystals of haemozoin (chloroquine, lumefantrine, amodiaquine, quinine, mefloquine and halofantrine). Yet, trophozoites are more metabolically active than earlier stages, with intense protein synthesis, several of which are expressed mostly or exclusively at this stage [157].

Violacein is not an exception for this behavior, showing to be more active against trophozoite stages (Figure 15). However, despite similar preference for killing later stages of *P. falciparum,* when compared to other antimalarials violacein seems to present a different mode of action due to its ability to kill multi-drug resistant parasites at same dose as it kills sensitive 3D7 parasites (Figure 14).

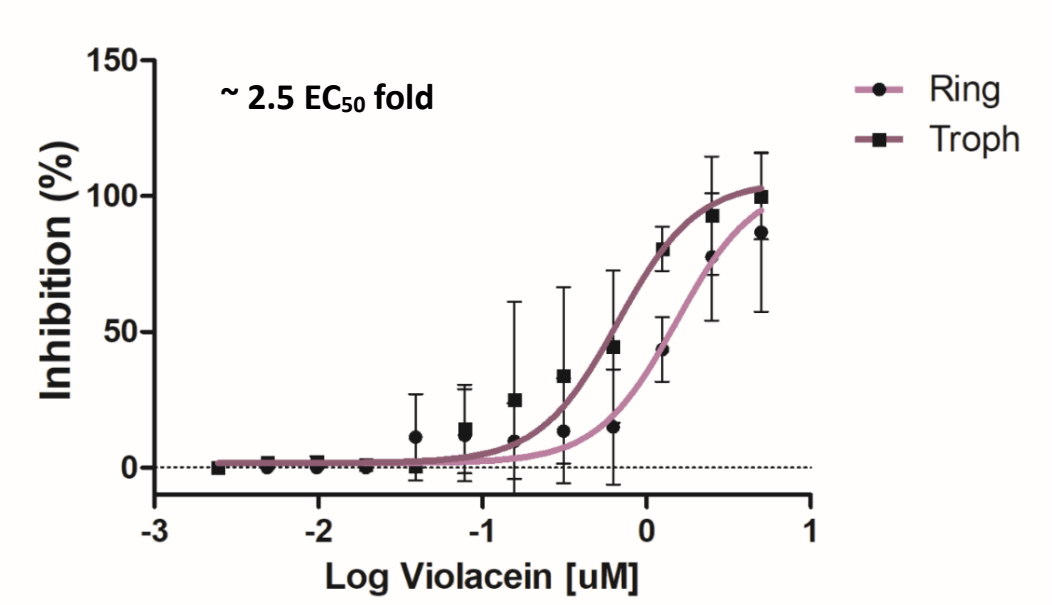

Figure 15. Violacein stage specificity within asexual parasites. Highly synchronized 3D7 parasites were tested against different doses of violacein at early ring stage (0-3 h post invasion) for 20 h or at early trophozoite (23-26 h post invasion) for 20 h of drug exposure.

5.3. Violacein speed of action

Importantly, the mode of action of a compound can give us a hint regarding its speed of action. In the case of artemisinin, despite completely activation by haem endoperoxide cleavage at trophozoite stage, parasite endogenous haem biosynthesis is enough to activate the drug sufficiently to kill both rings and trophs at similar EC_{50}, this data explains why ART and derivatives are considered fast antimalarial drugs [123], [158]. Pyrimethamine for instance, is a folic acid antagonist; its mechanism of action is based on the inhibition of dihydrofolate reductase, blocking parasite biosynthesis of purines and pyrimidines. Not surprisingly, pyrimethamine is a slow killing drug, acting at schizonts stages that require nucleic acid synthesis for the development of merozoites [159]. Interestingly

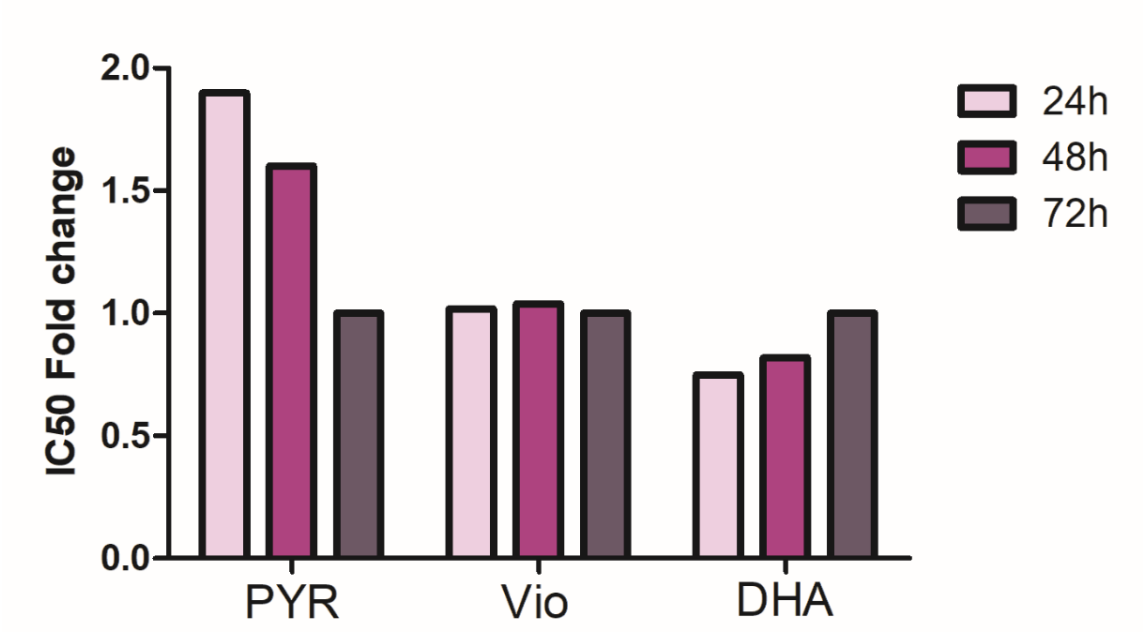

Figure 16. Violacein speed of action. Assynchronized 3D7 parasites were tested against violacein during different times, 24 h and 48 h for determination of EC_{50} fold changes in relation to EC_{50} determined at 72 h. Pyrimethamine (PYR) and dihydroartemisinin were used as controls for slow and fast killing compounds respectively. Data representative of one experiment.

5.4. Violacein liver stage activity

Malaria infection in humans' starts within the liver, when sporozoites released into bloodstream during mosquito blood meal reaches the liver parenchyma, infecting hepatocytes. Despite the importance of strategies targeting liver stage parasites for malaria vaccine development [160], [161], the majority of drug discovery approaches tackles the symptomatic phase, with nearly the totality of commercial drugs being active exclusively against blood stage parasites [162]. Not even chloroquine, nor artemisinin, drugs considered gold standard in malaria treatment, have activity against liver stage parasites [162]. In the past, only compounds with good EC_{50} values against erythrocytic stages are tested across hepatic parasites [163], probably due to laborious manual work required for mosquito dissection to collect reasonable amount of sporozoites [164]. However, this standard drug discovery pipeline ends up limiting transmission blocking and chemo preventive strategies for disease control policies, as many molecules active against liver stage have different drug scaffolds and putative targets from known antimalarial drugs [165]. Thus, there is no correlation

between activity against blood and hepatic parasites. For that reason, despite an EC_{50} of ~400 nM against symptomatic forms, we decided to test if whether violacein also possess liver stage activity.

Violacein activity against liver stage parasites were performed in collaboration with Prof. Dr. Pedro Cravo, from New University from Lisbon, Portugal. For this experiment, human hepatome cells (Huh7) were seeded until confluency, treated with violacein and subsequently incubated for 46 h with *P. berghei* sporozoites, expressing luciferase (Pb- Luci), previously collected from salivary glands of infected *Anopheles stephensi* mosquito [166]. Cellular confluency and parasite infection after drug treatment were measured through AlamarBlue® and luciferin solution readings respectively and atovaquone was used as a control. As shown in Table 2, violacein has low-mild activity against liver stage parasites, with an estimated EC_{50} between 1-2 μM, two to four times higher than the one obtained for asexual blood stages. At concentrations above 2 μM we can observe an effect of the compound on cell confluency, which can be attributed to violacein antitumor properties (Figure 17).

Table 2. Liver stage activity of violacein

	Liver stage activity (% ± SE)	
Compound	Huh7 Confluency (%)	Infection (%)
Violacein 0.5 μM	107.4 ± 0.9	75.4 ± 10.4
Violacein 1 μM	124.2 ± 7.5	54.9 ± 4.3
Violacein 2 μM	89.8 ± 13.9	40.8 ± 6.0
Violacein 5 μM	23.2 ± 2.3	2.7 ± 2.6
Atovaquone 10 nM	115.7 ± 4.3	1.4 ± 0.7

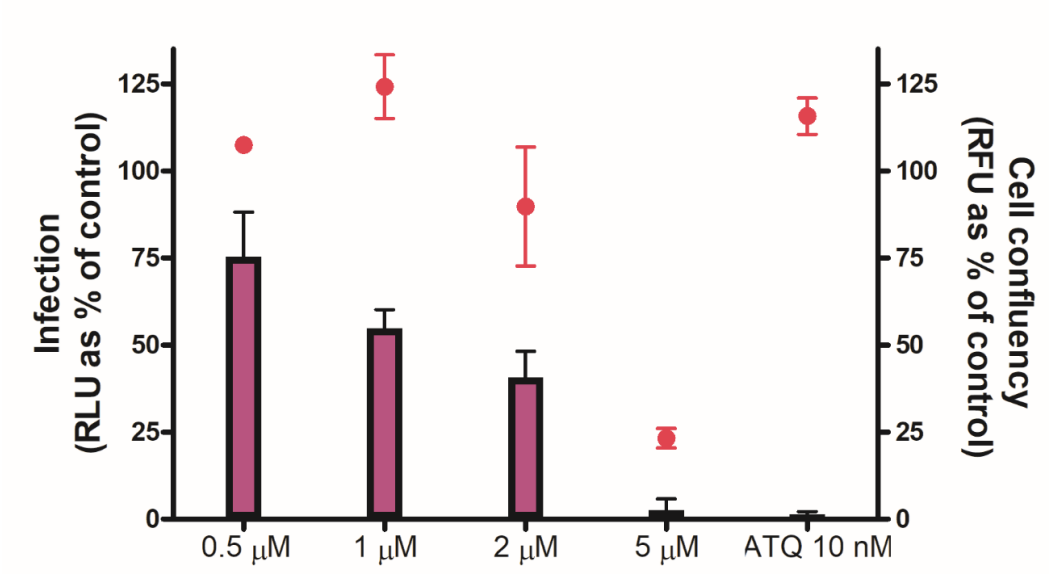

Figure 17. *P. berghei* liver stages *in vitro* infection rates upon violacein treatment. Parasite load in Huh7 cells was assessed by the relative luminescence 48 h after infection. Atovaquone (ATQ) was included as control. Bars represent infection loads ± SD. Red circles indicate Huh7 confluency.

5.5. Violacein gametocide activity

Only sexual stage parasites are able to transmit the disease from humans to mosquitos, giving continuity to malaria cycle. Thus, strategies that prevent gametocyte uptake by mosquitos or block parasite sexual stage development are required to reduce malaria burden, representing critical steps towards eradication policies [167].

P. falciparum gametocytes undergo five different stages of maturation (I-V) in a period of 10 to 12 days until full maturity (gametocyte V). Simultaneously with maturation, both, parasite and host RBC cytoskeleton undergo structural changes to achieve an elongated shape of sickle (“falx”, from Latin), which baptizes the parasite with the name of *P. falciparum* [168]. Interestingly, within all gametocyte stages, only mature forms at stage V are able to infect mosquitos, being attractive drug targets to block disease transmission.

The 8-aminoquinolones compounds have always shown good gametocide properties when compared with other antimalarial drug scaffolds [167], [169]. Currently, primaquine is the only FDA approved drug able to kill quiescent forms of *Plasmodium* parasites [169], [170]. Despite the ability to efficiently kill sexual stages, the use of primaquine to treat malaria relapses and reduce gametocyte burden raises

concerns regarding its safety on patients with G6PD deficiency, as they are unable to cope with primaquine induced oxidative stress [89], [171], reinforcing the need for new active compounds.

Interestingly, when early stage gametocytes (Stage I and II) were treated with violacein for 24 h, there was a massive drop on the number of gametocytes, indicating that violacein has promising transmission blocking properties, as it indirectly affects total gametocyte burden (Figure 18). Curiously, when preliminary drug tests were performed on stage V parasites, violacein was shown to be more active than DHA, with an EC_{50} of ~270 nM against 2.6 µM observed for DHA (Figure 19), going against the profile traced by standard antimalarials for its preferential activity against sexual stages rather than assexuals.

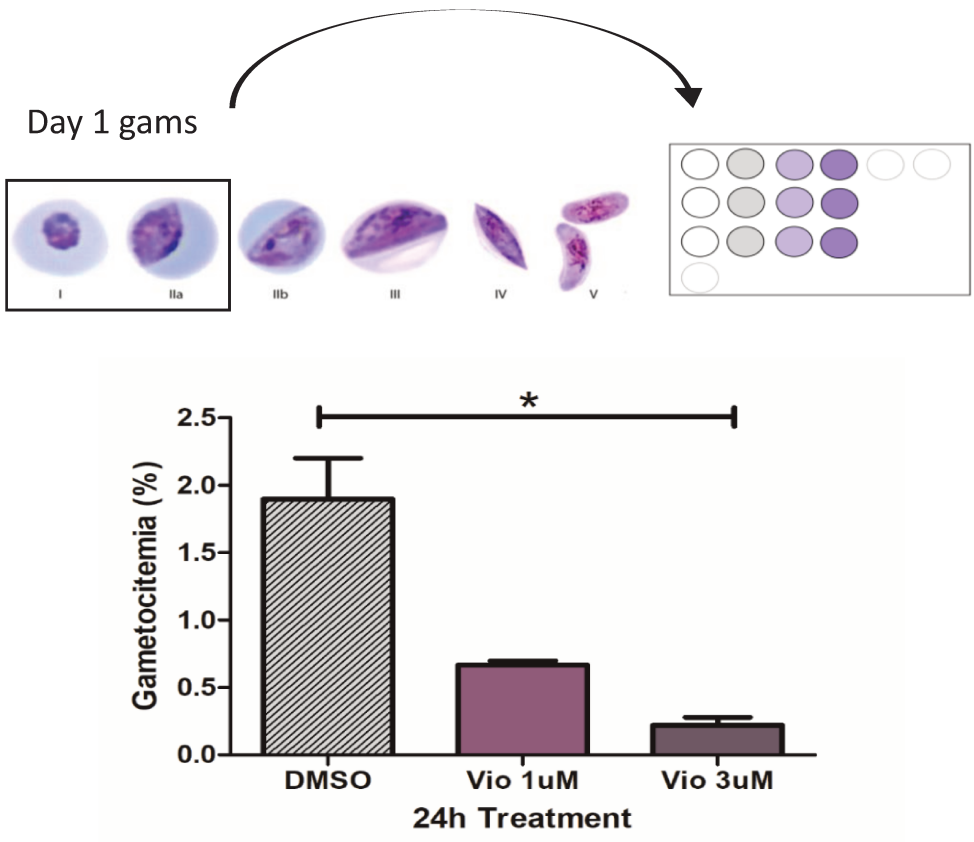

Figure 18. Violacein activity against early stage gametocytes. Stage I and II gametocytes, cultured in complete parasite media supplemented with 50 µM GNAC, were seeded into a 24 well plate and subsequently treated with violacein for 24h. Gametocytemia was assayed by Giemsa smears.

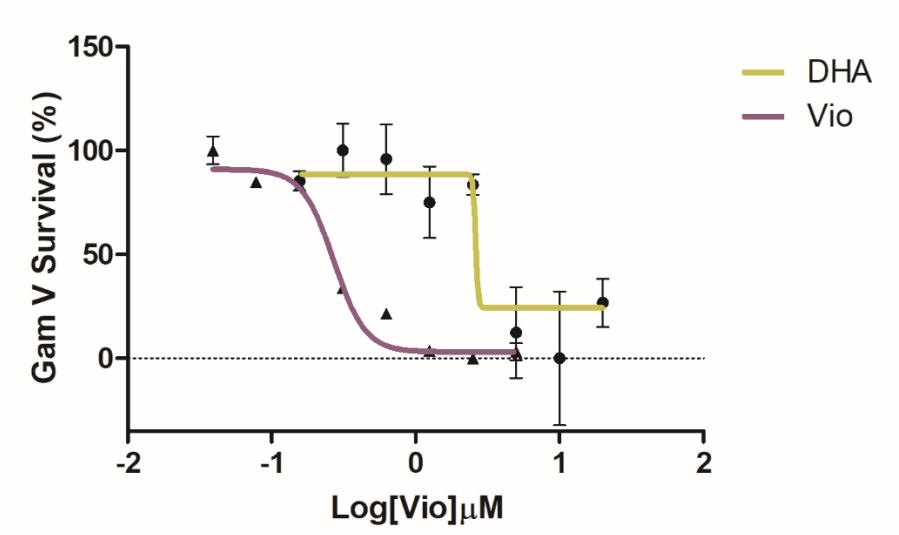

Figure 19. Violacein activity against stage V gametocytes. Stage V gametocytes (gam) were seeded into a 96 well plate in a concentration of 50.000 gametocytes/well and subsequently treated with different doses of DHA or violacein for 72 h prior 24 h incubation with AlamarBlue®. Results were plotted in a non-linear regression curve, GraphPad 5. DHA EC_{50}: 2.6 µM; violacein EC_{50}: 270 nM.

5.6. Ookluc Assay

To evaluate if violacein is able to affect parasite development on mosquito stages we used an elegant technique created by Dr. Daniel Bargieri (Instituto de Ciências Biomédicas – USP). Unlike conventional mosquito membrane feeding assays, quite laborious and time-consuming, we took advantage of the properties that gametocytes have to convert into ookinete *in vitro* under proper conditions, enabling chemical fertilization impairment analyses.

For this experiment, mutant *P. berghei* (Ookluc) gametocytes that expresses a Nano-luciferase reporter gene (nLuc), under control of an ookinete specific promoter, were incubated with different concentrations of violacein for 24 h in complete ookinete medium, followed by addition of a luciferin solution for luminometer readings [126]. Thus, is possible to associate luminescence signals with gamete fertilization and ookinete formation. Importantly, despite activity against early and late stage gametocytes, violacein had no biologically relevant effect on fertilization rate disruption, as the treatment at the higher dose tested was not active enough to avoid 50 % conversion into ookinetes (Figure 20 and Table 3).

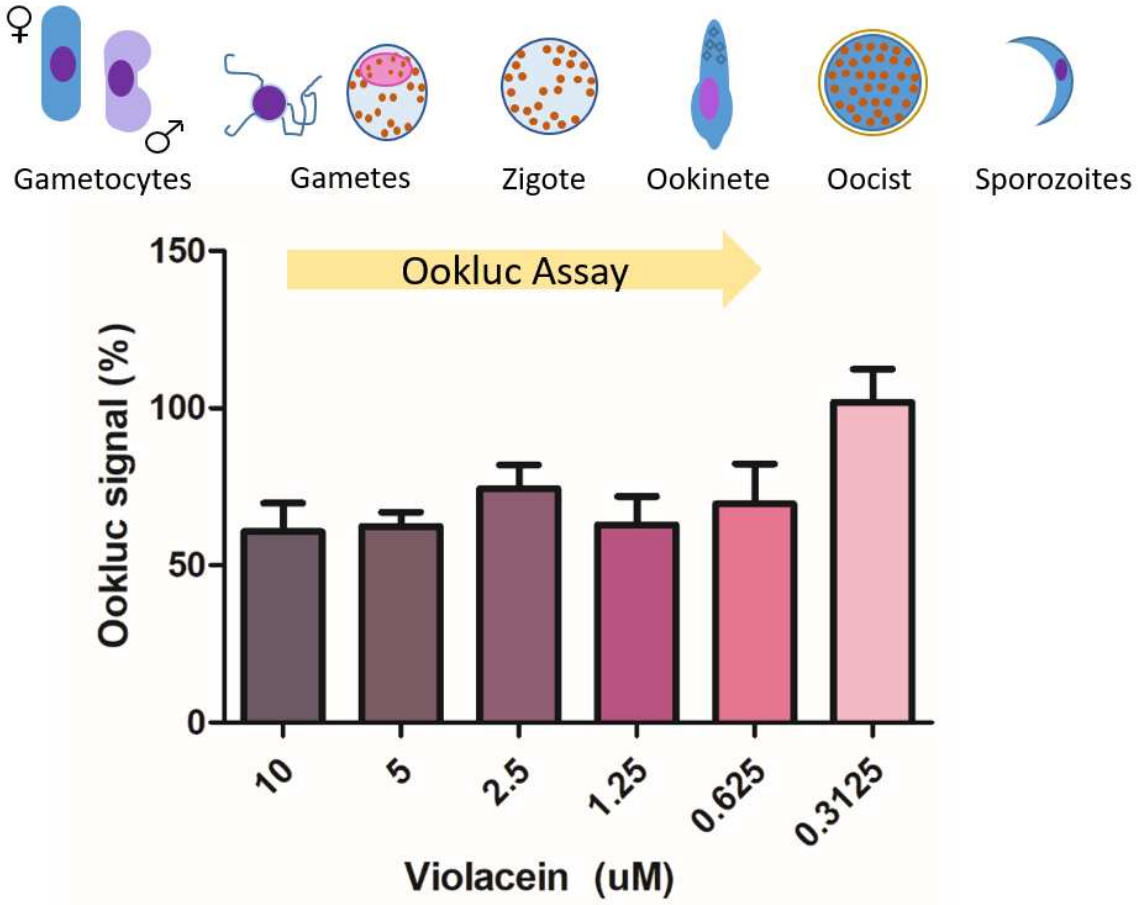

Figure 20. Gametocyte ookinete conversion upon violacein treatment. Ookluc gametocytes were drug treated with indicated doses of violacein for 24 h and luciferase substrate was added for enzyme activity readings. Violacein was not active enough to avoid 50 % of ookinete conversion at the highest dose tested (10 µM).

Table 3. Ookinete conversion under violacein treatment

Ookinete conversion (% ± SE)						
Violacein (µM)	10	5	2.5	1.25	0.625	0.312
Ookinete Conversion	60.64 ± 9.12	62.46 ± 4.45	74.41 ± 7.54	62.98 ± 8.91	69.53 ± 12.81	102.0 ± 10.48

5.7. Haploinsufficiency Chemical Genomic Profiling using yeast as a model

The budding yeast is the first and best characterized eukaryote cell to be fully sequenced, sharing numerous biochemical pathways with higher eukaryotes [172], [173]. Fast growth, low cost and easy gene manipulation made *Saccharomyces cerevisiae* a powerful tool to understand gene and protein function through creation of knockout and knockdown libraries covering all its genome [174]. Haploinsufficiency Chemical Genomic Profiling (CGP) approach is based on the premise that diploid yeast containing a gene expressed in heterozygosis will become hypersensitive to sublethal doses of an inhibitor targeting the product of this gene (Figure 21). Thus, understanding how small molecules and genes relate in a systemic view might clarify how genomic response is modulated by chemical treatments [128], [175], [176]. Because violacein has activity against several organisms from distinct phylums including higher eukaryotes, we decided to apply chemical genomic approach as an attempt to discover potential targets or pathways affected by this compound.

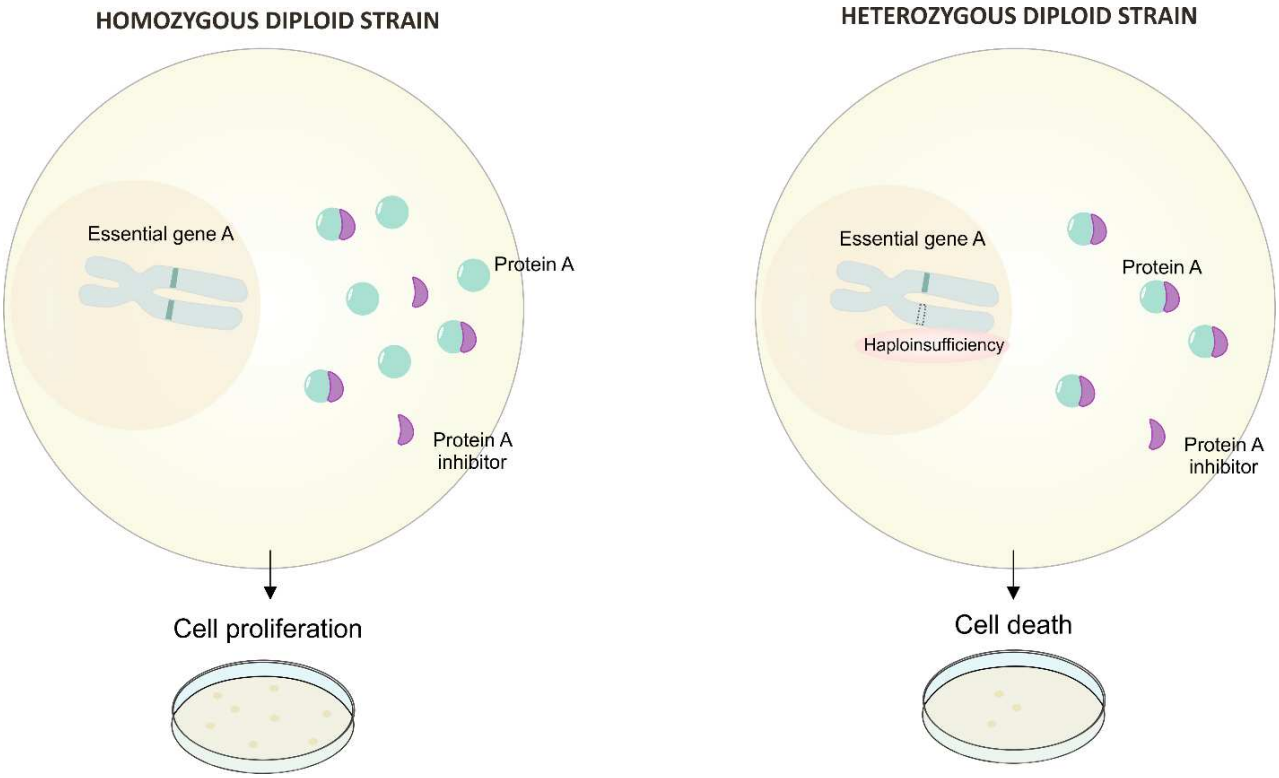

Figure 21. Hypothetical scheme showing Haploinsufficiency Chemical Genomic Profiling assay. How HIP can track the biochemical pathways affected by the pressure of a compound in heterozygous mutant yeast strains.

To determine which drug concentration to use in the chemo-genetic screen, we performed a drug assay in wild-type BY4743 yeast strain for 25 h starting with initial OD_{595} of 0.1, and selected the concentration able to inhibit 20 % of growth relative to control (EC_{20}). EC_{20} concentration was chosen due to its ability to affect yeast deletion strains without unspecific toxic effects that occurs at higher concentrations [130]. The tests revealed that the concentration of violacein capable of inhibiting 20 % of yeast growth was 8 µM (Figure 22).

After determination of ideal concentration, pools of the 6000 barcoded heterozygous yeast strains were cultured in the presence of violacein or DMSO for 5, 10, 15 and 20 generations prior to genomic analysis. We selected triplicates of mutant pools grown under drug pressure or DMSO for 10 generations for genomic DNA extraction and barcode quantification.

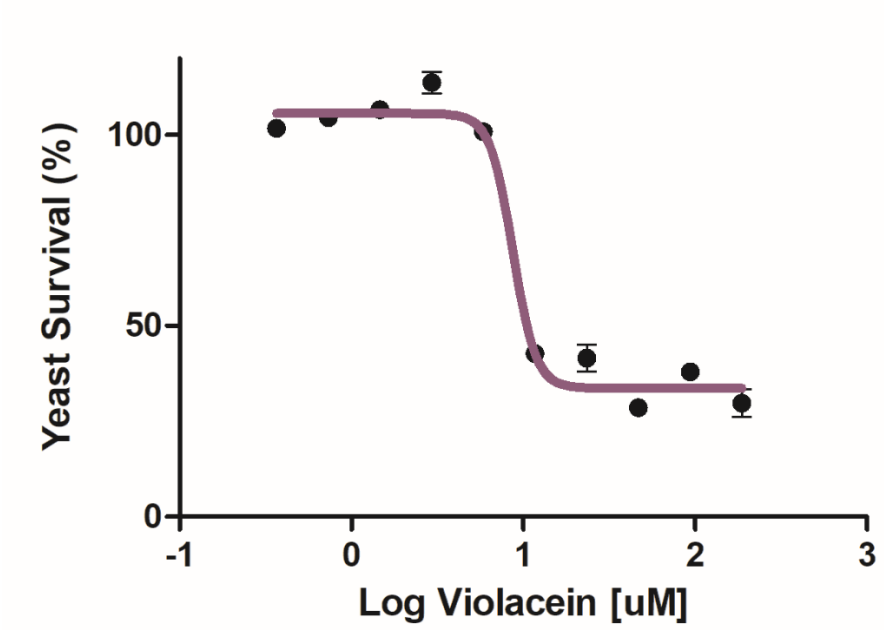

Figure 21. BY4743 wild-type yeast growth curve upon violacein treatment. BY4743 yeasts were incubated for 24 h in the presence of violacein and untreated controls. OD_{595} values were collected every 10 minutes to calculate the growth of treated yeasts in relation to the control. EC_{20} value calculated by a log nonlinear curve [violacein] x growth inhibition (%).

Comparisons between yeasts pools treated with violacein IC_{20} and equivalent concentration of vehicle control, made possible to identify which strains were most depleted in the mutant population against treated ones after 10 generations. The cutoff

values used to select the trial hits were p-value <0.001 and log2 fold change <0, (Figure 23). These reference values were used according to the protocol provided in the HIPHOP Database, which groups chemo-genomic screenings performed by the University of Toronto [136].

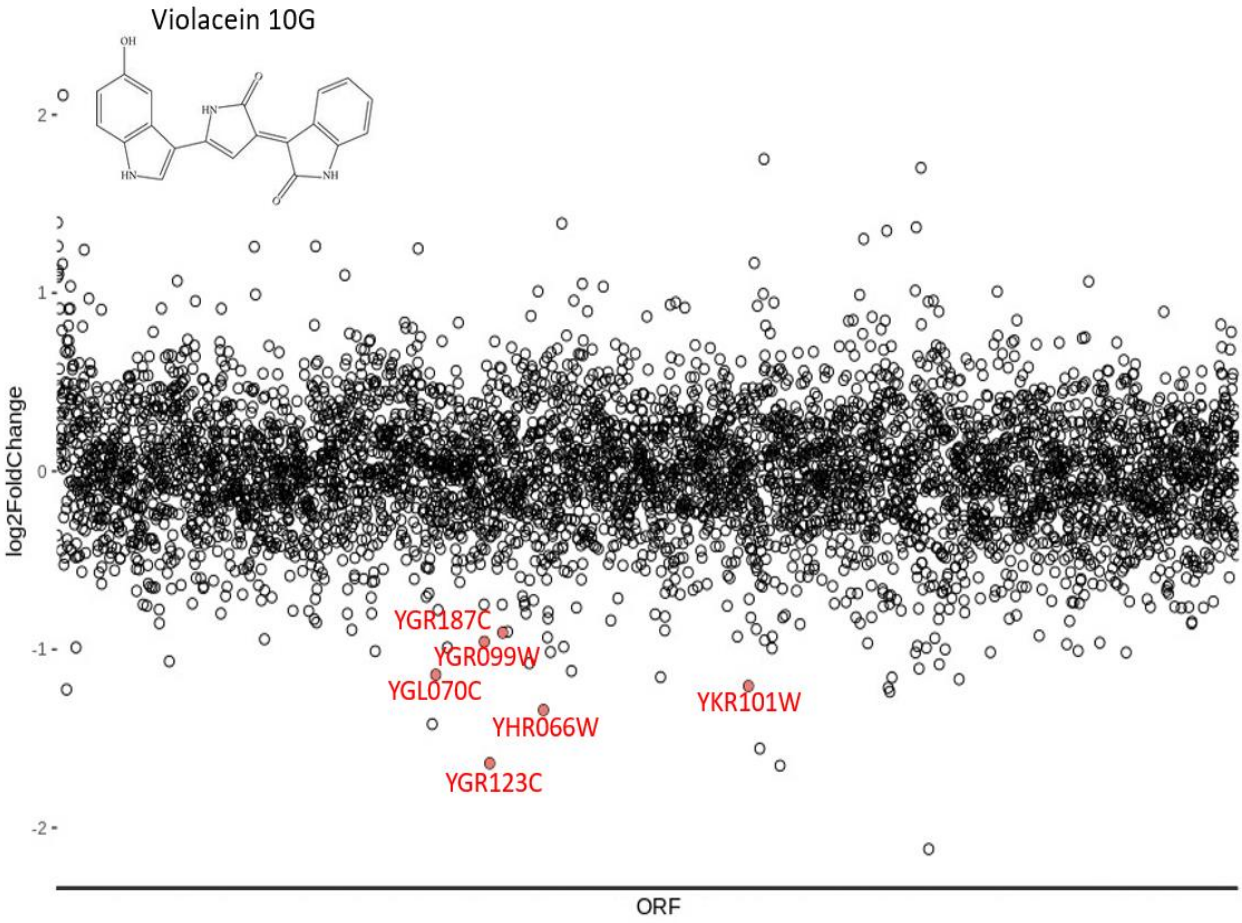

Figure 23. Haploinsufficiency profile of heterozygous yeast strains treated with violacein compared to the untreated control. The fold change log is plotted on the y-axis as a function of the deleted yeast strains ordered alphabetically by their respective ORF. The lower the strain log of fold change value, the greater is its sensibility to the compound. The red highlights in the chart represent the ORFS that meet the conditions p-value <0.001 and log2 fold change <0.

The Haploinsufficiency profile of diploid heterozygous yeast strains analysis allowed us to identify six violacein-sensitive ORFs, that is, six depleted strains with statistical significance under treatment with violacein for 10 generations (Table 4).

Table 4. Top Hits Fitness defect. Hits for CGP, violacein 10G

ORF	Pvalue	Null viability	Gene Ontology
YGL070C	0.000118	+	RNA polymerase II; response to DNA damage stimulus
YKR101W	0.000127	+	sequence-specific DNA binding
YGR123C	**0.000158**	**+**	**protein serine/threonine phosphatase activity; co-chaperone HSP90**
YGR187C	0.000569	+	molecular function unknown; relative distribution to the nucleus increases upon DNA replication stress
YHR066W	0.000598	+	rRNA binding; regulation of cell size
YGR099W	**0.000753**	**-**	**DNA binding; co-chaperone HSP90**

References:: SGD- **www.yeastgenome.org**

Interestingly, two of the putative targets pointed are co-chaperones that have the ability to complex with Hsp90 to develop innumerous functions within the cell, including kinase activity control and protein folding (found in bold, Table 4). The fact that two (out of six, 33% total hits) Hsp90 partner binding proteins appeared as hits on the screening, raises the possibility that violacein could be affecting Hsp90 function impairing its ability to interact with other cochaperones. It is possible that we couldn't find Hsp90 as a hit due to the existence of another isoform present on yeast genome that can buffer the absence of this essential chaperone under stressful situations [177]. Several proteins depend on Hsp90 for proper folding, final structure maturation, and binding activity, thus, inhibition of this chaperone leads to extensively degradation of client proteins that is usually mediated by the proteasome, affecting distinct biochemical pathways (for more information see https://www.picard.ch/downloads) [178].

Curiously, the extensive list of proteins regulated by Hsp90 include many oncoproteins and transcription factors that cope with cancer cell malignancy, being firstly suggested as a potential drug target in the 90s[179] . The initial skepticism surrounding the idea of chaperones as druggable targets was fed by concerns

regarding its toxicity on healthy cells, quickly surpassed by the success from initial efforts from academia and small biotechnology companies that developed these small inhibitors for potential cancer treatment, subsequently growing interest of big pharmaceutical companies. Only two decades after the first thought of targeting Hsp90 for cancer therapeutics, there were already 17 inhibitors at clinical trials, being one of the most pursuit targets for oncological treatment in earlier XXI century [125].

Hsp90 is known to interact with a battery of cochaperones that essentially aids on the performance of different tasks within the cell depending on the partner attached. The binding of TPR cochaperones to Hsp90 relies on interactions between their tetratricopeptide repeat (TPR) domains, where each member brings particular functions to the complex. Thus, Hsp90 function is suggested to be shaped by protein competition for binding sites to form specific complexes [180]. While humans possess two cytosolic *HSP90* genes containing terminal EEVD motif (common sequence present in both, Hsp90 and TPR cochaperone motif), in *Plasmodium* we can find only one *HSP90* gene carrying the same sequence pattern, sharing 64% identity with their human counterpart, and a conserved ATP binding pocket [32].

Importantly, chaperones are well known to cope with the UPS for proteostasis in mantainence of protein quality control. Hsp90 inhibition by small molecules leads to misfolding and degradation of client proteins by the proteasome [181]. Client polyubiquitination and proteolysis is mediated by E3 ubiquitin ligases, with cullin E3 ubiquitin ligase family playing an intrinsic role in ubiquitin-labelling of Hsp90 misfolded intermediates [182], [183]. Interestingly, cullin seems to play an important role in *Plasmodium* resistance to artemisinin and derivatives, as indirect cullin inhibition by Nedd8 inhibitor potently antagonizes DHA activity [43] and mutations at Kelch propeller domain, responsible for substrate binding for cullin-mediated ubiquitination, is also able to confer parasite ART resistance [68], [81], [82].

Several human Hsp90 inhibitors were shown to inhibit *Plasmodium* Hsp90 at low nanomolar doses, possibly due to high similarity between their ATP binding pockets [184], [32]. The same compounds also showed antimalarial activity against both, blood and liver stages highlightening chaperone inhibitors as potential antimalarial partner drugs since they are also able to cope synergistically with other compounds to increase antimalarial activity [184]. Taking that in consideration, we

developed *in silico* homology models for PfPP5, one of the cochaperones pointed as a hit on CGP, as well as PfHsp90, to evaluate if violacein could potentially bind these proteins. Tel2 was not analyzed as it is lacking in *Plasmodium*.

5.8. *In silico* analysis of violacein as a PfHsp90 inhibitor

In silico analysis of violacein were performed in collaboration with Profa. Dra. Carolina Horta Andrade and Dr. Bruno Neves at Federal University of Goiás, Goiânia.

The 3D structure of *Pf*PP5 not available on the PDB at the time this work was conducted. Consequently, homology models were built by comparing the *P. falciparum* primary sequences with sequences of homologue proteins (templates) for which 3D structures were available. After the homology modeling, the loops and terminus regions were structurally refined. Geometric analysis of modeled protein structure indicated the good quality of the backbone dihedral angles ψ and φ (95.15% of amino acids are within the favored Ramachandran regions, and 0% are outliers) and χ side-chain angles (96.18% of good rotamers, and 0% of poor rotamers). In addition, acceptable Clashscore (0.00) and MolProbity score (0.81) was obtained for this structure. The Clashscore is the number of steric clashes per 1000 atoms, whereas MolProbity score is a log-weighted combination of the percentage bad side-chain rotamers, percentage Ramachandran outliers, and Clashscore, giving one number that reflects the resolution of X-ray structures at which those values would be expected.[185], [186] So, the overall stereochemistry and conformation characteristics of amino acids, and the compatible chemical interaction environment indicate that generated *Pf*PP5 model could be useful to prospective molecular docking studies.

To further characterize the binding modes and the affinity of violacein with the investigated *P. falciparum* targets, molecular docking studies were performed using FRED program. As we can see in Table 5, the Chemgauss4 scores of docking indicated that violacein is able to perform relevant binding interactions with PfHsp90 (score of -11.68). The docking scores also indicated that violacein interacts with PfHsp90 in the same range of positive control (score of -12.97, experimental IC_{50} = 0.08 µM)[187]. On the other hand, less pronounced scores were observed for *Pf*PP5 (score of -6.57). The intermolecular interactions of violacein in ATP-binding site of *Pf*Hsp90 (Figure 24A and 24C) can be generalized as follows: the carbonyl and amine

groups of 2,3-dihydro-1H-pyrrol-2-one moiety can form hydrogen bonds (represented as black dashed lines) with the Lys44 and Asn92, respectively. The phenyl group of violacein can interact with hydrophobic pocket formed by Ile173, Ile77, Phe124, and Thr171. In addition, the hydroxyl group and amine of 2,3-dihydro-1H-indole moiety can form hydrogen bonds with Asn37 and Asp79, while the phenyl group forms a π-cation interaction with Arg98.

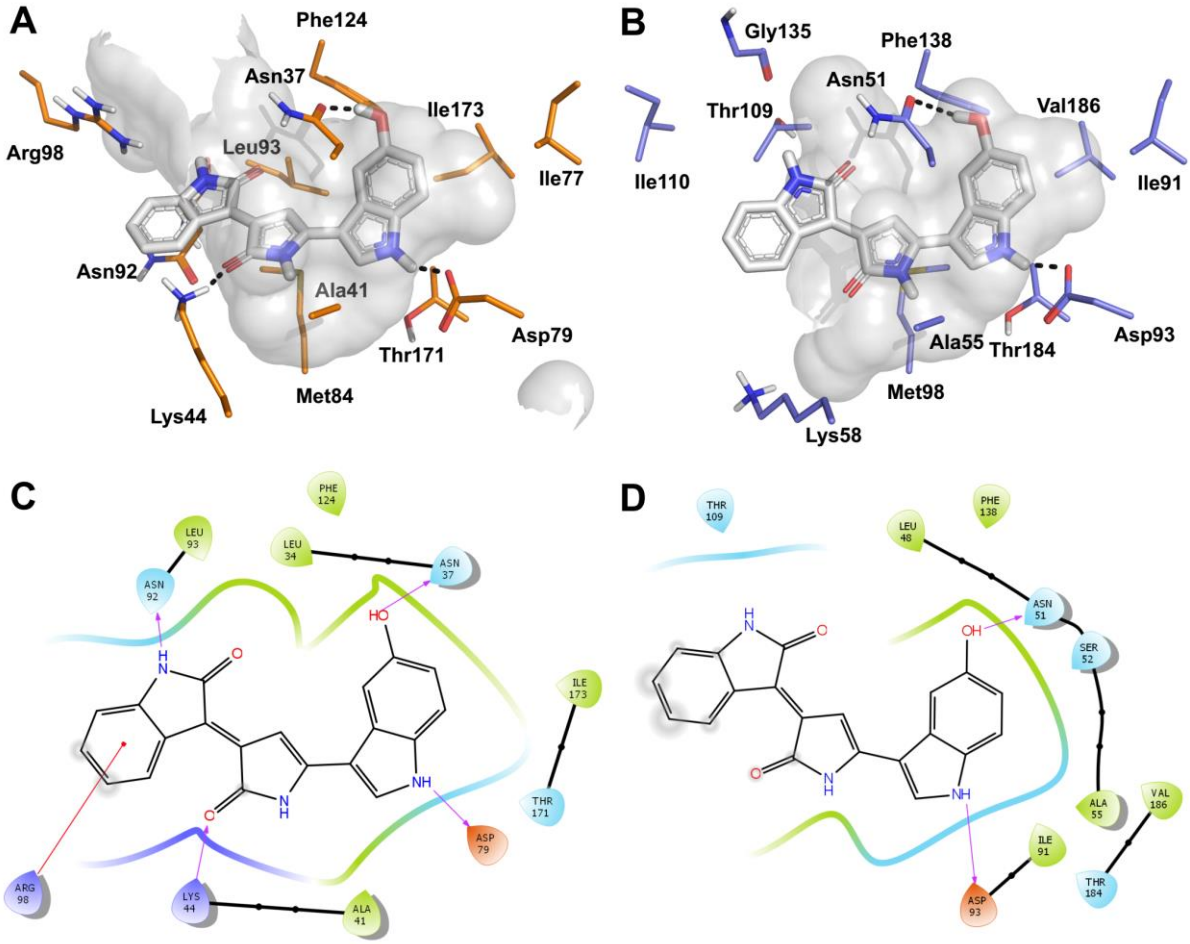

Figure 24. Predicted intermolecular interactions of violacein with ATP binding sites of *P. falciparum* Hsp90 (A and C, backbone in orange), and its human homologue (B and D, backbone in blue). Violacein is represented in stick models with carbon atoms colored gray, nitrogen in blue, oxygen in red, and hydrogen in white. In 2D interaction diagrams (C and D), hydrogen bonds are presented as magenta arrows and π-cation interaction as red lines.

In order to explore structural basis for selectivity, molecular docking was also carried with *h*Hsp90. Violacein interacts with a score similar to that obtained for *Pf*Hsp90 (-11.42, see Table 4), but with a reduced number of intermolecular interactions at the ATP-binding site of *h*Hsp90 (Figure 24B and 24D).

In addition, docking scores corroborates with experimental bioactivity data of positive control (-8.17), a selective inhibitor (*h*Hsp90 IC_{50} = 3.6 µM) 45 folds less potent for *h*Hsp90[187]. These results suggest that violacein may have similar affinity for both parasite and human proteins.

Table 5. Details of grids used in molecular docking studies and corresponding Chemgauss4 scores for violacein.

Protein target	Dimensions	Box volume	ChemGauss4 scores	
			Violacein	Control
*Pf*Hsp90	19.71 x 18.79 x 17.10	6336	-11.68	-12.97
*h*Hsp90	19.67 x 18.67 x 17.33	6363	-11.42	-8.17
*Pf*PP5	19.99 x 16.95 x 20.04	6788	-6.57	–
*h*PP5	19.67 x 14.94 x 20.23	6740	-7.25	–

5.9. Violacein and *Plasmodium* UPR and UPS responses

Evaluation of UPR and UPS responses in parasites treated with violacein were performed in collaboration with Dra. Leann Tillley and Dra. Natalie Spillman from Melnourne University, Australia. Because PfHsp90 chaperone was pointed as a promising target for violacein, we decided to investigate the two major regulatory branches of cell stress response in which chaperones play pivotal role in proteostasis mantainence: the Ubiquitin Proteasome System (UPS) and Unfolded Protein Response (UPR). As previously said, in UPS pathway, proteins damaged by cellular stress are preferentially refolded by chaperones, and in case of chaperone

overburden, damage proteins are ubiquitin tagged for proteasome degradation. In UPR, the cell cope to respond to stress by increasing cytokine production, transcription of chaperones and proteins involved in proteolytic systems, while translation of other proteins are shut down (Figure 4). In mammalian systems, three majoritarian arms compose UPR: IRE-1, PERK and ATF6, in *Plasmodium* this response is reduced to a modified PERK pathway that lacks transcriptional regulatory response. Under accumulation of misfolded proteins, BiP dissociates from PK4, a transmembrane kinase that undergoes autophosphorylation prior to phosphorylation of eIF2α, resulting in protein translation shut down, avoiding chaperone overload (Figure 25A). Thus, stress response in *Plasmodium* is controlled by decrease of protein synthesis (UPR branch) and degradation of misfolded proteins (UPS branch) [34]. To examine if UPR and UPS response are altered following violacein treatment, we sought to investigate eIF2α phosphorylation and ubiquitination profile of parasites treated with different doses of violacein. We found that unlike Dihydroartemisinin (DHA), violacein does not cause phosphorylation of eIF2α (Figure 25B), showing no signals of stress in ER. On the other hand, while for DHA treatment it was possible to note accumulation of ubiquitinated proteins in a dose dependent manner, in parasites treated with violacein we could see a slightly accumulation of polyubiquitinated proteins compared with the non-treated control at the lowest dose tested. However, there is a decrease in polyubiquitin signals for the highest concentration, implying in a chemical-induced deubiquitination profile (Figure 25C). Interestingly, the initial increase on protein polyubiquitination upon violacein treatment suggests that chaperone inhibition can lead to chaperone overload followed by protein misfolding and subsequent ubiquitin tagging for proteolysis. As proteins are sent for degradation, ubiquitin molecules are possibly being detached from substrates by the 26S proteasome, explaining the deubiquitination profile visualized for parasites treated with highest dose of violacein. In summary this data shows that violacein does not trigger the Unfolded Protein Response, as there is no accumulation of ubiquitinated proteins and eIF2α remains unphosphorylated. Altogether, data indicates that protein synthesis is still being carried on by parasites treated with violacein.

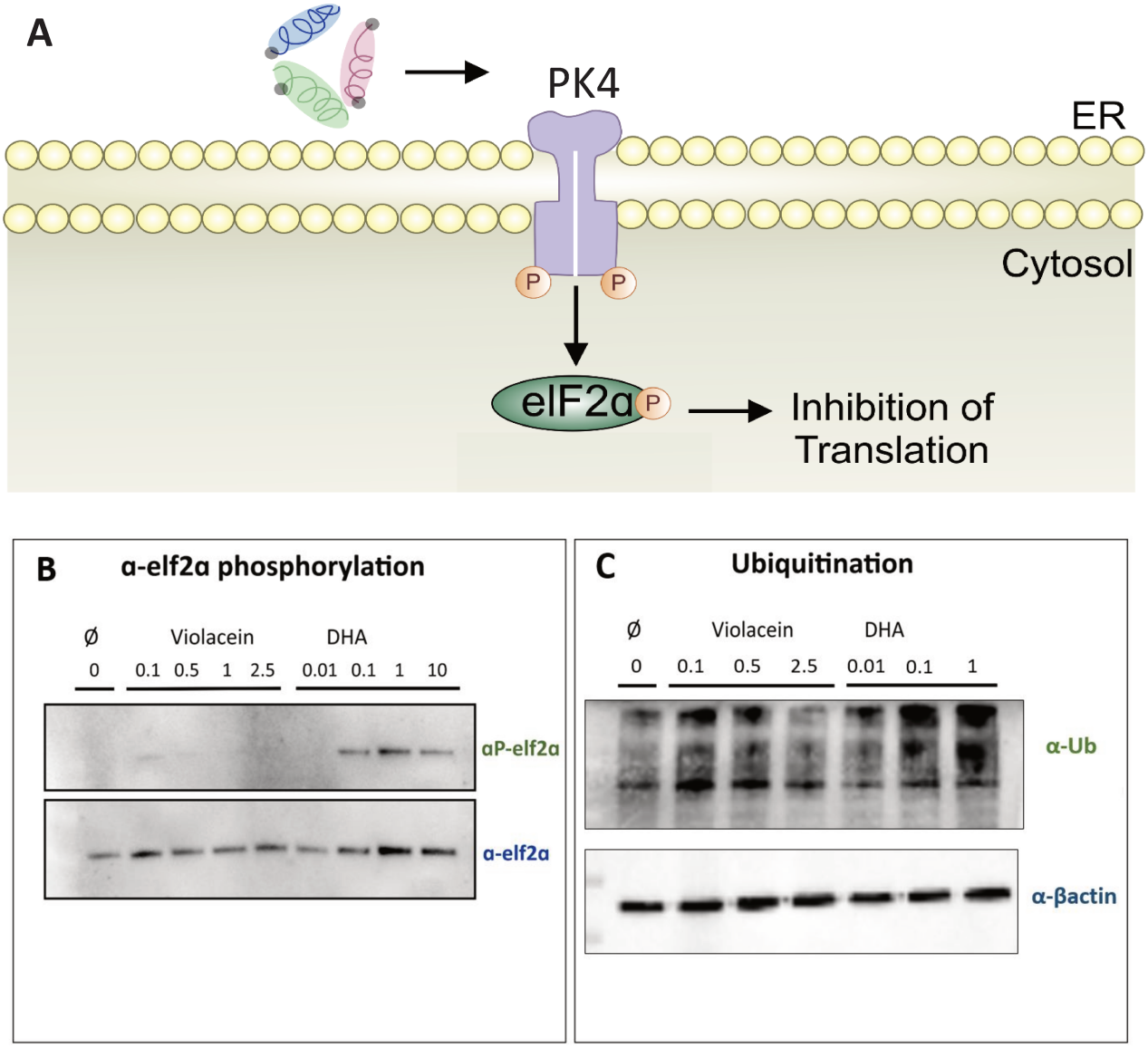

Figure 25. Unfolded protein response in *P. falciparum* upon violacein treatment. A) Scheme of PK4 pathway activation in *Plasmodium*. B) Western Blot against p-eIf2α. NF54 parental line parasites were treated with different doses of violacein, DHA or vehicle for 90 minutes at 37 ºC. Cell extracts went through SDS-PAGE and western blotting prior probing with anti phospho-eIf2α. The concentration of compound used for WB is shown bellow the name of each compound in µM. Membrane was stripped and reprobed with anti-eIf2α for protein load control. C) Western Blot against poly-ubiquitin. NF54 parental line parasites were treated with different doses of violacein, DHA or vehicle for 90 minutes at 37 ºC. Cell extracts went through SDS-PAGE and western blotting prior probing with anti poly-ubiquitin. The concentration of compound used for WB is shown bellow the name of each compound in µM. . Membrane was stripped and reprobed with anti GAPDH for protein load control.

5.10. Violacein and *Plasmodium* proteolysis system

In the past decade, researchers created a system that enable control of protein function using a “single ligand-single domain” strategy by fusing any protein to a ligand-binding domain that is engineered to be unstable and degraded by the proteasome pathway in the absence of its ligand [188]. When ligand binds to the destabilizing domain of the mutant protein, it shields it from degradation, restoring protein function. Several groups have been using similar techniques as a knockdown approach to understand protein function [129], [174], [189]. However, Dr. Spillman, from Bio21/ Melbourne University, adapted this method as a tool for surveillance of unfolded protein load induced by compounds in *P. falciparum* model. *P. falciparum* parasites were transfected with plasmids containing PfFKBP gene, a protein known to be quickly degraded by the proteasome, containing a destabilizing domain (DD) fused with a GFP reporter gene, enabling track of the mutant protein in presence of different compounds (figure 25A). Folded proteins are detected by flow cytometry (FC) through GFP fluorescence signals, while total amount of protein is obtained by western blotting (WB), using antibodies against GFP [43], [66]. Protein unfolding is noticed when mutant parasites treated with a compound of interest present a decrease on GFP signals when compared to GFP signaling from vehicle treated control, but show no lessen amount of total protein (WB). Since PfHSP90 chaperone was pointed as a possible target for violacein, Dr. Spillman’s technique was employed to investigate if violacein could be causing protein unfolding in *P. falciparum* (Figure 26).

The experiment was designed to contain a group of mutant parasites treated with violacein and five control groups: 1) DMSO (vehicle control), 2) WR (does not affect UPR/ UPS), 3) Shield (protects protein from degradation), 4) Dihydroartemisinin/DHA (causes protein unfolding) and 5) CPD-1 (indirect proteasome inhibitor). As expected, WR showed a response similar with the one observed in DMSO group. While Shield and CPD-1 presented curves above the line stablished by vehicle control, violacein showed a FC profile resembling the one observed for Dihydroartemisinin (DHA), with both compounds exhibiting GFP signal bellow DMSO background line (Figure 25B). When we analyze FC data together with WB, It is possible to note that Shield does not cause activation of proteasome pathway, once proteins have their folded state stabilized in a dose response manner. DHA promotes accumulation of unfolded proteins, as GFP signal remains bellow

background control line, indicating loss of GFP native conformation, but WB shows that protein accumulates in a dose dependent manner, due to partial inhibition of proteasome induced by the drug [43]. Violacein on the other hand, seems to be causing protein damage/unfolding without proteasome inhibition, resulting in a decreased signal observed both in FC and WB (Figure 26B and 26C).

When we analyze all the data together, we can suggest that despite no activation of the Unfolding Protein Response (as there is no accumulation of polyubiquitinated proteins), proteins are being unfolded by violacein treatment. Possibly, protein unfolding happens due to chaperone overburden, leading to misfolding of client proteins that are firstly tagged with polyubiquitin chains and then, quickly degraded by the proteasome. Interestingly, even though our experiments have shown intense proteolysis induced by violacein, protein synthesis is still being carried on, probably in a way to compensate loss of essential proteins by the proteasome.

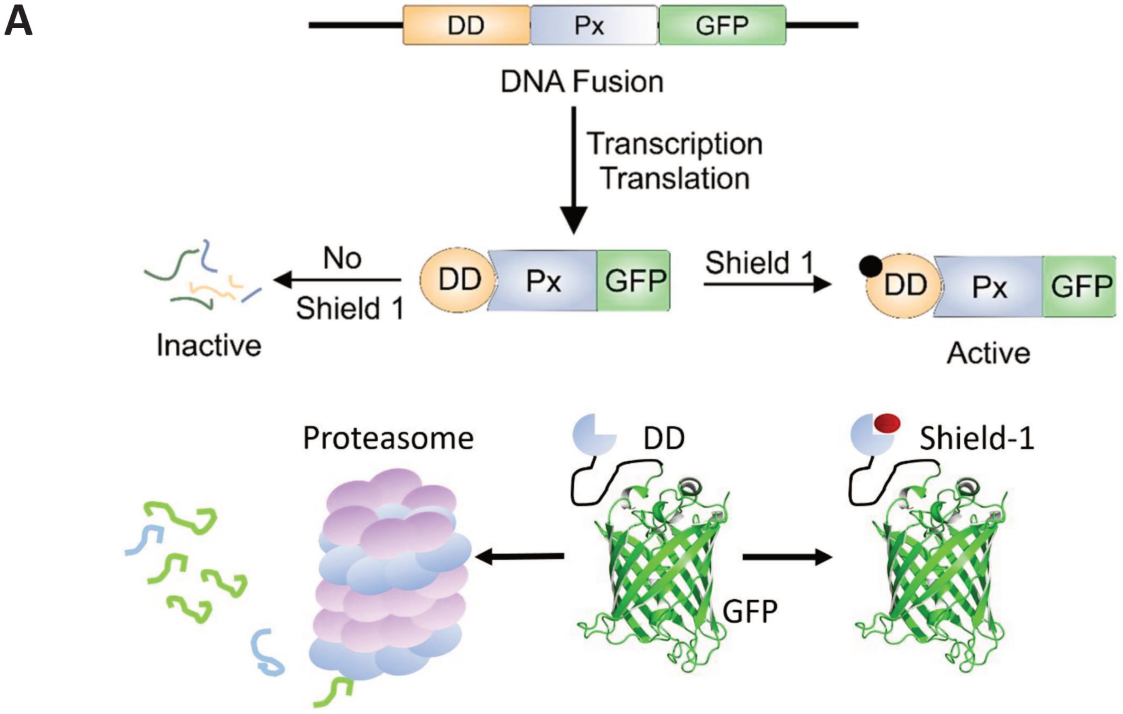
A
DD
Px
GFP
DNA Fusion
Transcription
Translation
No
Shield 1
Inactive
Shield 1
Active
Proteasome
DD
Shield-1
GFP

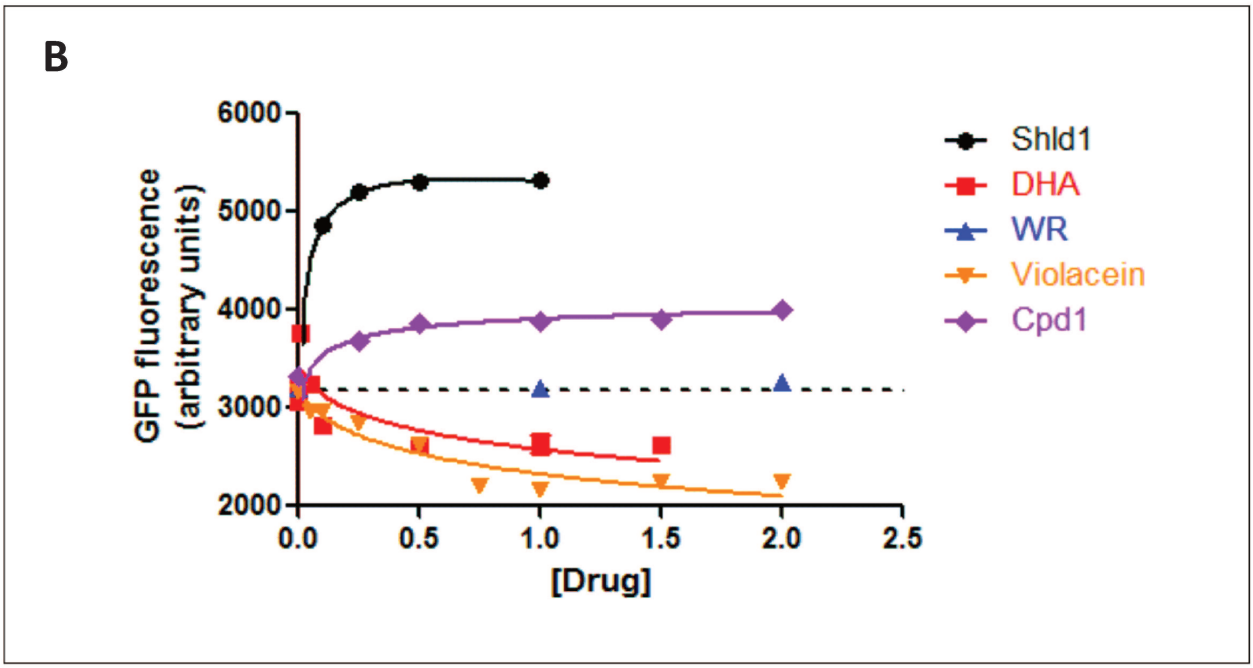
B
GFP fluorescence
(arbitrary units)
6000
5000
4000
3000
2000
0.0
0.5
1.0
1.5
2.0
2.5
[Drug]
Shld1
DHA
WR
Violacein
Cpd1

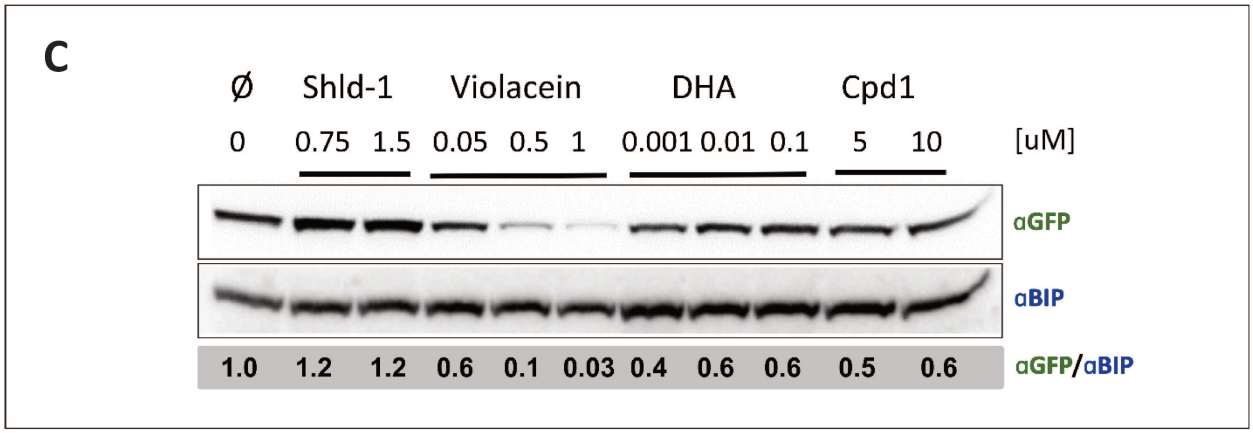
C
Ø
Shld-1
Violacein
DHA
Cpd1
0
0.75
1.5
0.05
0.5
1
0.001
0.01
0.1
5
10
[uM]
αGFP
αBIP
1.0
1.2
1.2
0.6
0.1
0.03
0.4
0.6
0.6
0.5
0.6
αGFP/αBIP

Figure 26. *P falciparum* UPS response upon violacein treatment. A) *P. falciparum* 3D7 plasmid construct and experiment design B) GFP fluorescence recorded by flow cytometry. Each curve represents GFP fluorescence signaling from parasites treated for 3 h at 37 °C with several concentrations (μM) of different compounds: Shield (causes protein stability, black), DHA (causes protein unfolding, red), WR (does not affect UPS/UPR, blue), CPD1(indirect proteasome inhibitor, purple) and violacein (orange). C) Western Blot against GFP**.** Same mutant parasites analyzed by flow cytometry were lysed and blotted against GFP. The concentration of compound used for WB is shown bellow the name of each compound in μM. Membrane was stripped and reprobed with anti BIP for protein load control. Densitometry analysis of the ratio between αGFP/ αBIP performed by ImageJ are shown in the gray box

5.11. Circular dichroism analysis for PfHSP90-violacein interactions

Violacein biophysical and biochemical binding analysis of were performed in collaboration with Prof. Dr. Júlio César Borges and PhD candidate Noeli Soares Silva, from São Paulo University, São Carlos.

Despite suggestions from chemical genomic profiling and increased protein unfolding and degradation (typical features of chaperone inhibitors), there is no direct evidence showing that violacein inhibits PfHsp90 function. Taking advantage of the properties that proteins have to deviate light due to its chirality, we used optical spectroscopy analysis to understand how violacein biophysically affects PfHsp90.

Circular Dichroism (CD) spectroscopy is a technique that measures the differences in absortion of right handed and left handed circularly polaryzed light by a solution containing molecules of interest. Only chiral molecules such as proteins are able to deviate light, producing CD signals. The chiral recurrent content of proteins, alpha-helix and beta-sheets, produces strong bands, specific to each protein, on far-ultraviolet spectra. When a molecule binds to a specific protein, it changes its CD spectrum profile due to eletron reorganization leading to chiral pertubations [190]–[193]. Circular dichroism (CD) was employed to vizualize changes in folding and protein dynamics on full lenght PfHsp90 when pre-incubated with violacein.

The collected and curated data shows that even low doses of violacein (proportion 1:1, PfHSP90:violacein) were able to promote changes in PfHsp90 CD spectra, changing protein secondary structure configuration (Figure 27). Violacein promoted a substancial gain in α-helix structure (6%) together with loss (4%) in β-sheet structures when compared to PfHsp90 non-bound state. Importantly, violacein is a non-chiral molecule, unable to produce signal, reinforcing that the changes

observed in protein light deviation were boosted by conformational changes promoted to accommodate violacein binding.

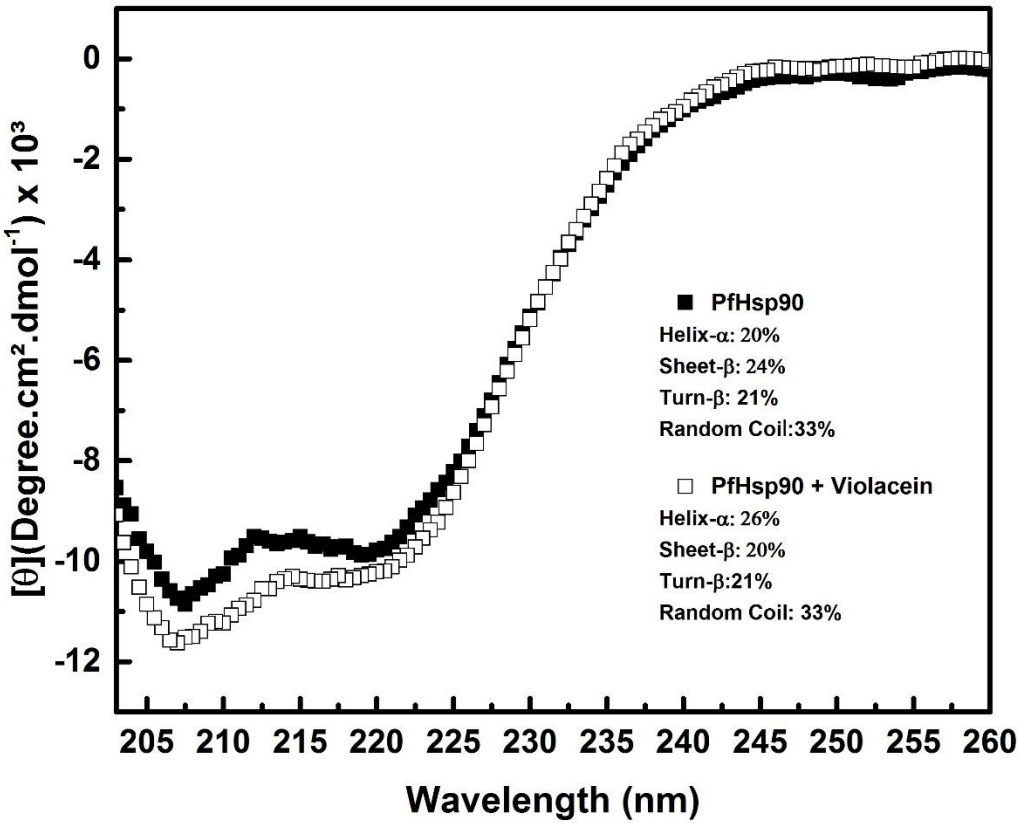

Figure 27. PfHsp90 CD far-UV spectra in the presence or absence of violacein. Black and White squares represents CD readings of PfHsp90 alone or pre-incubated for 30 minutes with violacein (proportion 1:1, PfHsp90:violacein) respectively.

5.12. Differential Scanning Calorimetry for PfHSP90-violacein interactions

Spectra profile changes on circular dichroism from PfHsp90 in the presence of violacein showed us a hint of protein-compound interactions. To further characterize unfolding and binding energetics, we used Differential Scanning Calorimetry (DSC) technique for comparisson analysis of results obtained for full length PfHsp90 alone or pre-incubated with violacein (proportion 1:5, PfHsp90:violacein) for 1 hour (Figure 28).

DSC can provide thermodinamics and thermalstability information that underlies biological samples by measuring the heat capacity of a system when a

temperature gradient is applied, that is, DSC can measure the heat change during protein thermal denaturation [194]. The set-up of DSC is composed by two separate containers or crucibles, one for sample of interest and another for reference solvent/ buffer (the same used for sample preparation). Both containers are connected to individual identical heaters and subjected to a heatflow. The temperature sensors increases linearly and the heatflow to maintain both containers at the same temperature is recorded as a temperature function, allowing characterization of protein thermo-properties like melting points, or thermal transition temperature (Tm) and proccess enthalpy (ΔH) [194]–[196]. When we look at the melting curve profile of PfHsp90 alone, we can notice two melting temperature peaks, the first happens at 41 °C and the second one at 58 °C (Figure 28, table 6). Clearly, the first peak corresponds to N-terminal domain melting point as it gains thermalstability at the presence of its natural binder, ADP, lingering Tm_1 up to 7°C forward (Table 6). Violacein was also able to displace N-terminal domain, but not C-terminal domain (second temperature pick) melting temperature in a similar fashion, but less pronouced, as ADP (Table 6). Interestingly, when ADP and violacein were incubated together we can see that violacein is not able to displace the preferential binding of ADP to the chaperone (Table 6).

Worth notice that the ADP concentration used for a 7 °C deslocation on Tm_1 was 100 times higher than the amount of protein. For violacein we used a concentration only 5 times higher than the one used for PfHsp90, and we were able to notice a gain in thermalstability of 2 °C at first melting temperature. The Tm_1 postponing, when PfHsp90 is incubated with violacein, is followed by an increase on total enthalpy process (ΔH_1), that is, the energy required to complete the transitional state of N-terminal domain unfolding is higher after violacein treatment. Thus, our DSC matches with previous docking results, reinforcing the idea that violacein binds the N-terminal domain, which comprises the PfHsp90 ATP binding pocket.

Table 6. Differential Scanning Calorimetry analysis

Conditions	Diferential Scanning Calorimetry			
	Tm_1	ΔH_1	Tm_2	ΔH_2
PfHsp90	41,0 ± 0,2	60 ± 10	58,0 ± 0,3	80 ± 10
PfHsp90 + Violacein	43,0 ± 0,2	100 ± 10	58,1 ± 0,2	80 ± 10
PfHsp90 + ADP*	48,1 ± 0,2	130 ± 10	56,5 ± 0,2	100 ± 10
PfHsp90 + ADP+ Violacein *	48,9 ± 0,1	100 ± 10	57,0 ± 0,3	120 ± 10

* Performed in the presence of $MgCl_2$.

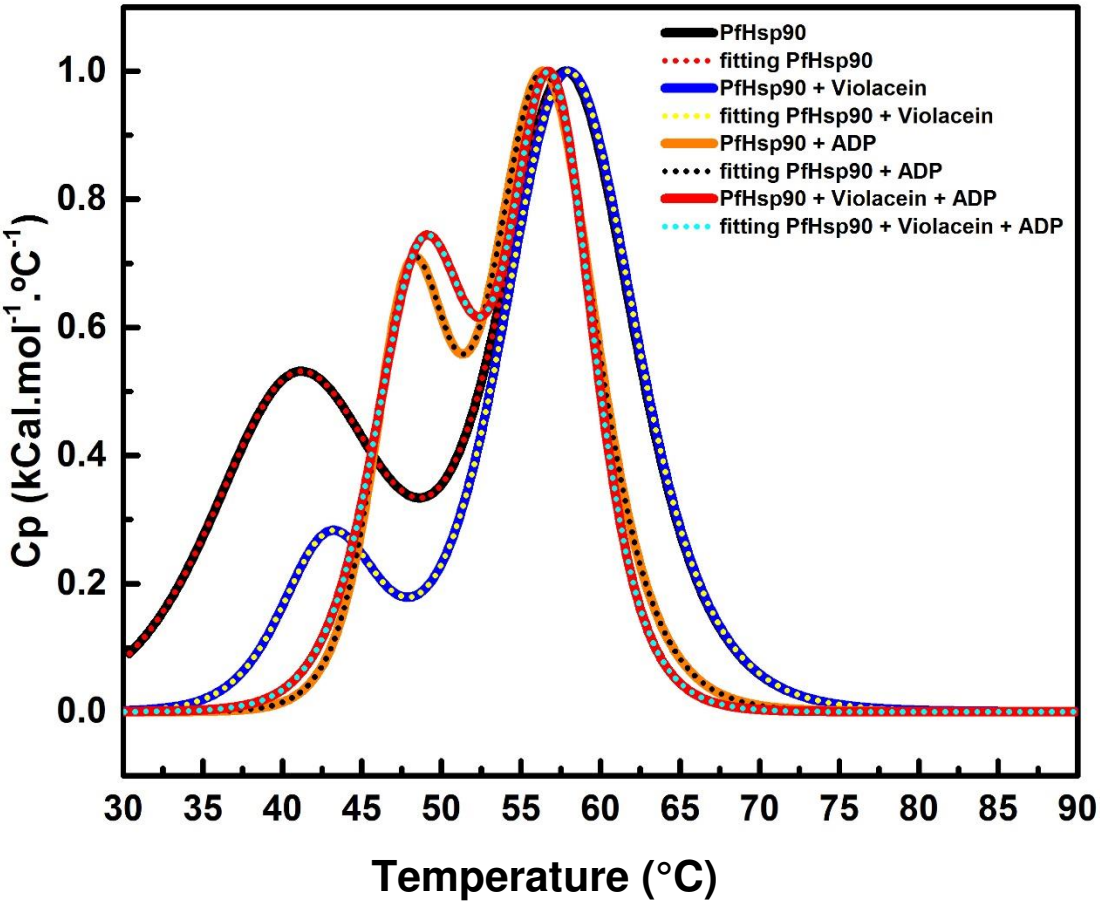

Figure 28. DSC data for full length PfHsp90 incubated with ADP, violacein or both. Continuous line represents DSC curve for full length PfHsp90 (Black), PfHsp90 + violacein (blue), PfHsp90 + ADP (orange) and PfHsp90 + ADP + violacein (red). Dotted line represents DSC fitting curves for full length PfHsp90 (red), PfHsp90 + violacein (yellow), PfHsp90 + ADP (black) and PfHsp90 + violacein + ADP (light blue).

5.13. PfHsp90 ATPase activity upon violacein treatment

Hsp90 proteins are dimeric macromolecules able to reach different conformations driven by an ATP cycle. After ATP binding to chaperone NH_2-terminal domain, Hsp90 slowly achieves the first intermediate state (E1). In this state, the segment lid (C-terminal domain) is closed, but the N-terminal domain remains open in a scissor-like shape, permissive for client substrates interactions. The second intermediate state (E2) is marked by the transient dimerization of the NH_2-terminal domain, culminating on its repositioning. Hsp90 then acquires a "closed" conformation, within which ATP is hydrolyzed releasing ADP and Pi (inorganic phosphate), returning Hsp90 back to the open conformation [197].

Among several compounds known to affect Hsp90-dependent processes, the natural product geldanamycin (GA) is probably the best characterized Hsp90 inhibitor so far [198]. Similarly to violacein, geldanamycin is a compound derived from the secondary metabolism of bacteria, being active against a wide variety of organisms that ranges from prokaryotes to complex eukaryotes [199]. Only 30 years after is discovery as a new bioactive molecule, geldanamycin mechanism of action was elucidated showing crystalographic evidence of molecular binding to human Hsp90 [200].

The initial thoughts regarding Hsp90 activity were based on hypotesis that Hsp90 only worked in a dependent cooperation with cochaperones, and cofactors to develop its role in preventing agreggates and folding mature proteins into their quaternary states [201]. Despite evidence of a conserved nucleotide binding pocket, highlightened when yeast Hsp90 crystal structure was solved, cientists remained skeptical regarding its ATPase activity, unequivocally atributting the ATPase interactions to be driven by Hsp70 when complexed with Hsp90 [201]. Importantly, Hsp90 was shown not only to bind ATP, but to depend on ATP hydrolysis for *in vivo* activity, as mutations in ATP binding pocket impairing nucleotide binding and hydrolysis caused fitness defects in yeast [201]–[204].

Importantly, GA binding site happens in the NH_2-terminal domain within the ATP binding pocket [198], [200]. Indeed, inhibition of Hsp90 by GA happens through competition for nucleotide binding site, culminating in misfolding and degradation of inumerous client protein [205].

For PfHsp90 ATPase activity in the presence of compound, we incubated full length protein pre-treated with different concentrations of violacein prior ATP addition in a way to monitor its hydrolysis into ADP and Pi. Surprisingly, even though previous experiments suggested that violacein could be inhibiting PfHsp90 in a similar way as geldanamycin, by competing with nucleotide binding pocket at the N-terminal domain, our ATPase activity assays pointed the oposite. Instead of inhibiting ATP binding and hydrolysis, violacein seemed to enhance PfHsp90 activation in a dose dependent manner (Figure 29). Although unexpected, compounds that increase Hsp90 ATPase activity have been described before [206]. Tamoxifen was reported to promote relevant docking interactions with Hsp90 ATP binding pocket, being suggested as a competitor of nucleotide binding, inhibiting chaperone activity. However, when ATPase activity assay was performed with full length protein there were a considerable increase in ATP hydrolysis [206].It is important to note that Hsp90 activity relies on tight regulation of ATP hydrolysis for propper functioning as inhibition leads to misfolding and activation culminates in enhaced client aggregation [197], [207]–[210]. Thus, despite modest activation of Hsp90 ATPase activity, is possible that violacein interferes with chaperone function through binding in a distinct site of PfHsp90 N-terminal domain, other than the nucleotide binding pocket.

Importantly, client folding by Hsp90 relies on the energy released from ATP-driven cycle, in which Hsp90 undergoes strikingly conformational remodeling allowing client maturation [211]. The regulation of protein folding activation cycle starts with client protein transfer into Hsp90 dimer. When ATP binds NH_2 terminal domain of Hsp90, the dimeric chaperone dramatically changes its conformation from an “open state” (passive of interacting with unfolded clients) to a “closed state” that will eventually culminates in protein folding and ATP hydrolyses (figure 30). This proccess is highly dependent on Hsp90 interaction with regulatory proteins, the cochaperones, which provides intrinsic assistance along the folding cycle [197].

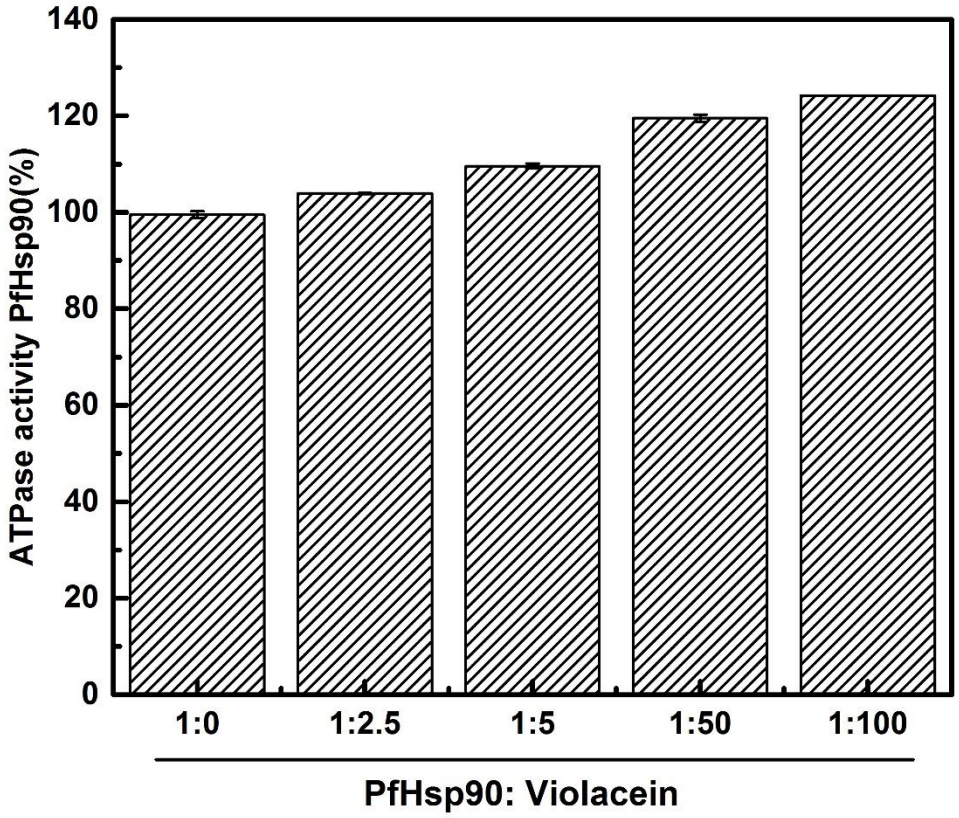

Figure 29. PfHsp90 ATPase activity following violacein pre-treatment. Full length PfHsp90 was incubated or not with different doses of violacein for 1 h prior to ATP incubation and free Pi detection. Bars represent ATPase activity (%) compared to non-treated controls. Concentrations of violacein are expressed in proportions relative to concentration of PfHsp90 as described at the bottom of bars.

From the many cochaperones that interact with Hsp90, Aha1 is the only one known to enhance its ATPase activity [208], [212]. Studies have shown that overexpression of Aha1 in transgenic mouse promoted accumulation of insoluble and oligomeric microtubule-associated protein tau. Tau is able to aggregate causing neurotoxicity promoting cognitive damage [208]. The fact that treatments with Aha1 inhibitor results in solubilization of Tau aggregates suggests that hyperstimulation of Hsp90 ATPase activity might lead to premature release of client protein due to quicker ATP turnover.

Thus, doses of violacein able to enhance PfHsp90 ATPase activity might be able to impair chaperone protein folding cycle, contributing to early release of a non-mature folded protein.

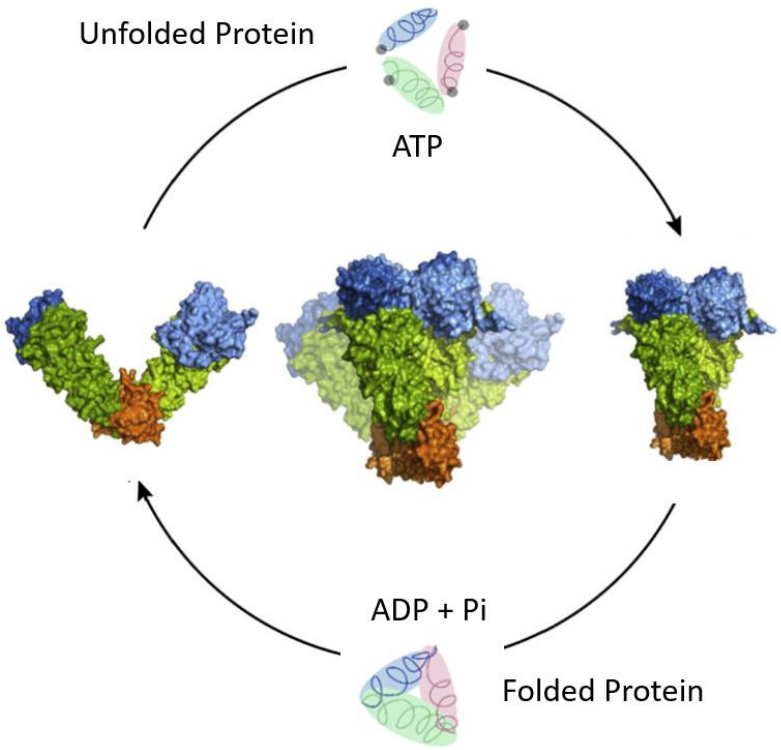

Figure 30. PfHsp90 ATPase folding cycle (Adapted from Li and colleagues, 2012). Hsp90 dimer in a "scissor-like" open conformation binds to ATP and interacts with client substrate. ATP binding leads to protein remodeling that undergoes from "open state" to a "closed state". Client folding is performed with energy released from ATP hydrolysis liberating ADP and inorganic phosphate. After ATP hydrolysis, Hsp90 releases folded protein and rearranges itself again in an open conformation, giving continuity to ATP binding cycle.

5.14. PfHsp90 prevention of aggregation upon violacein treatment

Protein aggegation is known to contribute to several diseases [213]. One of the key features of chaperones as Hsp90, is their ability to assist solubilization and protein refolding, preventing aggregation [214]. We can easily monitor aggregation by light scatter measurements at a determined wavelength, that is, the higher amount of protein clumps, higher will be light absorbance signals [215]. For this experiment we evaluated if the capacity of PfHsp90 to prevent malate dehydrogenase (MDH) aggregation could be disturbed by chaperone-violacein interactions *in vitro*. Although a small impairment on PfHsp90 function, our results didn't show significant changes (~15 % inhibition) in chaperone capability to prevent aggregation even though violacein contributed to acceleration of MDH aggregation (Figure 31A).

It worthnotice that although interactions of Hsp90 multiple domains is required for its full activity, isolated small fragments of Hsp90, ranging from N-terminal to C-terminal domain, were previously shown to prevent protein aggregation [216]. Thus, these studies raise the possibility that even if a compound is able to inhibit one of the domains, Hsp90 would still be able to prevent aggregation through client interactions with other sites of the protein.

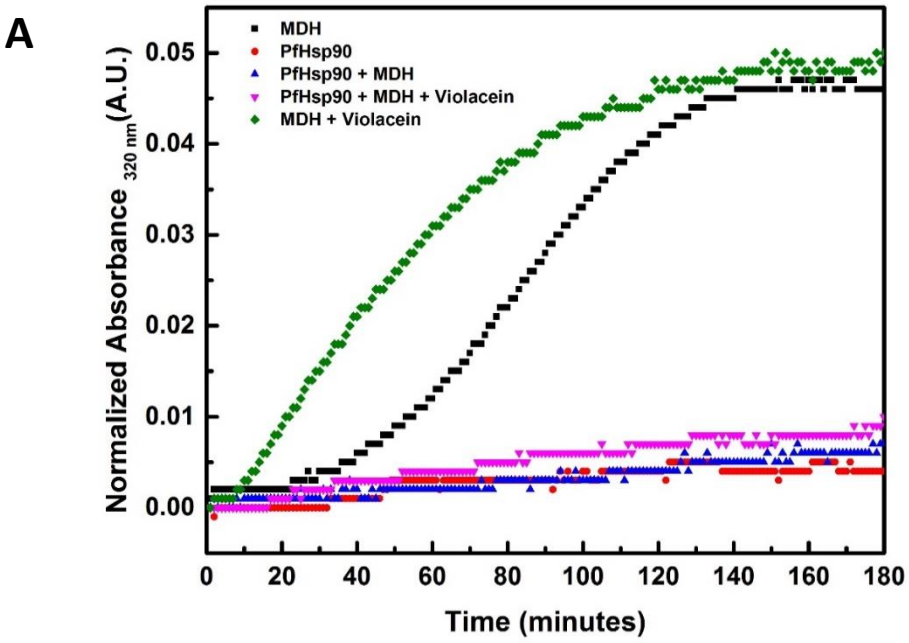

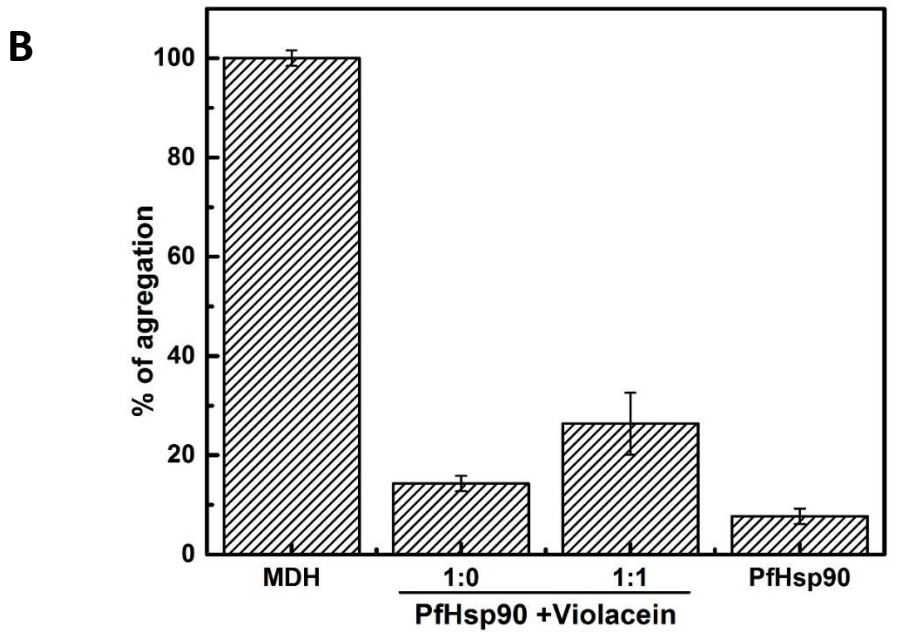

Figure 31. PfHsp90 capability to prevent MDH aggregation upon violacein pre-treatment. Full length PfHsp90 was incubated or not with violacein in an equimolar proportion for 30 minutes prior to MDH incubation. Temperature was raised until 42 °C and consecutives absorbance readings were recorded for 3 h. A) Normalized absorbance data over time for: MDH alone (Black plots), PfHsp90 alone (red plots), PfHsp90 + MDH (blue plots), PfHsp90 + violacein + MDH (pink plots) and MDH + violacein (green plots). B) Bars represent aggregation data (%) compared to non-treated controls. Concentrations of violacein are expressed in proportions relative to concentration of PfHsp90 as described at bottom of the graph.

5.15. Violacein affects the chaperone system machinery

Chaperones as Hsp90 work as hubs on the process of protein quality control, building an interface between protein folding and degradation by the proteasome. Hsp90 inhibitors are able to quickly shift the mode of action of these chaperones from folding to protein degradation, promoting proteostasis imbalance and cellular incapacity to cope with proteotoxic stress [217]. Violacein was shown to induce protein unfolding followed by intense proteasome degradation, commom features of chaperone inhibitors [181], [218], [219].

Although we have shown that violacein is able to cause alterations on secondary structure of PfHsp90, induce N-terminal domain thermalstability and enhance ATPase activity of full length protein in a dose dependent manner, we don't know if this response is specific for PfHsp90 or if violacein is able to affect other chaperones. Chemical genomic profiling is a powerfull tool for elucidating compounds mode of action by pointing either specific targets or biochemical pathways involved on molecule bioactivity mechanism. When we look at Chemical genomic profiling data from all yeast strains carring heterozygous mutant for proteins involved in the chaperone system (178 genes found in www.yeastgenome.org), we can observe that treated groups present higher fitness defects compared with vehicle treated controls (Figure 32). This is a strong indication that violacein can be affecting other components of the chaperone system, reinforcing the need of a potent stress response by the organism to overcome drug effects for survival. To verify if violacein is targeting PfHsp90 exclusively, we tested if violacein was able to affect two essential chaperones for parasite survival: the CCT complex (TriC) and PfHsp70.

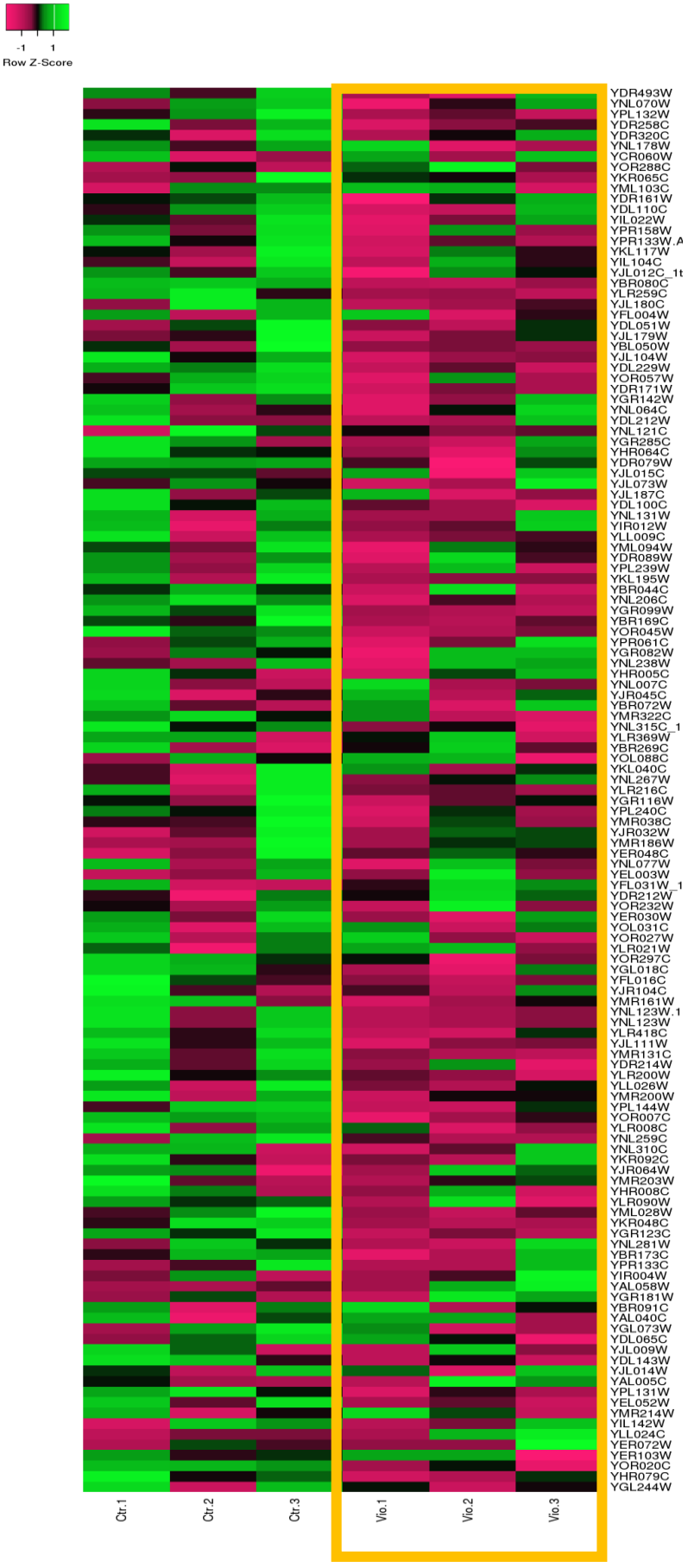
-1
1
Row Z-Score
YDR493W
YNL070W
YPL132W
YDR258C
YDR320C
YNL178W
YCR060W
YOR288C
YKR065C
YML103C
YDR161W
YDL110C
YIL022W
YPR158W
YPR133W_A
YKL117W
YIL104C
YJL012C_1t
YBR080C
YLR259C
YJL180C
YFL004W
YDL051W
YJL179W
YBL050W
YJL104W
YDL229W
YOR057W
YDR171W
YGR142W
YNL064C
YDL212W
YNL121C
YGR285C
YHR064C
YDR079W
YJL015C
YJL073W
YJL187C
YDL100C
YNL131W
YIR012W
YLL009C
YML094W
YDR089W
YPL239W
YKL195W
YBR044C
YNL206C
YGR099W
YBR169C
YOR045W
YPR061C
YGR082W
YNL238W
YHR005C
YNL007C
YJR045C
YBR072W
YMR322C
YNL315C_1
YLR369W
YBR269C
YOL088C
YKL040C
YNL267W
YLR216C
YGR116W
YPL240C
YMR038C
YJR032W
YMR186W
YER048C
YNL077W
YEL003W
YFL031W_1
YDR212W
YOR232W
YER030W
YOL031C
YOR027W
YLR021W
YOR297C
YGL018C
YFL016C
YJR104C
YMR161W
YNL123W.1
YNL123W
YLR418C
YJL111W
YMR131C
YDR214W
YLR200W
YLL026W
YMR200W
YPL144W
YOR007C
YLR008C
YNL259C
YNL310C
YKR092C
YJR064W
YMR203W
YHR008C
YLR090W
YML028W
YKR048C
YGR123C
YNL281W
YBR173C
YPR133C
YIR004W
YAL058W
YGR181W
YBR091C
YAL040C
YGL073W
YDL065C
YJL009W
YDL143W
YJL014W
YAL005C
YPL131W
YEL052W
YMR214W
YIL142W
YLL024C
YER072W
YER103W
YOR020C
YHR079C
YGL244W
Ctr.1
Ctr.2
Ctr.3
Vio.1
Vio.2
Vio.3

Figure 32. Heatmap showing Fitness defect scores from yeast strains carring heterozygous mutant for proteins involved in the chaperone system. Each column represents fitness defect data collected for all mutant strains carrying heterozygous genes for components of the chaperone system (178 genes found in www.yeastgenome.org). While the first 3 columns represents triplicate from pools treated with vehicle control; the columns highlightened by a yellow square, show fitness defect data from pools treated with sublethal doses of violacein (as annotated bellow the graph). Red color express defects in growth, while green color represents improved growth.

5.16. Violacein activity on knockdown *P.falciparum* TRiC (Hsp60)

TRiC complex is a highly conserved protein folding machine composed by two rings containing eight or nine subunits each, which are organized in a cylindrical shape forming a central cavity able to bind to soluble polypeptides. The correct folding of these polypeptides occurs inside the cavity in an ATP dependent manner [220]. Despite initially thoughts that actin and tubulin were the only substrates for TRiC, today it is known that it can fold other proteins and interact with around 10% of newly synthesized proteins in the cell [220]–[222].

In malaria, TRiC seems to be important for the parasite to acquire resistance against the antimalarial drug artemisinin [15], [70]. Transcriptomic analysis of 1043 *P. falciparum* isolates from patients with malaria from Southeast Asia correlated the increased levels of mRNAs for chaperone systems like PROSC and TRiC with parasite artemisinin resistance [42]. Interestingly, TRiC from the red blood cell seems to be involved in the traffic of PfEMP1, the most virulent factor of severe malaria [28]. Despite recent discoveries showing that TRiC might be important for malaria, little is known about its role in malaria pathogenesis, probably due to the lack of a specific inhibitor.

To verify if violacein is able to interfere on *Plasmodium* CCT complex, we decided to test if mutant knockdown parasites for TRiC were more susceptible to violacein treatment than their wild type counterparts. Unlike PfHsp90, is not convenient to express all the eight different subunits of *Plasmodium* CCT complex for biophysical and biochemical assays. For this experiment, we used a regulatable ϴTRiC knockdown parasite line developed by Dra. Spillman and coworkers, from Melbourne University. For this approach, a plasmid containing a Tet repressor (TetR-DOZI) gene and repeated sequences of Tet-Repressor binding aptamer array was

introduced in the 3' UTR of PfΘTRiC [151]. DOZI molecule (development of zygote inhibited) has the ability to bind to aptamer sequences of the mRNA targeting it for degradation. When a compound called aTc (anhydrous tetracycline) is present, it binds to Tet repressor molecule preventing its interaction with aptamer sequences, consequently, DOZI's ability to modify mRNA is blocked, maintaining normal expression levels of PfΘTRiC (Figure 33). We used two different *P. falciparum* mutant strains varying only in the number of aptamer repeats: A3 strain (6 aptamers) and B8 (10 aptamers). The higher the number of aptamer sequences in a strain, more dramatic is its effect in targeting mRNA for degradation. Interestingly, even low doses of aTc seems to protect PfΘTRiC mRNA from Tet-Repressor's effect (Figure 34A and 34B). To examine if PfΘTRiC knockdown strains were more sensitive to violacein than parasites with normal expression of PfΘTRiC, we performed a violacein dose-response curve in both parasites to see if we could find any shift in EC_{50} concentration. Previous study has shown that PfTRiC is essential for parasite growth [151]. When aTc was removed from mutants at ring stage, parasites could develop normally until trophozoite stage, being incapable of forming normal schizonts, with no rings recovered in the next cycle. Removal of aTc at trophozoite stage results in growth arrest, while when aTc is removed at schizonts stage, next cycle rings develop normally until being arrested at trophozoite stage. With this data we can conclude that TRiC is important mostly in trophozoite stage, affecting formation of healthy schizonts and merozoites. Because of impairment in invasion and ΘTRiC knockdown parasites inability to develop into next cycle, we opted to perform drug assays within the same cycle. For that, 0.5 µM of aTc was removed or not from ring stage mutant parasites for 20 h, this period is enough to ensure knockdown was achieved in cell lines with no aTc (Figure 34C). After 20 h, parasites were treated with different doses of violacein for 3h, washed and stained with rhodamine 123 for mitochondrial staining. Despite a trend, we couldn't see any significant change between EC_{50} from both parasites, knockdown and control (Figure 35A and 35B).

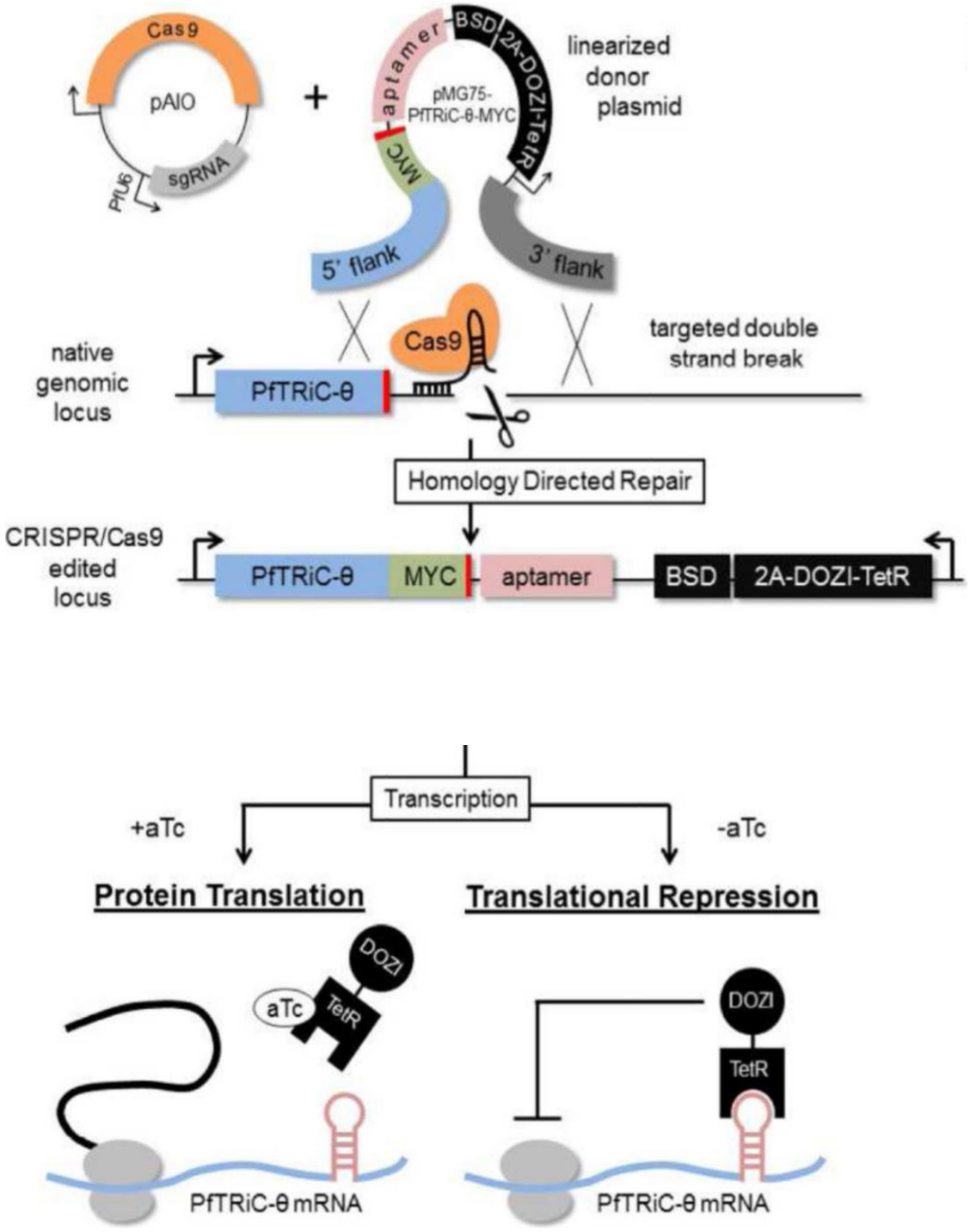

Figure 33. Schematic outlining the strategy used to design PfΘTRiC conditional knockdown (adapted from Spillman and colleagues, 2017)

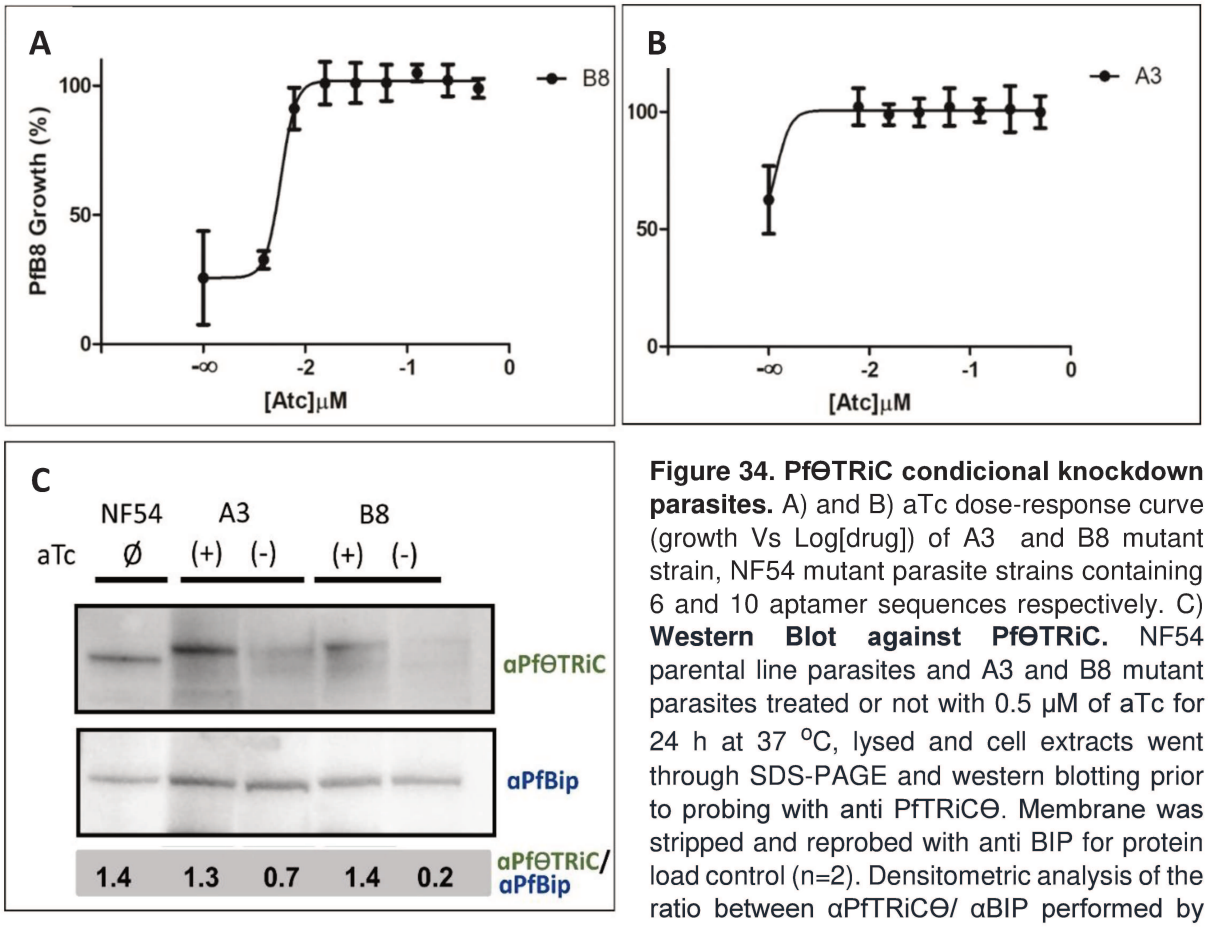

Figure 34. PfΘTRiC condicional knockdown parasites. A) and B) aTc dose-response curve (growth Vs Log[drug]) of A3 and B8 mutant strain, NF54 mutant parasite strains containing 6 and 10 aptamer sequences respectively. C) **Western Blot against PfΘTRiC.** NF54 parental line parasites and A3 and B8 mutant parasites treated or not with 0.5 µM of aTc for 24 h at 37 ^{o}C, lysed and cell extracts went through SDS-PAGE and western blotting prior to probing with anti PfTRiCΘ. Membrane was stripped and reprobed with anti BIP for protein load control (n=2). Densitometric analysis of the ratio between αPfTRiCΘ/ αBIP performed by ImageJ are shown in the gray box.

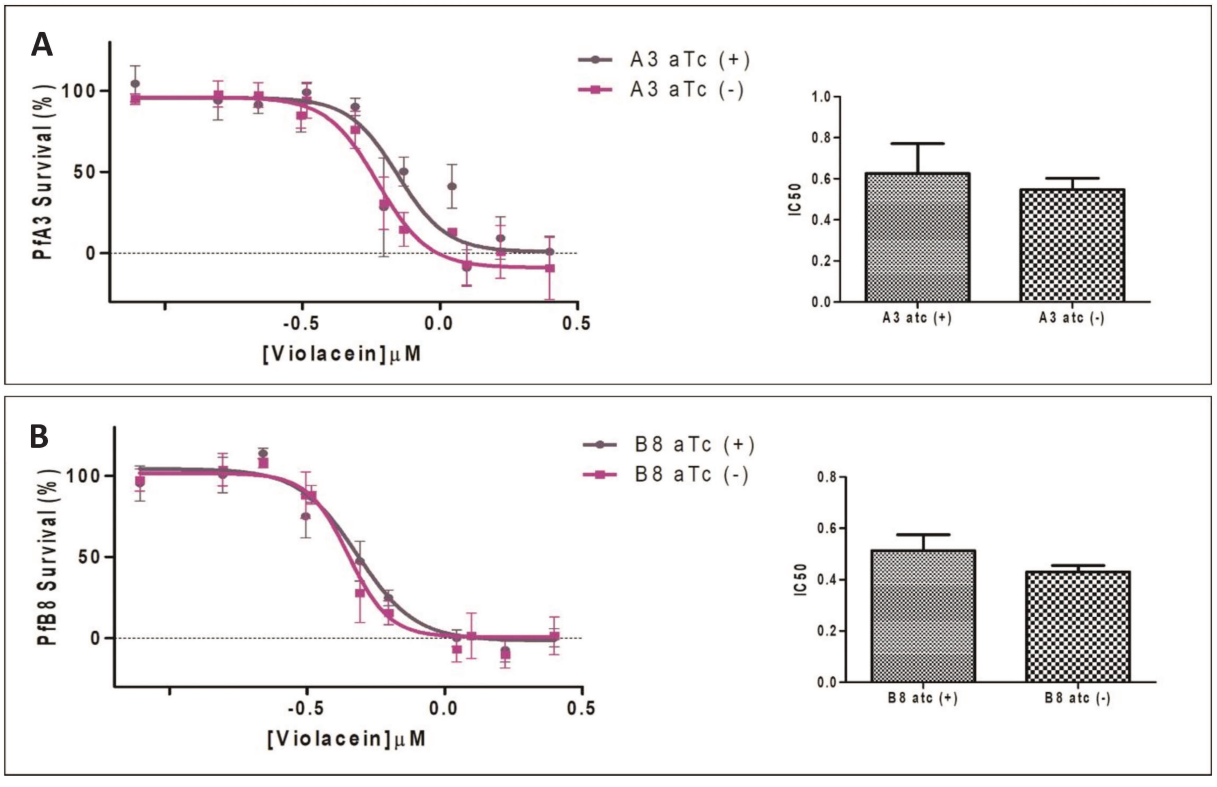

Figure 35. PfTRiC knockdown EC50 shift upon violacein treatment. A) and B) Violacein dose-response curve (normalized mitochondrial staining signal Vs Log [drug]) of PfA3 and PfB8 respectively. At ring stage, mutants were treated or not with 0.5 µM of aTc for 20 h at 37 ºC prior to 3 h incubation with different doses of violacein, parasites were then stained with rhodamine 123 for mitochondrial staining of trophozoites. At the side of each dose-response graph there is a bar graph showing the average of EC_{50} values collected from three different experiments comparing PfΘTRiC knockdown cell lines with normal PfΘTRiC cell lines. P>0.05, GraphPad4.

5.17. PfHsp70 ATPase activity upon violacein treatment

Similar to both, Hsp90 and TRiC, heat shock protein 70 (Hsp70) are highly conserved proteins across different species, phylums and kingdoms, being one of the major components of the Heat Shock family [223], [224].

There are three major processess assisted by Hsp70 on folding of non-native proteins: native state folding, prevention of aggregation and solubilization of aggregates for futher refolding [225]. Akin other chaperoes, for client protein folding, Hsp70 also relies on ATP-expendind cycles, within which it differs from Hsp90 and TRiC, as it doesn't requires dimerization or any other kind of complex organization for fully ATP-cycle completion, being able to promote client folding in a monomeric state. In therms of structure, Hsp70 has a nucleotide binding domain (NBD) and a peptide binding domain (PBD). The nucleotide domain is comprised by two lobes (I and II) containing two subdomains each (IA, IB, IIA and IIB), in which ATP is bound when tightly surrounded by both NBD lobes in a sanduwich-like organization. The peptide binding domain is structured by two subdomains: alpha (α-PBD) and beta (β-PBD). When Hsp70 hydrolyses ATP into ADP, client peptides with long exposed hydrophobic chains bind to β-PBD channel (usually delivered by cochapeones), forming strong chemical interactions, in which α-PBD folds into β-PBD for subsequent peptide refolding. Whereas when ADP is exchanged by ATP (usually with cochaperone aid), the chaperone goes through dramatic conformational remodeling that results on decreased binding affinity for the substrate, causing its subsequent release [226]. There are six genes enconding Hsp70 chaperones on *P. falciparum* genome, three of them encodes cytosolic chaperones and three encodes specific isoforms from mitochondria, endoplasmatic reticulum and microssomes [32], [34], [227].

Unlike the CCT complex, expression and purification of PfHsp70 is highly achievable. Thus, we performed biochemical assays on the major *P. falciparum* cytosolic isoform, PfHsp70-1, to verify if violacein is able to affect PfHsp70 ATPase cycle as an indirect measurement of proteostasis impairment.

Curiously, even with the ability to stimulate PfHsp90 ATPase activity under high concentrations and despite no signs of activity against PfCCT complex, violacein was shown to completely inhibit PfHsp70 at low concentrations (Figure 36), with nearly 100% of chaperone ATPase activity inhibition at a proportion of 1 to 2.5 (PfHSP70:violacein). This result suggests that inhibition of Hsp70 can be a major contributor for the imbalance on stress response highlightned on Chemical Genomic Profiling screening, as abnormal regulation of Hsp70 nucleotide cycle is essential for yeast survival [228]. Therefore, we propose that violacein is able to impair PfHsp70 ATP hydrolysis, in a way that the chaperone never achieves a conformation with high affinity for the client peptide, making substrate folding unsustainable.

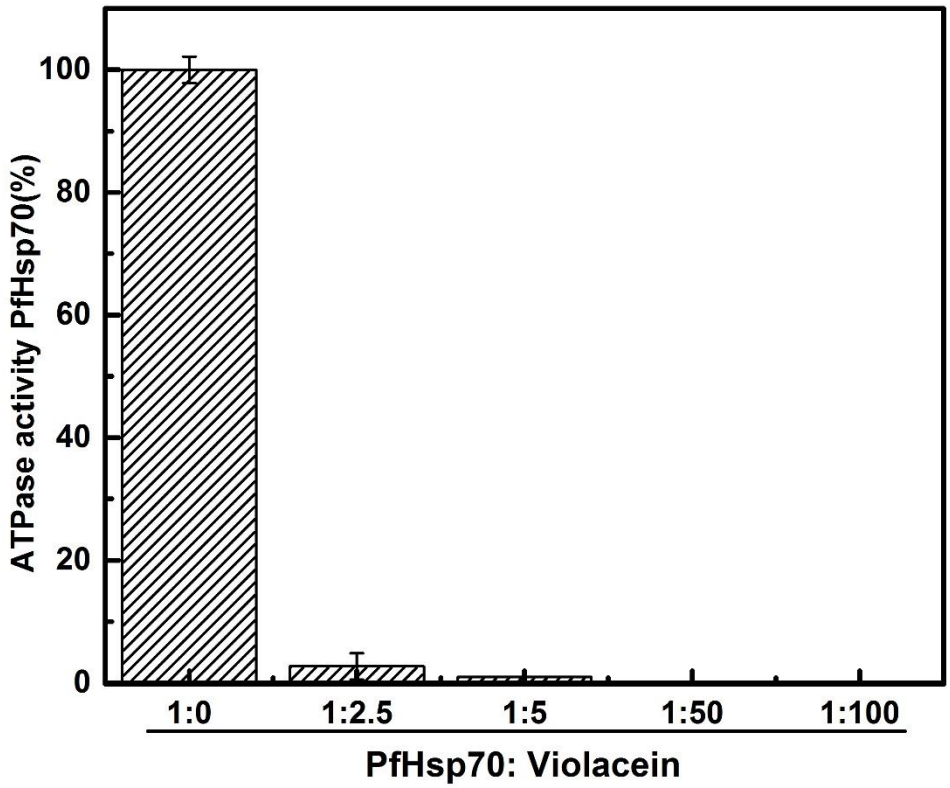

Figure 36. PfHsp70 ATPase activity following violacein treatment. Full length PfHsp70 was incubated or not with different doses of violacein for 1 h prior to ATP incubation and free Pi detection. Bars represent ATPase activity (%) compared to non-treated controls. Concentrations of violacein are expressed in proportions relative to concentration of PfHsp70 as described at bottom of the graph.

5.18. PfHsp70 prevention of aggregation upon violacein treatment

The high negative correlation between protein expression and aggregation rates suggests that proteins co-evolved to become soluble enough within specific niches to develop their biological functions, in an extremely small edge of stability [229]. Multiple types of environmental variations such as heat, pH, and protein concentration or even mutations and chemical interference can destabilize proteins making them prone to loss of function due to aggregation.

One of chaperones major functions within the cell is their ability to aid protein disaggregation, allowing cellular survival even under stress conditions. Studies performed *in vitro* and *in vivo* have linked temperature-induced aggregate clearance with the presence of chaperones Hsp104 (from yeast) and ClpB (from *E. coli*) that were later shown inability to disaggregate proteins by themselves, acting in majority as Hsp70 cooperators on protein disaggregation process [214].

Hsp70 is also able to prevent aggregation through recognition and rescue of exposed hydrophobic substrate regions by its β-Peptide Binding Domain. To evaluate if PfHsp70 has its ability to prevent aggregation preserved in the presence of violacein, we monitored Malate Dehydrogenase protein aggregation rates at 42 °C under different conditions. Unlike PfHsp90, in the presence of violacein PfHsp70 ability to prevent protein aggregation at equimolar concentrations of chaperone and compound was greatly decreased (~70% aggregation) (Figure 37). This data raises the possibility that violacein might impair substrate binding to PfHsp70. Interestingly, violacein was previously shown (Figure 36) to impair PfHsp70 ATP hydrolysis that culminates in decreased affinity for substrate binding. However, with the present information, we cannot affirm how violacein interacts with PfHsp70 due to its bidirectional heterotrophic allosteric mechanism, in which alterations on the Nucleotide Binding Domain reflects on the Peptide Binding Domain [230]. It is interesting to note that violacein accelerates MDH aggregation in a chaperone non-dependent fashion, shedding light on a different mechanism involving non-specific

protein damage, reinforcing the need of a strong cellular stress response to avoid proteostasis collapse.

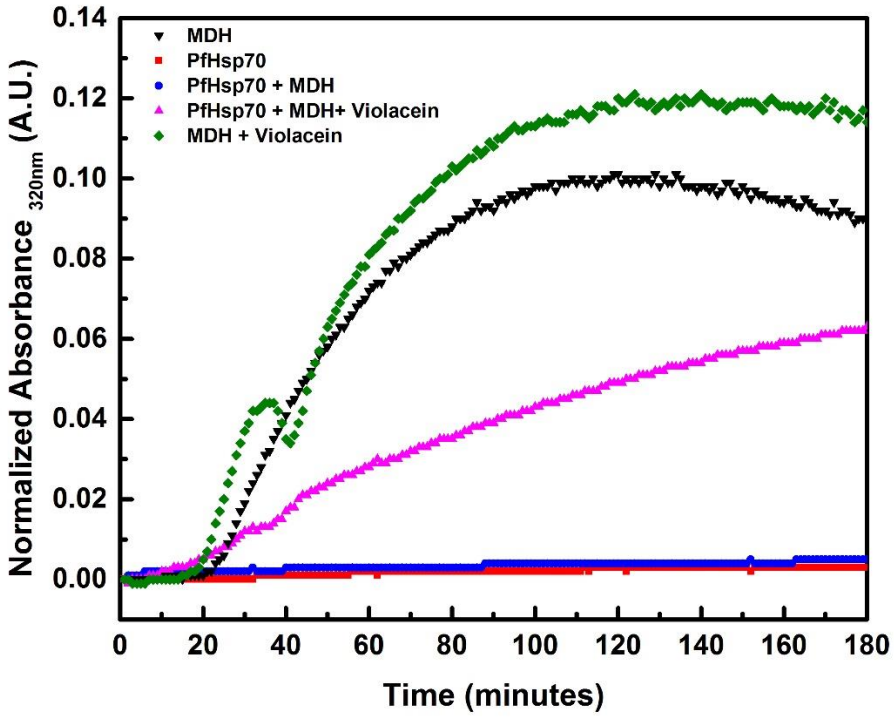

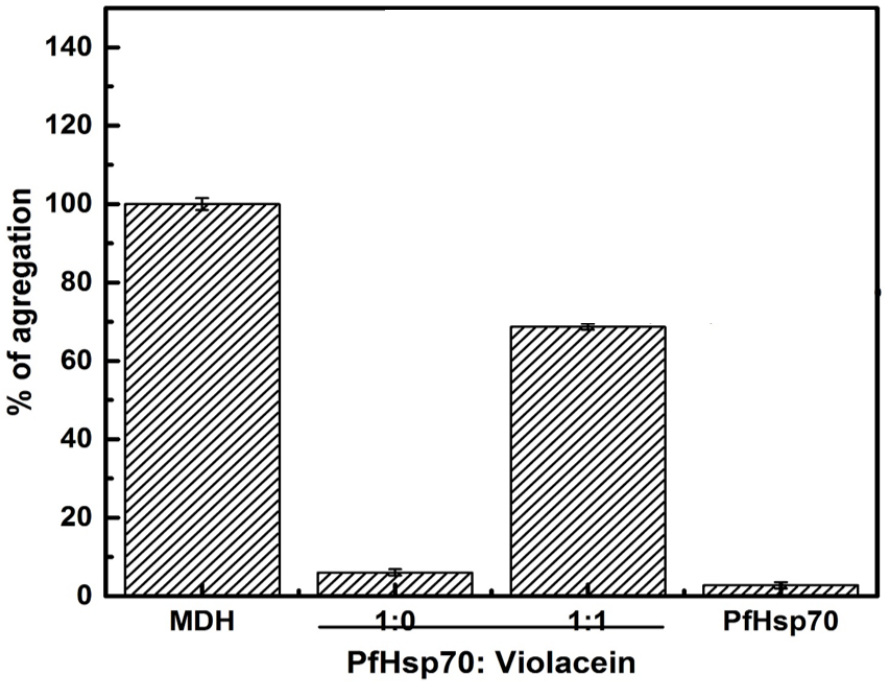

Figure 37. PfHsp70 capability to prevent MDH aggregation upon violacein pre-treatment. Full length PfHsp70 was incubated or not with violacein in an equimolar proportion for 30 minutes prior to MDH incubation. Temperature was raised until 42 °C and consecutives absorbance readings were recorded for 3 h. A) Normalized absorbance data over time for: MDH alone (Black plots), PfHsp70 alone (red plots), PfHsp70 + MDH (blue plots), PfHsp70 + violacein + MDH (pink plots) and MDH + violacein (green plots). B) Bars represent aggregation data (%) compared to non-treated controls. Concentrations of violacein are expressed in proportions relative to concentration of PfHsp70 as described at bottom of the graph.

5.19. Final Remarks

Plasmodium parasites need to deal with different types of adversities to establish malaria infection, having evolved to digest haemoglobin as their main source of amino acids. The toxic reactive oxygen species (ROS) and toxic free haem (ferri/ ferroprotoporphyrin IX) generated as a result of haemoglobin degradation represents a threat for parasite survival [31]. In fact, many of the commercially available antimalarial compounds, such as chloroquine, causes *Plasmodium* death by impairing parasite detoxification system, blocking free haem conversion into non-toxic β-haematin [156].

Furthermore, parasite faces nearly 10 °C heat shock during transmission from the anopheline mosquito to the human host, with constant temperature variations derived from patients fever episodes. Not surprisingly, genes from the chaperone system compose around 2 % of *Plasmodium* genome [32]. The importance of chaperones for malaria pathogenesis and treatment was reinforced by studies suggesting that high levels of *Plasmodium* mRNAs for chaperone systems like PROSC and TRiC correlates with parasite resistance to artemisinin [42]. Indeed artemisinin induces promiscuous protein damage and accumulation of polyubiquitinated proteins as a result of partial proteasome inhibition, causing parasite death due to proteostasis collapse. It makes sense that parasites with stronger chaperone network would be more likely to survive artemisinin treatment, especially during early ring stages, within which artemisinin is not fully activated [43], [68], [76]. Similar to artemisinin, compounds hitting the proteasome have also shown relevant antimalarial activity, promoting parasite death through proteotoxic stress pathway, highlightening a growing interest for compounds targeting *Plasmodium* stress response [40], [46], [63], [64], [66], [68], [184].

Violacein is a natural tryptophan-derived purple compound produced during the secondary metabolism of several gram-negative bacteria [96]. In the present work, we suggest through Chemical Haploinsufficiency Profiling screening, followed by biochemical and biophysical validation, that violacein targets the chaperone system response, with two Hsp90 co-chaperones appearing as potential targets at HIP. When we looked at data from all yeast strains carring heterozygous genes for proteins involved in the chaperone system we could observe a clear pattern of compound-induced fitness defects, suggesting that the chaperone pathway could be affected as a whole.

We have investigated violacein interaction with three major components of chaperone system: PfHsp90, PfTRiC and PfHsp70. In summary, our data showed that violacein is able to bind, thermostabilize PfHsp90 NH2-terminal domain and increase chaperone ATPase activity at high concentrations, possibly leading to early release of client proteins as a consequence of quick ATP turnover. Importantly, despite no clear signs of interplay with PfTRiC, violacein was shown to interact with PfHsp70, being able to completely inhibit chaperone ATPase cycle, which culminates in decreased affinity for unfolded substrates. Moreover, PfHsp70 becomes unable to prevent protein aggregation in the presence of violacein, emphasizing our data collected from CGP. Interestingly, the compound is able to accelerate protein aggregation in a chaperone non-dependent fashion, shedding light on a different mechanism involving non-specific protein damage.

Consistent with our results pointing chaperones as violacein target, parasites treated with the molecule presented protein unfolding and intense proteasome degradation (commom features of chaperone inhibitors), but no signs of endoplasmatic reticulum stress activation [181], [218], [219]. It is possible that parasite still carries on protein synthesis in a way to compensate proteolysis of essential proteins that were targeted to the proteasome as a consequence of chaperone overload. However, protein synthesis itself is an error-prone process that relies on chaperones to succeed, reinforcing violacein-induced proteostasis collapse (Figure 39).

To finalize, we propose that violacein is able to inhibit PfHsp70 at biologically relevant doses, suggesting that it might also be able to affect PfHsp90 activity; as

PfHsp90 activity *in vivo* is complex and highly dependent on interactions with cochaperones, difficult conditions to faithfully reproduce experimentally. Both chaperones are essential and extremelly conserved across different phylums and kingdoms with several proteins relying on an orchestrated activity from both chaperones to be correctelly folded [232]. Thus, their inhibition is consistent with violacein activity against a wide variety of organisms, including cancer cells, reinforcing the existence of a shared mechanism of action.

Lastly, violacein most interesting activity within malaria context happens to be on gametocytes. The transmissive forms of the parasite have been extensively persuit as targets on transmission blocking strategies [167]. Currently, the only FDA approved drug active against late stage gametocytes is primaquine [169]. The use of primaquine for malaria treatment raises concern regarding its safety due to its haemolytic profile on patients with G6PD deficience, boosting the need for better drugs [89]. Curiously, violacein have shown good activity against Stage V gametocytes, being around 10 times more active than DHA (Violacein EC_{50}~ 270 nM) and nearly 2 times more active on gametocytes than on asexual stages. Our data reinforce previous studies highlightening the importance of a sharp chaperone-proteasome system required for proper parasite protein turnover; an essential process required by parasites during gametocyte development and sexual differentiation [62], [233].

Similar to proteasome inhibitors, chaperone inhibitors might face the same obstacles regarding compound selectivity for the parasite target due to high rates of protein conservation. Moreover, violacein small molecule might provide a good scafold to be considerate for future antimalarial drug design approaches due to its transmission blocking properties.

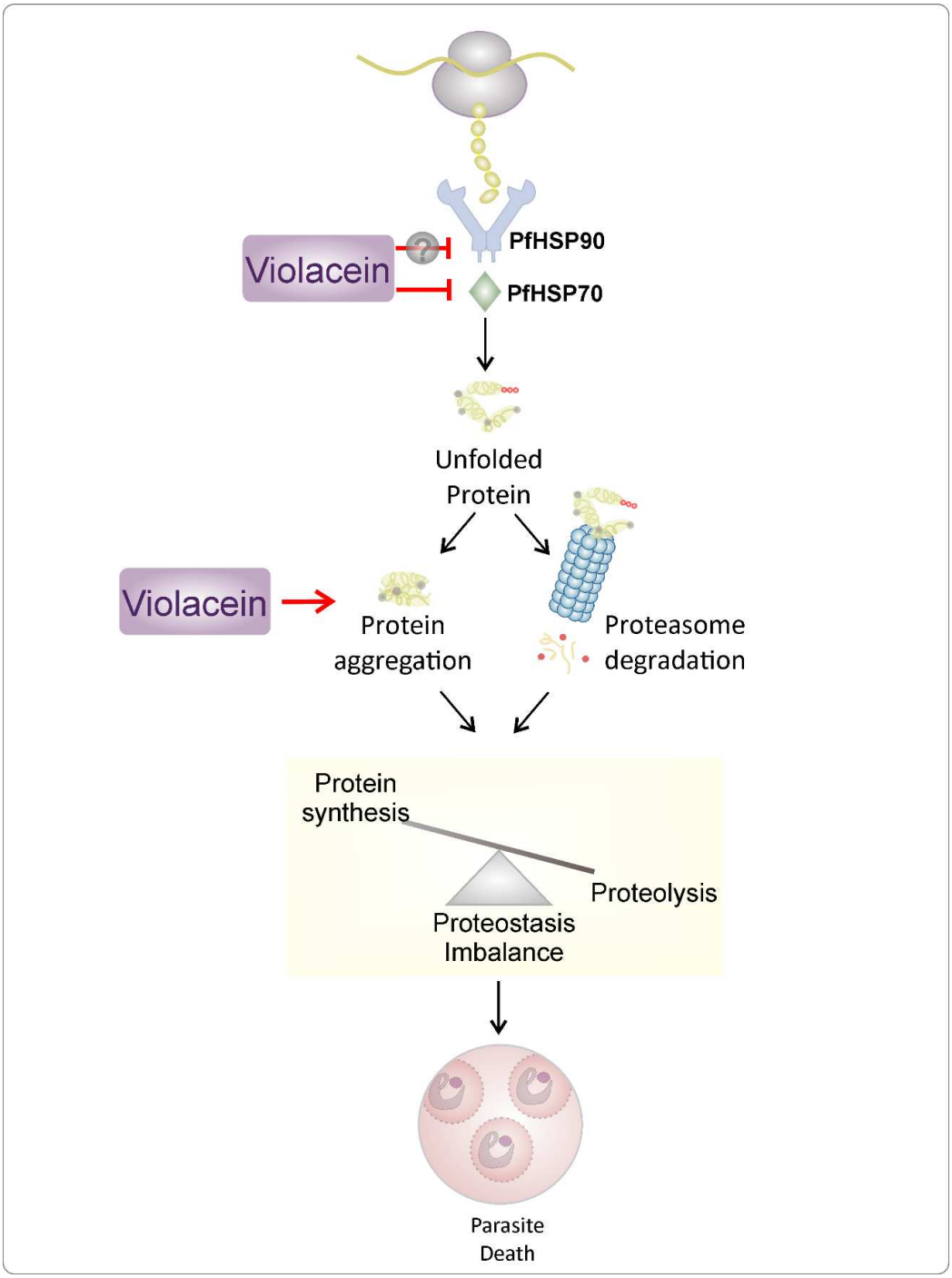

Figure 39. Proposed violacein mechanism of action in *Plasmodium*. Violacein promotes PfHsp70 inhibition with possible impairment on PfHsp90 chaperone activity, preventing folding of damaged and newly synthesized peptides added to induction of protein aggregation in a chaperone non-dependent fashion. Chaperone overburden shifts its function towards proteolytic pathways, culminating in protein polyubiquitination and intense proteasome degradation that leads to a proteostasis imbalance causing parasite death. Despite intense proteolysis, protein synthesis is still being carried on, possibly in an attempt to compensate loss of essential proteins by the proteasome, reinforcing violacein-induced proteostasis collapse.

6. Conclusions

1. Violacein has activity against *Plasmodium falciparum* strains *in vitro*
2. When it comes to asexual activity violacein is more active against trophozoite stages
3. Violacein is a fast acting compound
4. Violacein has low-mid activity against liver stage parasites
5. Violacein is more active against sexual stages rather than asexuals, but is not able to prevent mosquito fertilization
6. Violacein causes parasite protein unfolding, polyubiquitination followed by intense protein degradation by the proteasome
7. Violacein binds PfHsp90 NH2-terminal domain and increases chaperone ATPase activity in a dose-dependent manner at high concentrations
8. Violacein binds the peptide binding domain of PfHsp70 and inhibits chaperone ATPase activity at low doses, impairing its ability to prevent aggregation
9. Violacein is able to accelerate protein aggregation in a chaperone non-dependent fashion
10. Violacein seems to cause *Plasmodium* death through proteostasis imbalance as a consequence of chaperone system collapse

7. References

[1] *World malaria report 2017*. 2017.

[2] *World malaria report 2018*. 2018.

[3] F. E. G. Cox, “History of the discovery of the malaria parasites and their vectors,” no. Figure 1, pp. 1–9, 2010.

[4] “World Malaria Report 2015,” 2015.

[5] W. M. Report, *World malaria report 2016*. 2016.

[6] A. F. Cowman, D. Berry, and J. Baum, “The cellular and molecular basis for malaria parasite invasion of the human red blood cell,” *J. Cell Biol.*, vol. 198, no. 6, pp. 961–971, 2012.

[7] T. F. De Koning-ward, M. W. A. Dixon, L. Tilley, and P. R. Gilson, “Plasmodium species: master renovators of their host cells,” *Nat. Publ. Gr.*, 2016.

[8] A. F. Cowman, J. Healer, D. Marapana, and K. Marsh, “Review Malaria : Biology and Disease,” *Cell*, vol. 167, no. 3, pp. 610–624, 2016.

[9] E. I. N. The, “W OMEN ’ S H EALTH IN THE D EVELOPING W ORLD Malaria and Pregnancy :,” vol. 2, no. 3, pp. 186–192, 2009.

[10] D. D. Laishram, P. L. Sutton, N. Nanda, V. L. Sharma, R. C. Sobti, and J. M. Carlton, “The complexities of malaria disease manifestations with a focus on asymptomatic malaria,” *Malar. J.*, vol. 11, no. 1, p. 29, 2012.

[11] I. Chen, S. E. Clarke, R. Gosling, B. Hamainza, and G. Killeen, “‘ Asymptomatic ’ Malaria : A Chronic and Debilitating Infection That Should Be Treated,” pp. 1–11, 2016.

[12] E. Talundzic, S. A. Okoth, and K. Congpuong, “Selection and Spread of Artemisinin-Resistant Alleles in Thailand Prior to the Global Artemisinin Resistance Containment Campaign,” pp. 1–14, 2015.

[13] H. Noedl *et al.*, “Artemisinin Resistance in Cambodia : A Clinical Trial Designed to Address an Emerging Problem in Southeast Asia,” vol. 51, no. June, 2018.

[14] J. M. Anderson *et al.*, “Spread of Artemisinin Resistance in,” 2014.

[15] “The 2015 Nobel Prize in Physiology or Medicine - Press Release.” .

[16] X. Su and L. H. Miller, “HHS Public Access,” vol. 58, no. 11, pp. 1175–1179, 2016.

[17] S. M. Chenet, S. A. Okoth, C. S. Huber, and J. Chandrabose, “Independent Emergence of the Plasmodium falciparum Kelch Propeller Domain Mutant Allele C580Y in Guyana,” vol. 213, no. June, pp. 2016–2019, 2018.

[18] A. J. Tatem, D. L. Smith, P. W. Gething, C. W. Kabaria, R. W. Snow, and S. I. Hay, “Malaria Elimination 2 Ranking of elimination feasibility between malaria-endemic countries,” *Lancet*, vol. 376, no. 9752, pp. 1579–1591, 2010.

[19] A. Sturm, R. Menard, and V. T. Heussler, “Manipulation of Host Hepatocytes,” vol. 1287, no. 2006, 2014.

[20] B. Nyboer, K. Heiss, A. Mueller, and A. Ingmundson, “International Journal of Medical Microbiology The Plasmodium liver-stage parasitophorous vacuole : A front-line of communication between parasite and host,” *Int. J. Med. Microbiol.*, vol. 308, no. 1, pp. 107–117, 2018.

[21] S. Charpian and J. M. Przyborski, “Protein transport across the parasitophorous vacuole of Plasmodium falciparum: Into the great wide open,” *Traffic*, vol. 9, no. 2, pp. 157–165, 2008.

[22] M. Moras, S. D. Lefevre, and M. A. Ostuni, “From Erythroblasts to Mature Red Blood Cells: Organelle Clearance in Mammals,” *Front. Physiol.*, vol. 8, no. December, pp. 1–9, 2017.

[23] C. A. Moxon, G. E. Grau, and A. G. Craig, “Malaria : modification of the red blood cell and consequences in the human host,” pp. 670–679, 2011.

[24] M. J. Weiss and C. O. Santos, “Review article Chaperoning erythropoiesis,”

vol. 113, no. 10, pp. 2136–2145, 2016.

[25] M. J. Weiss and C. O. Santos, “Review article Chaperoning erythropoiesis,” vol. 113, no. 10, pp. 2136–2145, 2018.

[26] A. Ghosh, G. Garee, E. A. Sweeny, Y. Nakamura, and D. J. Stuehr, “Hsp90 chaperones hemoglobin maturation in erythroid and nonerythroid cells,” pp. 1117–1126, 2018.

[27] C. T. Wagner, I. Y. Lu, M. H. Hoffman, W. Q. Sun, J. D. Trent, and J. Connor, “T-complex Polypeptide-1 Interacts with the Erythrocyte Cytoskeleton in Response to Elevated Temperatures,” *J. Biol. Chem.*, vol. 279, no. 16, pp. 16223–16228, 2004.

[28] S. Batinovic *et al.*, “An exported protein-interacting complex involved in the trafficking of virulence determinants in Plasmodium-infected erythrocytes,” *Nat. Commun.*, vol. 8, no. May, pp. 1–14, 2017.

[29] P. Inácio *et al.*, “Parasite-induced ER stress response in hepatocytes facilitates Plasmodium liver stage infection,” vol. 16, no. 8, pp. 955–964, 2015.

[30] E. Jortzik and K. Becker, “International Journal of Medical Microbiology Thioredoxin and glutathione systems in Plasmodium falciparum,” *Int. J. Med. Microbiol.*, vol. 302, no. 4–5, pp. 187–194, 2012.

[31] K. Becker, L. Tilley, J. L. Vennerstrom, D. Roberts, S. Rogerson, and H. Ginsburg, “Oxidative stress in malaria parasite-infected erythrocytes : host – parasite interactions,” vol. 34, pp. 163–189, 2004.

[32] P. Acharya, R. Kumar, and U. Tatu, “Chaperoning a cellular upheaval in malaria: Heat shock proteins in Plasmodium falciparum,” *Mol. Biochem. Parasitol.*, vol. 153, no. 2, pp. 85–94, 2007.

[33] G. Banumathy, V. Singh, and U. Tatu, “Host chaperones are recruited in membrane-bound complexes by Plasmodium falciparum,” *J. Biol. Chem.*, vol. 277, no. 6, pp. 3902–3912, 2002.

[34] S. Külzer *et al.*, “Plasmodium falciparum-encoded exported hsp70/hsp40 chaperone/co-chaperone complexes within the host erythrocyte,” *Cell.*

Microbiol., vol. 14, no. 11, pp. 1784–1795, 2012.

[35] L. Neckers and U. Tatu, “Molecular Chaperones in Pathogen Virulence: Emerging New Targets for Therapy,” *Cell Host Microbe*, vol. 4, no. 6, pp. 519–527, 2008.

[36] S. J. C. Gosline *et al.*, “Intracellular eukaryotic parasites have a distinct unfolded protein response,” *PLoS One*, vol. 6, no. 4, 2011.

[37] A. Buchberger, B. Bukau, and T. Sommer, “Protein Quality Control in the Cytosol and the Endoplasmic Reticulum: Brothers in Arms,” *Mol. Cell*, vol. 40, no. 2, pp. 238–252, 2010.

[38] G. C. Brown, “Total cell protein concentration as an evolutionary constraint on the metabolic control distribution in cells,” *J. Theor. Biol.*, vol. 153, no. 2, pp. 195–203, 1991.

[39] S. Külzer *et al.*, “Parasite-encoded Hsp40 proteins define novel mobile structures in the cytosol of the P. falciparum-infected erythrocyte,” *Cell. Microbiol.*, vol. 12, no. 10, pp. 1398–1420, 2010.

[40] S. R. Pavithra, R. Kumar, and U. Tatu, “Systems analysis of chaperone networks in the malarial parasite Plasmodium falciparum,” *PLoS Comput. Biol.*, vol. 3, no. 9, pp. 1701–1715, 2007.

[41] R. M. Fairhurst, “Year Makes,” vol. 28, no. 5, pp. 417–425, 2016.

[42] S. Mok *et al.*, “Europe PMC Funders Group Population transcriptomics of human malaria parasites reveals the mechanism of artemisinin resistance,” vol. 347, no. 6220, pp. 431–435, 2017.

[43] J. L. Bridgford *et al.*, “proteins and inhibiting the proteasome,” *Nat. Commun.*, no. 2018, pp. 1–9.

[44] N. Ponts *et al.*, “Unraveling the Ubiquitome of the Human Malaria Parasite * □,” vol. 286, no. 46, pp. 40320–40330, 2011.

[45] S. Chaubey, M. Grover, and U. Tatu, “Endoplasmic Reticulum Stress Triggers Gametocytogenesis in the Malaria Parasite □,” vol. 289, no. 24, pp. 16662–

16674, 2014.

[46] L. Galluzzi, A. Diotallevi, and M. Magnani, “Endoplasmic reticulum stress and unfolded protein response in infection by intracellular parasites,” *Futur. Sci. OA*, vol. 3, no. 3, p. FSO198, 2017.

[47] F. C. Koyama, M. F. Azevedo, A. Budu, and D. Chakrabarti, “Melatonin-Induced Temporal Up-Regulation of Gene Expression Related to Ubiquitin / Proteasome System (UPS) in the Human Malaria Parasite Plasmodium falciparum,” pp. 22320–22330, 2014.

[48] P. Res, “Ubiquitin proteasome system and the atypical kinase PfPK7 are involved in melatonin signaling in Plasmodium falciparum,” 2012.

[49] P. H. Scarpelli, C. Currà, and C. R. S. Garcia, “Ubiquitin Proteasome System as a Potential Drug Target for Malaria,” pp. 1–6, 2018.

[50] C. Spycher *et al.*, “An ER-directed transcriptional response to unfolded protein stress in the absence of conserved sensor-transducer proteins in Giardia lamblia,” vol. 88, no. April, pp. 754–771, 2013.

[51] K. M. Krishnan and K. C. Williamson, “The proteasome as a target to combat malaria : Hits and Misses,” *Transl. Res.*, 2018.

[52] S. Rathore *et al.*, “A cyanobacterial serine protease of Plasmodium falciparum is targeted to the apicoplast and plays an important role in its growth and development,” vol. 77, no. June, pp. 873–890, 2010.

[53] S. Rathore *et al.*, “Disruption of a mitochondrial protease machinery in Plasmodium falciparum is an intrinsic signal for parasite cell death,” *Cell Death Dis.*, vol. 2, no. 11, pp. e231-12, 2011.

[54] M. J. C. and S. Urbe, “Minireview Ubiquitin : Same Molecule , Different Degradation Pathways,” *Cell*, vol. 143, no. 5, pp. 682–685, 2010.

[55] N. Gallastegui and M. Groll, “The 26S proteasome : assembly and function of a destructive machine,” *Trends Biochem. Sci.*, vol. 35, no. 11, pp. 634–642, 2010.

[56] K. Hofmann, “Ubiquitin-binding domains and their role in the DNA damage response,” vol. 8, pp. 544–556, 2009.

[57] L. Hicke, “A New Ticket for Entry into Budding Vesicles — Ubiquitin,” vol. 106, pp. 527–530, 2001.

[58] M. Nigel, H. Arndt, and G. Pradel, “International Journal for Parasitology : Drugs and Drug Resistance The proteasome of malaria parasites : A multi-stage drug target for chemotherapeutic intervention ?,” *Int. J. Parasitol. Drugs Drug Resist.*, vol. 2, pp. 1–10, 2012.

[59] L. Wang *et al.*, “Characterization of the 26S proteasome network in Plasmodium falciparum,” *Nat. Publ. Gr.*, pp. 1–14, 2015.

[60] D. D. Chung, N. Ponts, J. Prudhomme, E. M. Rodrigues, and K. G. Le Roch, “Characterization of the Ubiquitylating Components of the Human Malaria Parasite ’ s Protein Degradation Pathway,” vol. 7, no. 8, pp. 1–12, 2012.

[61] M. N. Aminake *et al.*, “Thiostrepton and Derivatives Exhibit Antimalarial and Gametocytocidal Activity by Dually Targeting Parasite,” vol. 55, no. 4, pp. 1338–1348, 2011.

[62] B. Czesny, S. Goshu, J. L. Cook, and K. C. Williamson, “The Proteasome Inhibitor Epoxomicin Has Potent Plasmodium falciparum Gametocytocidal Activity □,” vol. 53, no. 10, pp. 4080–4085, 2009.

[63] E. Yoo *et al.*, “Defining the determinants of specificity of Plasmodium proteasome inhibitors Defining the determinants of specificity of Plasmodium proteasome inhibitors,” 2018.

[64] S. M. Gantt *et al.*, “Proteasome Inhibitors Block Development of Plasmodium spp .,” vol. 42, no. 10, pp. 2731–2738, 1998.

[65] S. Crunkhorn, “Novel proteasome inhibitor combats malaria,” *Nat. Publ. Gr.*, vol. 15, no. 4, pp. 232–233, 2016.

[66] S. C. Xie *et al.*, “Target Validation and Identi fi cation of Novel Boronate Inhibitors of the Plasmodium falciparum Proteasome,” 2018.

[67] A. Manuscript and M. Outcomes, “NIH Public Access,” vol. 30, no. 5, pp. 600–604, 2014.

[68] C. Dogovski *et al.*, “Targeting the Cell Stress Response of Plasmodium falciparum to Overcome Artemisinin Resistance,” *PLoS Biol.*, vol. 13, no. 4, pp. 1–26, 2015.

[69] H. Li, A. J. O. Donoghue, W. A. Van Der Linden, and S. C. Xie, “HHS Public Access,” vol. 530, no. 7589, pp. 233–236, 2016.

[70] Y. Tu, “c o m m e n ta ry The discovery of artemisinin (qinghaosu) and gifts from Chinese medicine,” *Nat. Publ. Gr.*, vol. 17, no. 10, pp. 1217–1220, 2011.

[71] I. E. Effers, “Chloroquine-resistant Plasmodium falciparum malaria in Kenya,” pp. 228–229, 1979.

[72] T. E. Wellems and C. V Plowe, “Chloroquine-Resistant Malaria,” pp. 770–776.

[73] C. Haemorheology, “Cigarette smoking in pregnancy and fetal hyperviscosity Plasmodium malaria resistant to chloroquine in a Zambian living in Idiopathic hypoparathyroidism associated with stable untreated Idiopathic hypoparathyroidism is rare and characteristically occurs,” vol. 286, no. April, pp. 1315–1316, 1983.

[74] M. Dhorda *et al.*, “Spread of artemisinin-resistant Plasmodium falciparum in Myanmar : a cross-sectional survey of the K13 molecular marker,” pp. 21–26.

[75] H. M. Ismail *et al.*, “A Click Chemistry-Based Proteomic Approach Reveals that 1 , 2 , 4-Trioxolane and Artemisinin Antimalarials Share a Common Protein Alkylation Profile,” pp. 6401–6405, 2016.

[76] J. Wang *et al.*, “Haem-activated promiscuous targeting of artemisinin in Plasmodium falciparum,” *Nat. Commun.*, vol. 6, pp. 1–11, 2015.

[77] N. Klonis, D. J. Creek, and L. Tilley, “Iron and heme metabolism in Plasmodium falciparum and the mechanism of action of artemisinins,” *Curr. Opin. Microbiol.*, vol. 16, no. 6, pp. 722–727, 2013.

[78] P. M. O. Neill, V. E. Barton, and S. A. Ward, “The Molecular Mechanism of

Action of Artemisinin—The Debate Continues," pp. 1705–1721, 2010.

[79] J. Li and B. Zhou, "Biological Actions of Artemisinin: Insights from Medicinal Chemistry Studies," pp. 1378–1397, 2010.

[80] F. Ariey *et al.*, "HHS Public Access," vol. 505, no. 7481, pp. 50–55, 2016.

[81] J. Straimer *et al.*, "Reports K13-propeller mutations confer artemisinin resistance in Plasmodium falciparum clinical isolates," no. December, pp. 1–7, 2014.

[82] A. P. Ramadani *et al.*, "Plasmodium falciparum clinical isolates," vol. 347, no. 6220, pp. 428–431, 2015.

[83] J. R. Broach and J. Thorner, "High-throughput screening for drug discovery," vol. 384, no. November, pp. 14–16, 1996.

[84] A. L. Harvey, R. Edrada-ebel, and R. J. Quinn, "The re-emergence of natural products for drug discovery in the genomics era," no. January, 2015.

[85] G. M. Rishton, "Natural Products as a Robust Source of New Drugs and Drug Leads : Past Successes and Present Day Issues," 2008.

[86] D. J. Newman and G. M. Cragg, "Natural Products as Sources of New Drugs over the Last 25 Years ⊥," pp. 461–477, 2007.

[87] J. Achan *et al.*, "Quinine , an old anti-malarial drug in a modern world : role in the treatment of malaria," *Malar. J.*, vol. 10, no. 1, p. 144, 2011.

[88] S. R. Meshnick and M. J. Dobson, "The History of Antimalarial Drugs," pp. 15–26.

[89] E. A. Ashley, J. Recht, and N. J. White, "Primaquine : the risks and the benefits," pp. 1–7, 2014.

[90] H. Ginsburg and E. Deharo, "A call for using natural compounds in the development of new antimalarial treatments – an introduction," *Malar. J.*, vol. 10, no. Suppl 1, p. S1, 2011.

[91] M. Coleman, S. Casimiro, and J. Hemingway, "Operational Impact of DDT

Reintroduction for Malaria Control on Anopheles arabiensis in Mozambique," no. Who 1957, 2008.

[92] "© 1961 Nature Publishing Group," 1961.

[93] T. Meeting, "Interruption of Malaria Transmission by Chloroquinized Salt in Guyana With Observations on a Chloroquine-Resistant Strain of Plasmodium falciparum," pp. 283–301, 1967.

[94] N. Products, "W H Y ARE SECONDARY METABOLITES (NATURAL PRODUCTS)," vol. 52, no. 6, pp. 1189–1208, 1989.

[95] D. A. Dias, S. Urban, and U. Roessner, "A Historical Overview of Natural Products in Drug Discovery," pp. 303–336, 2012.

[96] N. Durán *et al.*, "Advances in Chromobacterium violaceum and properties of violacein-Its main secondary metabolite: A review," *Biotechnol. Adv.*, vol. 34, no. 5, pp. 1030–1045, 2016.

[97] M. Kanelli *et al.*, "Microbial Production of Violacein and Process Optimization for Dyeing Polyamide Fabrics With Acquired Antimicrobial Properties," vol. 9, no. July, pp. 1–13, 2018.

[98] E. Bilsland *et al.*, "Antiplasmodial and trypanocidal activity of violacein and deoxyviolacein produced from synthetic operons," *BMC Biotechnol.*, vol. 18, no. 1, 2018.

[99] G. T. Sigurdson, P. Tang, and M. M, "Natural Colorants : Food Colorants from Natural Sources," no. December 2016, pp. 1–20, 2017.

[100] K. H. Mcclean *et al.*, "Quorum sensing and Chrornobacteriurn violaceurn : exploitation of violacein production and inhibition for the detection of N-acyl homoserine lactones," no. 1 997, 2018.

[101] A. Maria, D. S. Leal, J. Dara, F. De Queiroz, S. Regina, and B. De Medeiros, "Violacein induces cell death by triggering mitochondrial membrane hyperpolarization in vitro," *BMC Microbiol.*, pp. 4–11, 2015.

[102] P. R. Gonçalves, K. J. P. Rocha-Brito, M. R. N. Fernandes, J. L. Abrantes, N.

Durán, and C. V. Ferreira-Halder, “Violacein induces death of RAS-mutated metastatic melanoma by impairing autophagy process,” *Tumor Biol.*, vol. 37, no. 10, pp. 14049–14058, 2016.

[103] D. D. de Carvalho, F. T. M. Costa, N. Duran, and M. Haun, “Cytotoxic activity of violacein in human colon cancer cells,” *Toxicol. Vitr.*, vol. 20, no. 8, pp. 1514–1521, 2006.

[104] N. Bromberg *et al.*, “Violacein cytotoxicity on human blood lymphocytes and effect on phosphatases,” vol. 6366, 2008.

[105] S. Melo, G. Z. Justo, and N. Dura, “Violacein and its b -cyclodextrin complexes induce apoptosis and differentiation in HL60 cells,” vol. 186, pp. 217–225, 2003.

[106] V. S. Saraiva, J. Marshall, J. Cools-lartigue, and M. N. B. Jr, “Cytotoxic effects of violacein in human uveal melanoma cell lines,” pp. 421–424.

[107] K. C. S. Queiroz *et al.*, “Violacein Induces Death of Resistant Leukaemia Cells via Kinome Reprogramming , Endoplasmic Reticulum Stress and Golgi Apparatus Collapse,” vol. 7, no. 10, 2012.

[108] A. Manuscript, “metastasis,” vol. 455, no. 0, pp. 107–112, 2015.

[109] C. R. Andrighetti-Fröhner, R. V. Antonio, T. B. Creczynski-Pasa, C. R. M. Barardi, and C. M. O. Simões, “Cytotoxicity and Potential Antiviral Evaluation of Violacein Produced by Chromobacterium violaceum,” *Mem. Inst. Oswaldo Cruz*, vol. 98, no. 6, pp. 843–848, 2003.

[110] H. Im, S. Y. Choi, S. Son, and R. J. Mitchell, “Combined Application of Bacterial Predation and Violacein to Kill Polymicrobial Pathogenic Communities,” *Sci. Rep.*, vol. 7, no. 1, pp. 1–10, 2017.

[111] S. Anju, N. S. Kumar, B. Krishnakumar, and B. S. D. Kumar, “Synergistic combination of violacein and azoles that leads to enhanced killing of major human pathogenic dermatophytic fungi Trichophyton rubrum,” *Front. Cell. Infect. Microbiol.*, vol. 5, no. November, p. 3389, 2015.

[112] M. H. Becker, R. M. Brucker, C. R. Schwantes, R. N. Harris, and K. P. C.

Minbiole, “The Bacterially Produced Metabolite Violacein Is Associated with Survival of Amphibians Infected with a Lethal Fungus □,” vol. 75, no. 21, pp. 6635–6638, 2009.

[113] S. C. P. Lopes *et al.*, “Violacein extracted from Chromobacterium violaceum inhibits Plasmodium growth in vitro and in vivo,” *Antimicrob. Agents Chemother.*, vol. 53, no. 5, pp. 2149–2152, 2009.

[114] C. Verı, C. L. Bos, H. H. Versteeg, G. Z. Justo, and N. Dura, “Molecular mechanism of violacein-mediated human leukemia cell death,” vol. 104, no. 5, pp. 1459–1465, 2018.

[115] A. A. Alshatwi, P. Subash-babu, and P. Antonisamy, “Experimental and Toxicologic Pathology Violacein induces apoptosis in human breast cancer cells through up regulation of BAX , p53 and down regulation of MDM2,” *Exp. Toxicol. Pathol.*, 2015.

[116] A. C. G. Cauz *et al.*, “Violacein targets the cytoplasmic membrane of bacteria,” *ACS Infect. Dis.*, vol. 5, no. 4, pp. 539–549, 2019.

[117] D. Walliker *et al.*, “Genetic Analysis of the Human Malaria Parasite,” *Science (80-.).*, vol. 236, no. November, pp. 1661–1666, 1986.

[118] A. M. J. Oduola, W. K. Milhous, N. F. Weatherly, J. H. Bowdre, and R. E. Desjardins, “Plasmodium falciparum: Induction of resistance to mefloquine in cloned strains by continuous drug exposure in vitro,” *Exp. Parasitol.*, vol. 67, no. 2, pp. 354–360, 1988.

[119] M. Microscopy, S. Operating, and S. Precautions, “Preparation of Giemsa Stock Solution,” pp. 1–3, 2016.

[120] C. Lambros and J. P. Vanderberg, “Falciparum of Plasmodium Synch Stages in Culture,” *J. Parasitol.*, vol. 65, no. 3, pp. 418–420, 1979.

[121] J. B. Jensen and W. Trager, “Plasmodium falciparum in culture: use of outdated erthrocytes and description of the candle jar method.,” *J. Parasitol.*, vol. 63, no. 5, pp. 883–6, 1977.

[122] J. D. Johnson, R. A. Dennull, L. Gerena, M. Lopez-Sanchez, N. E. Roncal,

and N. C. Waters, “Assessment and continued validation of the malaria SYBR Green I-based fluorescence assay for use in malaria drug screening,” *Antimicrob. Agents Chemother.*, vol. 51, no. 6, pp. 1926–1933, 2007.

[123] C. Le Manach *et al.*, “Fast in vitro methods to determine the speed of action and the stage-specificity of anti-malarials in Plasmodium falciparum,” *Malar. J.*, vol. 12, no. 1, pp. 1–7, 2013.

[124] M. K. Dearnley *et al.*, “Origin , composition , organization and function of the inner membrane complex of Plasmodium falciparum gametocytes,” 2011.

[125] A. Manuscript, “NIH Public Access,” vol. 177, no. 2, pp. 160–163, 2012.

[126] J. Calit *et al.*, “Screening the Pathogen Box for Molecules Active against Plasmodium Sexual Stages Using a New Nanoluciferase-Based Transgenic Line of P. berghei Identifies Transmission-Blocking Compounds,” *Antimicrob. Agents Chemother.*, vol. 62, no. 11, 2018.

[127] J. Calit *et al.*, “Screening the Pathogen Box against Plasmodium sexual stages using a new nanoluciferase based transgenic line of P. berghei identifies transmission-blocking compounds,” *Antimicrob. Agents Chemother.*, no. September, 2018.

[128] A. B. Parsons *et al.*, “Integration of chemical-genetic and genetic interaction data links bioactive compounds to cellular target pathways,” *Nat. Biotechnol.*, vol. 22, no. 1, pp. 62–69, 2004.

[129] J. S. Schneekloth *et al.*, “Chemical Genetic Control of Protein Levels: Selective in Vivo Targeted Degradation,” *J. Am. Chem. Soc.*, vol. 126, no. 12, pp. 3748–3754, 2004.

[130] S. E. Pierce, R. W. Davis, C. Nislow, and G. Giaever, “Genome-wide analysis of barcoded Saccharomyces cerevisiae gene-deletion mutants in pooled cultures,” 2007.

[131] P. Ewels, M. Magnusson, S. Lundin, and M. Käller, “MultiQC: Summarize analysis results for multiple tools and samples in a single report,” *Bioinformatics*, vol. 32, no. 19, pp. 3047–3048, 2016.

[132] M. Martin, “Cutadapt removes adapter sequences from high-throughput sequencing reads kenkyuhi hojokin gan rinsho kenkyu jigyo.,” *EMBnet.journal*, vol. 17, no. 1, pp. 10–12, 2013.

[133] I. Latar, “Et Al. , 2005;,” vol. 13, no. 7, pp. 1–6, 2013.

[134] M. I. Love, W. Huber, and S. Anders, “Moderated estimation of fold change and dispersion for RNA-seq data with DESeq2,” *Genome Biol.*, vol. 15, no. 12, pp. 1–21, 2014.

[135] S. Anders and W. Huber, “Differential expression analysis for sequence count data,” *Genome Biol.*, vol. 11, no. 10, p. R106, 2010.

[136] A. Y. Lee *et al.*, “Mapping the Cellular Response Chemogenomic Fitness Signatures,” *Science (80-.).*, vol. 344, no. April, pp. 208–212, 2014.

[137] H. M. Berman *et al.*, “The Protein Data Bank,” vol. 28, no. 1, pp. 235–242, 2000.

[138] C. Bi *et al.*, “The RCSB Protein Data Bank : views of structural biology for basic and applied research and education,” vol. 43, no. November 2014, pp. 345–356, 2015.

[139] F. Kiefer, K. Arnold, and M. Ku, “The SWISS-MODEL Repository and associated resources,” vol. 37, no. October 2008, pp. 387–392, 2009.

[140] K. Arnold, L. Bordoli, and T. Schwede, “Structural bioinformatics The SWISS-MODEL workspace : a web-based environment for protein structure homology modelling,” vol. 22, no. 2, pp. 195–201, 2006.

[141] J. Ko, H. Park, L. Heo, and C. Seok, “GalaxyWEB server for protein structure prediction and refinement,” vol. 40, no. May, pp. 294–297, 2012.

[142] V. B. Chen *et al.*, “research papers MolProbity : all-atom structure validation for macromolecular crystallography research papers,” pp. 12–21, 2010.

[143] B. J. Hintze, S. M. Lewis, J. S. Richardson, and D. C. Richardson, “distributions for model validation,” no. January, pp. 1177–1189, 2016.

[144] P. C. D. Hawkins, A. G. Skillman, G. L. Warren, B. A. Ellingson, and M. T.

Stahl, “Conformer Generation with OMEGA : Algorithm and Validation Using High Quality Structures from the Protein Databank and Cambridge Structural Database,” vol. 11, pp. 572–584, 2010.

[145] A. Jakalian, D. B. Jack, and C. I. Bayly, “Fast , Efficient Generation of High-Quality Atomic Charges . AM1-BCC Model : II . Parameterization and Validation,” 2002.

[146] J. C. Gordon, J. B. Myers, T. Folta, V. Shoja, L. S. Heath, and A. Onufriev, “H ++ : a server for estimating p K a s and adding missing hydrogens to macromolecules,” vol. 33, pp. 368–371, 2005.

[147] M. Mcgann, “FRED Pose Prediction and Virtual Screening Accuracy,” no. 1, pp. 578–596, 2011.

[148] M. Mcgann, “FRED and HYBRID docking performance on standardized datasets,” 2012.

[149] B. R. Pooria Gill, Tahereh Tohidi Moghadam, “Differential Scanning Calorimetry Techniques: Applications in Biology and Nanoscience,” *J. Biomol. Tech.*, vol. 21, no. 4, pp. 167–193, 2010.

[150] T. V. Seraphim *et al.*, “The C-terminal region of the human p23 chaperone modulates its structure and function,” *Arch. Biochem. Biophys.*, vol. 565, pp. 57–67, 2015.

[151] N. J. Spillman, J. R. Beck, S. M. Ganesan, J. C. Niles, and D. E. Goldberg, “The chaperonin TRiC forms an oligomeric complex in the malaria parasite cytosol,” *Cell. Microbiol.*, vol. 19, no. 6, 2017.

[152] L. R. Pratt-riccio *et al.*, “Antibodies against the Plasmodium falciparum glutamate-rich protein from naturally exposed individuals living in a Brazilian malaria-endemic area can inhibit in vitro parasite growth,” vol. 106, pp. 34–43, 2011.

[153] D. J. Johnson *et al.*, “NIH Public Access,” vol. 15, no. 6, pp. 867–877, 2010.

[154] V. C. Corey *et al.*, “A broad analysis of resistance development in the malaria parasite,” *Nat. Commun.*, vol. 7, no. May, pp. 1–9, 2016.

[155] M. I. Veiga *et al.*, “Globally prevalent PfMDR1 mutations modulate Plasmodium falciparum susceptibility to artemisinin-based combination therapies,” *Nat. Commun.*, vol. 7, no. May, 2016.

[156] A. Ecker, A. M. Lehane, J. Clain, and D. A. Fidock, “PfCRT and its role in antimalarial drug resistance,” *Trends Parasitol.*, vol. 28, no. 11, pp. 504–514, 2012.

[157] I. W. Sherman, “Amino acid metabolism and protein synthesis in malarial parasites *,” vol. 55, pp. 265–276, 1977.

[158] X. C. Ding *et al.*, “P . falciparum In Vitro Killing Rates Allow to Discriminate between Different Antimalarial Mode-of-Action,” vol. 7, no. 2, 2012.

[159] L. M. Fohl and D. S. Roos, “Fitness effects of DHFR-TS mutations associated with pyrimethamine resistance in apicomplexan parasites,” *Mol. Microbiol.*, vol. 50, no. 4, pp. 1319–1327, 2003.

[160] C. H. Coelho, J. Yai, A. Doritchamou, I. Zaidi, and P. E. Duffy, “Advances in malaria vaccine development : report from the 2017 malaria vaccine symposium,” *npj Vaccines*, no. August 2017, 2018.

[161] J. E. Epstein *et al.*, “malaria vaccines,” vol. 33, no. 52, pp. 7452–7461, 2016.

[162] B. Blasco, D. Leroy, and D. A. Fidock, “Antimalarial drug resistance : linking Plasmodium falciparum parasite biology to the clinic,” vol. 23, no. 8, pp. 917–928, 2017.

[163] E. R. Derbyshire, M. M. Mota, and J. Clardy, “The Next Opportunity in Anti-Malaria Drug Discovery : The Liver Stage,” vol. 7, no. 9, 2011.

[164] A. Gego *et al.*, “New Approach for High-Throughput Screening of Drug Activity on Plasmodium Liver Stages,” vol. 50, no. 4, pp. 1586–1589, 2006.

[165] E. R. Derbyshire, M. Prudêncio, M. M. Mota, and J. Clardy, “Liver-stage malaria parasites vulnerable to diverse chemical scaffolds,” vol. 109, no. 22, pp. 8511–8516, 2012.

[166] R. Faleiro, D. S. Karunarathne, and J. M. Horne-debets, “The Contribution of

Co-signaling Pathways to Anti-malarial T Cell Immunity," vol. 9, no. December, pp. 1–8, 2018.

[167] A. S. Butterworth, T. S. Skinner-adams, D. O. N. L. Gardiner, and K. R. Trenholme, "Plasmodium falciparum gametocytes : with a view to a kill," pp. 1718–1734, 2013.

[168] M. W. A. Dixon, M. K. Dearnley, E. Hanssen, T. Gilberger, and L. Tilley, "Shape-shifting gametocytes : how and why does P . falciparum go banana-shaped ?," *Trends Parasitol.*, vol. 28, no. 11, pp. 471–478, 2012.

[169] N. J. White, "Primaquine to prevent transmission of falciparum malaria," *Lancet Infect. Dis.*, vol. 13, no. 2, pp. 175–181, 2013.

[170] D. Fernando, C. Rodrigo, and S. Rajapakse, "Primaquine in vivax malaria : an update and review on management issues," *Malar. J.*, vol. 10, no. 1, p. 351, 2011.

[171] T. Journal, "B L 00 that IIIIIIIIIIIIIII1II \ IIIUI1IIIIII \ II11," 2019.

[172] D. Botstein, S. A. Chervitz, and J. M. Cherry, "Yeast as a model organism," *Science (80-.).*, vol. 277, no. 5330, pp. 1259–1260, 1997.

[173] A. Goffeau *et al.*, "Life with 6000 Genes conveniently among the different interna- Old Questions and New Answers The genome . At the beginning of the se- of its more complex relatives in the eukary- cerevisiae has been completely sequenced Schizosaccharomyces pombe indicate," *Science (80-.).*, vol. 274, no. October, pp. 546–567, 1996.

[174] E. C. Park, D. Finley, and J. W. Szostak, "A strategy for the generation of conditional mutations by protein destabilization.," *Proc. Natl. Acad. Sci. U. S. A.*, vol. 89, no. 4, pp. 1249–1252, 1992.

[175] M. J. Marton *et al.*, "Drug target validation and identification of secondary drug target effects using DNA microarrays.," *Nat. Med.*, vol. 4, no. 11, pp. 1293–1301, 1998.

[176] A. B. Parsons *et al.*, "Resource Exploring the Mode-of-Action of Bioactive Compounds by Chemical-Genetic Profiling in Yeast," pp. 611–625, 2006.

[177] A. Silva *et al.*, “Involvement of Yeast HSP90 Isoforms in Response to Stress and Cell Death Induced by Acetic Acid,” *PLoS One*, vol. 8, no. 8, 2013.

[178] H. Takai, Y. Xie, T. De Lange, and N. P. Pavletich, “Tel2 structure and function in the Hsp90-dependent maturation of mTOR and ATR complexes,” *Genes Dev.*, vol. 24, no. 18, pp. 2019–2030, 2010.

[179] L. Neckers and P. Workman, “Hsp90 molecular chaperone inhibitors: Are we there yet?,” *Clin. Cancer Res.*, vol. 18, no. 1, pp. 64–76, 2012.

[180] A. Burgess, K. Shah, O. Hough, and K. Hynynen, “HHS Public Access,” vol. 15, no. 5, pp. 477–491, 2016.

[181] C. Esser, S. Alberti, and J. Höhfeld, “Cooperation of molecular chaperones with the ubiquitin/proteasome system,” *Biochim. Biophys. Acta - Mol. Cell Res.*, vol. 1695, no. 1–3, pp. 171–188, 2004.

[182] E. S. Ehrlich *et al.*, “Regulation of Hsp90 client proteins by a Cullin5-RING E3 ubiquitin ligase,” *Proc. Natl. Acad. Sci.*, vol. 106, no. 48, pp. 20330–20335, 2009.

[183] J. R. Manjarrez, L. Sun, T. Prince, and R. L. Matts, “Hsp90-dependent assembly of the DBC2/RhoBTB2-cullin3 E3-ligase complex,” *PLoS One*, vol. 9, no. 3, 2014.

[184] D. Posfai *et al.*, “Identification of Hsp90 inhibitors with Anti-Plasmodium activity,” *Antimicrob. Agents Chemother.*, vol. 62, no. 4, 2018.

[185] V. B. Chen *et al.*, “MolProbity : all-atom structure validation for macromolecular crystallography,” *Acta Crystallogr. Sect. D Biol. Crystallogr.*, vol. 66, no. 1, pp. 12–21, Jan. 2010.

[186] B. J. Hintze, S. M. Lewis, J. S. Richardson, and D. C. Richardson, “Molprobity’s ultimate rotamer-library distributions for model validation,” *Proteins Struct. Funct. Bioinforma.*, vol. 84, no. 9, pp. 1177–1189, Mar. 2016.

[187] T. Wang, P. Mäser, and D. Picard, “Inhibition of Plasmodium falciparum Hsp90 Contributes to the Antimalarial Activities of Aminoalcohol-carbazoles,” *J. Med. Chem.*, vol. 59, no. 13, pp. 6344–6352, 2016.

[188] T. J. Wandless, “NIH Public Access,” vol. 126, no. 5, pp. 995–1004, 2012.

[189] L. A. Banaszynski and T. J. Wandless, “Conditional Control of Protein Function,” *Chem. Biol.*, vol. 13, no. 1, pp. 11–21, 2006.

[190] A. Rodger, R. Marrington, D. Roper, and S. Windsor, “for the Study of Protein – Ligand Interactions,” vol. 305, pp. 343–363.

[191] G. Siligardi, R. Hussain, S. G. Patching, and M. K. Phillips-jones, “Biochimica et Biophysica Acta Ligand- and drug-binding studies of membrane proteins revealed through circular dichroism spectroscopy ☆,” *BBA - Biomembr.*, vol. 1838, no. 1, pp. 34–42, 2014.

[192] F. Zsila, “Subdomain IB Is the Third Major Drug Binding Region of Human Serum Albumin: Toward the Three-Sites Model,” 2013.

[193] F. Zsila, “Circular Dichroism Spectroscopic Detection of Ligand Binding Induced Subdomain IB Speci fi c Structural Adjustment of Human Serum Albumin,” 2013.

[194] M. S. Celej, S. A. Dassie, and G. D. Fidelio, “Differential scanning calorimetry as a tool to estimate binding parameters in multiligand binding proteins ´ n Gonza,” vol. 350, pp. 277–284, 2006.

[195] C. M. Johnson, “Differential scanning calorimetry as a tool for protein folding and stability,” *Arch. Biochem. Biophys.*, vol. 531, no. 1–2, pp. 100–109, 2013.

[196] I. B. Durowoju, K. S. Bhandal, J. Hu, B. Carpick, and M. Kirkitadze, “Differential Scanning Calorimetry — A Method for Assessing the Thermal Stability and Conformation of Protein Antigen,” no. March, pp. 1–8, 2017.

[197] L. H. Pearl, “Review The HSP90 Molecular Chaperone—An Enigmatic ATPase,” vol. 105, no. 8, 2016.

[198] H. Ochel and K. Eichhorn, “Geldanamycin : the prototype of a class of antitumor drugs targeting the heat shock protein 90 family of molecular chaperones,” vol. 6, pp. 105–112, 2001.

[199] A. Shonhai, “Plasmodial heat shock proteins: Targets for chemotherapy,”

FEMS Immunol. Med. Microbiol., vol. 58, no. 1, pp. 61–74, 2010.

[200] C. E. Stebbins, A. A. Russo, C. Schneider, N. Rosen, F. U. Hartl, and N. P. Pavletich, “Crystal Structure of an Hsp90 – Geldanamycin Complex : Targeting of a Protein Chaperone by an Antitumor Agent,” vol. 89, pp. 239–250, 1997.

[201] W. M. J. Obermann, H. Sondermann, A. A. Russo, N. P. Pavletich, and F. U. Hartl, “In Vivo Function of Hsp90 Is Dependent on ATP Binding and ATP Hydrolysis,” vol. 143, no. 4, pp. 901–910, 1998.

[202] B. Panaretou *et al.*, “ATP binding and hydrolysis are essential to the function of the Hsp90 molecular chaperone in vivo,” vol. 17, no. 16, pp. 4829–4836, 1998.

[203] J. P. Grenert, B. D. Johnson, and D. O. Toft, “The Importance of ATP Binding and Hydrolysis by Hsp90 in Formation and Function of Protein Heterocomplexes *,” vol. 274, no. 25, pp. 17525–17533, 1999.

[204] C. Prodromou *et al.*, “The ATPase cycle of Hsp90 drives a molecular ` clamp ’ via transient dimerization of the N-terminal domains,” vol. 19, no. 16, pp. 4383–4392, 2000.

[205] L. Whitesell, E. G. Mimnaugh, B. D. E. Costat, C. E. Myers, and L. M. Neckers, “Inhibition of heat shock protein HSP90-pp6Ov-src heteroprotein complex formation by benzoquinone ansamycins : Essential role for stress proteins in oncogenic transformation,” vol. 91, no. August, pp. 8324–8328, 1994.

[206] M. Schapira and W. A. Houry, “Tamoxifen Enhances the Hsp90 Molecular Chaperone ATPase Activity,” vol. 5, no. 4, pp. 1–8, 2010.

[207] C. Biology, C. S. Chua, H. Low, N. Lehming, and T. S. Sim, “The International Journal of Biochemistry Molecular analysis of Plasmodium falciparum co-chaperone Aha1 supports its interaction with and regulation of Hsp90 in the malaria parasite,” *Int. J. Biochem. Cell Biol.*, vol. 44, no. 1, pp. 233–245, 2012.

[208] L. B. Shelton *et al.*, “Hsp90 activator Aha1 drives production of pathological tau aggregates,” vol. 114, no. 36, pp. 9707–9712, 2017.

[209] S. H. Mclaughlin, H. W. Smith, and S. E. Jackson, “Stimulation of the Weak ATPase Activity of Human Hsp90 by a Client Protein,” 2002.

[210] S. Vali, R. Pallavi, and S. Kapoor, “Virtual prototyping study shows increased ATPase activity of Hsp90 to be the key determinant of cancer phenotype,” pp. 25–33, 2010.

[211] J. Li, J. Soroka, and J. Buchner, “Biochimica et Biophysica Acta The Hsp90 chaperone machinery : Conformational dynamics and regulation by,” *BBA - Mol. Cell Res.*, vol. 1823, no. 3, pp. 624–635, 2012.

[212] A. Wolmarans, B. Lee, L. Spyracopoulos, and P. Lapointe, “The Mechanism of Hsp90 ATPase Stimulation by Aha1,” no. August, pp. 1–15, 2016.

[213] A. Aguzzi and T. O. Connor, “Protein aggregation diseases : pathogenicity and therapeutic perspectives,” 2010.

[214] K. Liberek, “Focus Quality Control Chaperones in control of protein disaggregation,” vol. 27, no. 2, pp. 328–335, 2008.

[215] A. Penzkofer, “Protein aggregation studied by forward light scattering and light transmission analysis,” vol. 342, pp. 55–63, 2007.

[216] B. D. Johnson, A. Chadli, S. J. Felts, I. Bouhouche, M. G. Catelli, and D. O. Toft, “Hsp90 Chaperone Activity Requires the Full-length Protein and Interaction among Its Multiple Domains *,” vol. 275, no. 42, pp. 32499–32507, 2000.

[217] E. E. Nelson and A. E. Guyer, “NIH Public Access,” vol. 1, no. 3, pp. 233–245, 2012.

[218] S. A. D. Anishefsky, N. E. A. L. R. Osen, and F. U. L. H. Artl, “Pharmacologic shifting of a balance between protein refolding and degradation mediated by Hsp90,” vol. 93, no. December, pp. 14536–14541, 1996.

[219] E. G. Mimnaugh, C. Chavany, and L. Neckers, “Polyubiquitination and Proteasomal Degradation of the p185 c- erb B-2 Receptor Protein-tyrosine Kinase Induced by Geldanamycin *,” vol. 271, no. 37, pp. 22796–22801, 1996.

[220] A. S. Meyer, J. R. Gillespie, D. Walther, I. S. Millet, S. Doniach, and J. Frydman, “Closing the folding chamber of the eukaryotic chaperonin requires the transition state of ATP hydrolysis,” *Cell*, vol. 113, no. 3, pp. 369–381, 2003.

[221] C. D. McCallum, H. Do, A. E. Johnson, and J. Frydman, “The interaction of the chaperonin tailless complex polypeptide 1 (TCP1) ring complex (TRiC) with ribosome-bound nascent chains examined using photo- cross-linking,” *J. Cell Biol.*, vol. 149, no. 3, pp. 591–601, 2000.

[222] V. Thulasiraman, C. F. Yang, and J. Frydman, “In vivo newly translated polypeptides are sequestered in a protected folding environment,” *EMBO J.*, vol. 18, no. 1, pp. 85–95, 1999.

[223] F. U. Hartl, A. Bracher, and M. Hayer-Hartl, “Molecular chaperones in protein folding and proteostasis,” *Nature*, vol. 475, no. 7356, pp. 324–332, 2011.

[224] A. Shiber and T. Ravid, “Chaperoning Proteins for Destruction: Diverse Roles of Hsp70 Chaperones and their Co-Chaperones in Targeting Misfolded Proteins to the Proteasome,” pp. 704–724, 2014.

[225] M. P. Mayer and B. Bukau, “Cellular and Molecular Life Sciences Hsp70 chaperones : Cellular functions and molecular mechanism,” vol. 62, pp. 670–684, 2005.

[226] D. M. Cyr, “Previews Swapping Nucleotides , Tuning Hsp70,” pp. 945–947, 2008.

[227] A. Shonhai, A. Boshoff, and G. L. Blatch, “The structural and functional diversity of Hsp70 proteins from Plasmodium falciparum,” pp. 1803–1818, 2007.

[228] H. Raviol, H. Sadlish, F. Rodriguez, M. P. Mayer, and B. Bukau, “Chaperone network in the yeast cytosol : Hsp110 is revealed as an Hsp70 nucleotide exchange factor,” vol. 25, no. 11, pp. 2510–2518, 2006.

[229] G. G. Tartaglia, S. Pechmann, C. M. Dobson, and M. Vendruscolo, “Life on the edge : a link between gene expression levels and aggregation rates of human

proteins," vol. 32, no. 5, pp. 204–206, 2005.

[230] K. P. Silva and J. C. Borges, "The Molecular Chaperone Hsp70 Family Members Function by a Bidirec- tional Heterotrophic Allosteric Mechanism," pp. 132–142, 2011.

[231] N. J. Greenfield, "interactions," vol. 1, no. 6, pp. 2527–2535, 2009.

[232] G. W. Gitau, P. Mandal, G. L. Blatch, J. Przyborski, and A. Shonhai, "Characterisation of the Plasmodium falciparum Hsp70-Hsp90 organising protein (PfHop)," *Cell Stress Chaperones*, vol. 17, no. 2, pp. 191–202, 2012.

[233] L. A. Kirkman *et al.*, "Antimalarial proteasome inhibitor reveals collateral sensitivity from intersubunit interactions and fitness cost of resistance," vol. 115, no. 29, pp. 6863–6870, 2018.

[224] Antony, H. A., & Parija, S. C. (2016). Antimalarial drug resistance: An overview. *Tropical parasitology*, *6*(1), 30-41.

SUPPLEMENTARY MATERIAL

Annex I: Scientific production

During the period in which this thesis was developed, the student participated in scientific collaborations already published, accepted for publication or in the process of submission (not shown):

1. **Antiplasmodial and trypanocidal activity of violacein and deoxyviolacein produced from synthetic operons.**
   Bilsland E, **Tavella TA**, Krogh R, Stokes JE, Roberts A, Ajioka J, Spring DR, Andricopulo AD, Costa FTM, Oliver SG.
   BMC Biotechnology, 2018. Impact Factor: 2.4

2. **Hydroxyazole scaffold-based *Plasmodium falciparum* dihydroorotate dehydrogenase inhibitors: Synthesis, biological evaluation and X-ray structural studies.**
   Pippione AC, Sainas S, Goyal P, Fritzson I, Cassiano GC, Giraudo A, Giorgis M, **Tavella TA**, Bagnati R, Rolando B, Caing-Carlsson R, Costa FTM, Andrade CH, Al-Karadaghi S, Boschi D, Friemann R, Lolli ML.
   European Journal of Medicinal Chemistry, 2018. Impact Factor: 4.7

3. **Yeast-Based High-Throughput Screens for Antiparasitic Drug Discovery and Development.**
   Tavella TA, Sunnerhagen P, Costa FTM, Bilsland E.
   Current Topics in Medicinal Chemistry, 2017. Impact Factor: 2.5

4. **Targeting malaria protein kinases.**
   Cassiano GC, **Tavella TA,** Nascimento MN, PVL, Andrade CH, Maranhão Costa FTM
   Current Topics in Medicinal Chemistry, 2017. Impact Factor: 2.5

Annex II: Financial Support

This study was financed in part by the Coordenação de Aperfeiçoamento de Pessoal de Nível Superior - Brasil (CAPES) - Finance Code 001

Process number: 23038.013648/2018-51

Annex III: Authors Declaration

Declaração de Direitos Autorais

As cópias de artigos de minha autoria ou de minha co-autoria, já publicados ou submetidos para publicação em revistas científicas ou anais de congressos sujeitos a arbitragem, que constam na minha Dissertação/ Tese de doutorado intitulada, **Atividade antiplasmodial e mecanismo de ação da violaceína em *Plasmodium falciparum***, não infringem os dispositivos da Lei n°9.610/98, nem o direito autoral de qualquer editora.

Campinas, 25 de agosto de 2019

Assinatura:

Nome da autora: TATYANA ALMEIDA TAVELLA

RG: 14392423

Assinatura:

Nome do orientador: FABIO TRINDADE MARANHÃO COSTA

RG: 1263942

Annex IV: Bioethics Declaration

UNICAMP

COORDENADORIA DE PÓS-GRADUAÇÃO
INSTITUTO DE BIOLOGIA
Universidade Estadual de Campinas
Caixa Postal 6109. 13083-970, Campinas, SP, Brasil
Fone (19) 3521-6378. email: cpgib@unicamp.br

IB

DECLARAÇÃO

Em observância ao **§5º do Artigo 1º da Informação CCPG-UNICAMP/001/15**, referente a Bioética e Biossegurança, declaro que o conteúdo de minha Tese de Doutorado, intitulada "***Atividade antiplasmodial e mecanismo de ação da violaceína em Plasmodium falciparum***", desenvolvida no Programa de Pós-Graduação em Genética e Biologia Molecular do Instituto de Biologia da Unicamp, não versa sobre pesquisa envolvendo seres humanos, animais ou temas afetos a Biossegurança.

Assinatura: _____
Nome do(a) aluno(a): TATYANA ALMEIDA TAVELLA

Assinatura: _____
Nome do(a) orientador(a): FABIO TRINDADE MARANHÃO COSTA

Data: 25 de agosto de 2019, Campinas